2-1-2016

Passive aeration of wastewater using tray aerators

Ayman Mostafa El-Zahaby

The American University In Cairo
School of Science and Engineering

PASSIVE AERATION OF WASTEWATER USING TRAY AERATORS

BY

AYMAN MOSTAFA EL-ZAHABY

A thesis submitted in partial fulfillment of the requirements for the degree of

Masters of Science in Environmental Engineering

Under the supervision of:

Dr. Ahmed S. El-Gendy

Associate Professor and Director of the Environmental Engineering Program, Department of Construction Engineering

The American University in Cairo

Fall, 2016

Dedication

This work is dedicated to my wife Dina, my son Mostafa, and my daughter Layal for the hard times they suffered throughout my research.

Acknowledgment

This research work would never have been achieved without the support of many people. I owe them great gratitude and thanks for their continuous advice, patience, and encouragement.

I would like to acknowledge the great support I received from my thesis advisor, Dr. Ahmed El-Gendy. Thank you for your patience, and continuous advice. Your guidance in the methodology of addressing the thesis topic, and analyzing the results will always be a milestone in my life that I should never forget. I believe my research ability was developed mainly under your supervision.

My professor and mentor, Dr. Emad Imam, is also acknowledged for the support he provided through different courses that I received under his supervision, which marked my mind set. I owe you lot of thanks.

Thanks to Eng. Ahmed Saad and Mr. Mohamed Mostafa, from the Environmental lab, as well as Mr. Mohamed Saied, and Mr. Kassem Ali from the Waste Management lab for supporting me in the designing and conducting the experimental works. You were great company during my research journey.

Special thanks go to my loving wife Dina for her support, encouragement, and understanding. You afforded a lot taking care of our children while I was conducting this research. And to my beloved children Mostafa and Layal for their true love and tender smiles which always helped me keep going. I am totally grateful to my parents and big family who believed in me and offered prayers and words of encouragement throughout these years.

I could not have done it without all of you.

Abstract

Passive aeration units in water and wastewater treatment are aeration units that operate without the need for electric energy. They depend on dropping the water through the aerator, while increasing the surface area to volume ratio, and thus increasing the oxygen mass diffused into water. The passive units include cascade aerators, and tray aerators. On the contrary to cascade and spray aerators, tray aerators require a much smaller area for their installation. While researching the design of tray aerators, a shortage of literature pertaining to the topic was observed. The research objective is to develop a model for the design of tray aerators for the purpose of increasing the dissolved oxygen in wastewater.

This thesis investigated the design parameters affecting the aeration performance of tray aerators for wastewater treatment plants. A mathematical model was developed that predicts the aeration performance of a tray aerator system as a function of the flow rate, number of trays, tray area, spacing between trays, number and diameter of holes per tray. Results illustrate that the aeration performance is directly proportional to the tray area, the spacing between trays, and number of trays and is inversely proportional to the flow rate. The number and diameter of holes together with the flow rate define the flow regime into dripping or jetting. The spacing between trays, the number and diameter of holes had slight effect on the aeration performance.

The mass transfer coefficient (K_L) is reported to be a variable rather than a constant figure. An empirical equation for the estimation of K_L as a function in the spacing between trays, flow rate, and the total area of holes in the tray was developed from laboratory scale experiments. That equation is validated in the laboratory scale experiments, as well as in pilot scale application using real wastewater.

Table of Contents

List of Figures

List of Tables

List of Abbreviations

BOD	: Biological Oxygen Demand
CO_2	: Carbon Dioxide
$CoCl_2$	: Cobalt Chloride
DO	: Dissolved Oxygen
H_2O	: Water
Na_2SO_3	: Sodium Sulfite
Na_2SO_4	: Sodium Sulfate
TSS	: Total Suspended Solids
WS	: Wind Speed
WTP	: Water Treatment Plant
WWTP	: Waste Water Treatment Plant

List of Symbols

a	: Specific surface area=A/V, [m2/m3]
A	: Interfacial Area, [m2]
A_j	: Cross section area of the water jets, [m2]
C	: Concentration, [mg/Liter]
C_v	: Coefficient of velocity for flow through nozzle, [dimensionless]
C_d	: Coefficient of discharge for flow through nozzle, [dimensionless]
d	: Hole diameter, [m]
D	: Falling water drop/jet diameter, [m]
D_L	: Diffusivity of air in water, [m2/sec]
D_j	: Mean jet diameter, [m]
g	: Acceleration due to gravity [m/sec2] (9.81 m/sec2)
h	: Height of water film over tray, [m]
h’	: Corrected height of water film over tray, [m]
h_s	: Tray side height, [m]
H	: Overall system height, [m]
HLR	: Hydraulic loading rate=Q/A, [m3/m2/sec]
i	: Number of trays
J	: Rate of mass transfer per unit area or the mass flux, [mg/m2/sec]
K_L	: Overall liquid mass transfer coefficient, [m2]

L : Length, [m]

n : Number of holes per tray

n’ : Corrected number of holes per tray

N : Total number of trays in the system

Q : Flow rate, [m3/sec]

Q_{hole} : Flow rate per hole, [m3/sec]

S : Surface renewal rate, [1/sec]

SP : Spacing between trays, [m]

t : Time, [sec]

t_e : Exposure time, [sec]

T : Temperature, [^oC]

V : Volume, [m3]

v : Velocity, [m/sec]

δ : Film thickness, [m]

ρ : Density, [kg/m3] (997.2 kg/m3 for water at 24 deg.)

σ : Surface tension, [N/m] (0.073 N/m for water at 24 deg.)

BO : Bond number, [dimensionless]

We : Webber number, [dimensionless]

List of Subscripts

c	: Critical
f	: Water film over tray
j	: Water jet from tray
o	: Outer
S	: Saturation
0,1,2	: Initial, intermediate, final

1. Chapter 1: Introduction

Aeration is an important process in water and wastewater treatment plants. In Water Treatment Plants (*WTP*), aeration may be used for oxidation of iron and manganese ions, removal of sulfides, control of pH, and corrosion control. In Waste Water Treatment Plants (*WWTP*), aeration is mainly intended to increase the Dissolved Oxygen (*DO)* in waste water to the limits suitable for the aerobic degradation, as well as to keep the microorganisms in suspension state in the suspended growth biological treatment processes. There are various aeration systems known for *WWTPs*, most of them require energy for their operation. Therefore, the development of passive aeration units, which rely on the potential energy of water in the form of water head, should serve in reducing the operating costs of the *WWTP*.

1.1. Problem Statement

For developed and developing countries, installing adequate number of *WWTPs*, with sufficient design capacities is a great challenge. That challenge increases in its severity when the country is undergoing fast urbanization and development, due to the associated increase in water demand, and consequently an increase in produced waste water that needs to be treated. Furthermore, the investment cost as well as the running cost for *WWTPs* in many cases exceed the allocated budgets of those countries.

Electricity requirements for the aeration process within a biological *WWTP*, often exceed 50% of the total electricity consumption of the *WWTP* (Stoica et al. 2009). The power required to operate mechanical aerators ranges from 20-40 Kw/1000m3 (Tchobanoglous et al. 2004; Sabry et al. 2010). Taking an example from the United States, in which the water-related infrastructure (*WTPs* and *WWTPs*) represent around 3% of the county level total electricity (Hendrickson et al. 2015) from which aeration of wastewater represent a significant amount of energy.

Egypt, as a developing country, has around 60% of its population with access to sanitation facilities, while almost 100% of the population have access to improved water source (Odawara & Loayza 2010). Therefore, there is a need to provide sanitation facilities to the remaining 40% of the population. Country level electric energy figures indicate that the electricity consumed in Egypt is around 148TWh (International Energy Agency 2015). Thus, the additional electricity requirements that shall be associated with the aeration process of new *WWTPs* serving the remaining 40% of the population is estimated to be in the range of 590MWh. These 590MWh

would require additional power plants to be added, in addition to transmission lines to the *WWTPs*. This represents another investment cost adding to the investment cost of the WWTP. Furthermore, the conventional mechanical aeration process requires regular maintenance for the moving parts, and skilled labor to operate them (Sabry et al. 2010).

The aforementioned discussion clarifies the need to have an economical option for aeration that is easy to operate. These criteria can be met by using passive aeration techniques, such as cascade aerators, or tray aerator. Those passive aeration techniques would reduce the energy needed to increase the dissolved oxygen in wastewater for trickling filters, but do not replace the aeration for the suspension of microorganisms in activated sludge processes. Since cascade aerators require a large area footprint for their installation (Tchobanoglous et al. 2004; Lytle et al. 1998; Scott et al. 1955), the use of tray aerators can offer a more practical option for places where land availability is a constraint.

Literature about the design of tray aerators is limited and almost non-existing for their use for aeration purpose. However, a few studies, separated with long time duration, were published on the use of tray aerators for air stripping.

1.2. Objective

This research aims to investigate and develop a design model for tray aerators, as a passive aeration unit, that serves in increasing the DO of effluent from anaerobic treatment for sewage treatment in small communities. Design optimization is not covered in this work. Several factors affect the design criteria for any waste water aeration device, including the category of aerobic treatment unit that it serves, the chemical and physical properties of the water being aerated, the availability and cost of electric energy, the land availability, and the climatic conditions in which the unit will be installed.

1.3. General Approach

The following section summarizes the tasks planned to achieve the objectives of this research. The tasks are divided into three main phases: (i) derivation of a mathematical model that describes the

aeration of water using tray aerator, (ii) experimentally investigate the performance of tray aerators, and (iii) validating the performance of tray aerators using real wastewater.

1.3.1. Phase I - Mathematical Model

- Hydraulic design of tray aerator
- Aeration associated with thin films
- Aeration associated with falling water
- Overall aeration from tray aerators
- Develop software model to test the hydraulic design and the aeration performance from tray aerators

1.3.2. Phase II – Laboratory Study

- Prepare deoxygenated water
- Set-up a laboratory scale tray aerator
- Experiment a number of trays aerator designs using chemically deoxygenated water
- Compare aeration results from the experimented designs
- Investigate the validity of the mathematical model against the experimental results
- Propose an empirical equation for the volumetric mass transfer coefficient

1.3.3. Phase III - Pilot Scale Study

- Set-up four parallel pilot scale tray aerator trains in a WWTP
- Experiment the performance of each tray train for different wastewater flow rates

- Validate the aeration model developed from Phase I - Mathematical Model and corrected in Phase III - Pilot Scale Study

1.4. Thesis Structure

The thesis is divided into seven chapters.

Chapter 1 covers a general introduction of the subject, research motivation, objectives and related tasks and activities.

Chapter 2 presents a comprehensive literature review discussing the mass transfer principals, types of passive aeration systems, and the previous work related to tray aerators.

Chapter 3 encountered mathematical analysis for the flow of water over tray aerators as well as the aeration associated with the falling water and thin film formed above the trays. This analysis is then developed in a MATLab – Mathworks® function that predicts the flow regime and *DO* concentration achieved from each tray.

Chapter 4 discusses the laboratory scale experiments that were conducted using a tray aerator. This includes the deoxygenation techniques, the design of the laboratory scale tray aerator system, and conducting the experiments that tested the impact of different design parameters on the tray aerator efficiency. An empirical formula for the calculation of the oxygen mass transfer coefficient (K_L) is developed in this chapter.

Chapter 5 discusses the pilot scale application of the tray aerator system using real wastewater that is pretreated in an anaerobic unit. Results from this phase are compared against the model developed in previous chapters for validating their results using wastewater under real operating conditions.

Chapter 6 is a general discussion highlighting the results from the three phases of the study, and addresses the design procedure for tray aerators. A case study is illustrated pinpointing the design process inputs and outputs.

Chapter 7 summarizes conclusion and recommendations.

2. Chapter 2: Background and Review of Literature

2.1. Wastewater Treatment Background

Wastewater treatment has been practiced since the 1900s, however; until early 1970s, it only concerned with the removal of suspended solids, reduction of *BOD* and the elimination of pathogens (Tchobanoglous et al. 2004). From the 1970s to 1980s, due to the development in the studies on environmental impacts of wastewater discharge, and the focus on long term effects of the discharge of specific constituents on the receiving water bodies, the treatment of nutrients such as nitrogen and phosphorus were addressed, with higher treatment limits for the suspended solids, *BOD* and pathogenic control (Tchobanoglous et al. 2004). Since the 1980s, improvement of water quality continued to be addressed more strictly and with higher focus on constituents that have adverse consequences on the environment and the long term health issues (Tchobanoglous et al. 2004). Among those constituents are pesticides, industrial chemicals, phenolic compounds, volatile organic compounds, chlorine disinfection, and disinfection by products (Tchobanoglous et al. 2004). Many other constituents are published by the concerned environmental protection agencies (Tchobanoglous et al. 2004).

Wastewater can be defined as liquid waste, and includes domestic or municipal wastewater, and industrial wastewater (McGhee & Steel 1991). Domestic wastewater originates from the water used by a community for various daily applications. It can be classified into strong, medium or weak depending on the concentration of different contaminants (McGhee & Steel 1991). Industrial wastewater is the liquid discharged from industrial applications, such as manufacturing, dairy, food processing, textile…(McGhee & Steel 1991). Industrial wastewater contains, in addition to the organic and suspended constituents, heavy metals, phenolic compounds, and synthesized organic compounds (Tchobanoglous et al. 2004).

Proper collection and treatment of wastewater is essential for the preservation of both water resources and public health (Tchobanoglous et al. 2004). Wastewater collection from domestic uses was known until the 1940s (Tchobanoglous et al. 2004). With the significant growth in industrial applications after 1940, the separation of industrial wastewater from the domestic wastewater became a concern (Tchobanoglous et al. 2004). This was due to the nature of contaminants from industrial wastewater which had high concentrations of heavy metals and synthesized organic compounds that were not effectively treated in conventional wastewater treatment facilities (Tchobanoglous et al. 2004). Thus, industrial facilities had to install

pretreatment plants that collect their industrial waste and remove the non-conventional contaminants prior to the disposal of their waste to the wastewater collection networks (Tchobanoglous et al. 2004).

Regulations and standards for water disposal to receiving water bodies differ amongst countries (Tchobanoglous et al. 2004; McGhee & Steel 1991). In the United States, the regulations establish which bodies are quality limited, and which are effluent limited (McGhee & Steel 1991). Quality limited bodies define the maximum acceptable contamination levels throughout the receiving waterbodies without degradation from neither current nor future discharges, thus treatment degree and flow rate from each discharge source is tailored to meet those quality limits (McGhee & Steel 1991). On the other side, effluent limited standards define the allowable contamination load for each and every discharge source to the water body disregarding the water quality in the receiving water body (McGhee & Steel 1991). Effluent limited standards dictate that wastewater shall be treated to the level obtainable from secondary treatment processes (McGhee & Steel 1991).

2.1.1. Wastewater Treatment Processes

Wastewater may undergo several treatment processes prior to their final disposal to receiving waterbodies, which are generally water sources for downstream communities. Treatment processes are grouped into preliminary treatment, primary treatment, secondary treatment, and tertiary treatment (Tchobanoglous et al. 2004; McGhee & Steel 1991).

Preliminary treatment concerns with regulating the incoming flow rate, as well as the removal of constituents that may cause maintenance or operational problems to the subsequent processes (Tchobanoglous et al. 2004; McGhee & Steel 1991). Those constituents include large floating solids, grit and grease. The preliminary treatment is achieved using racks and coarse screens, grit chambers or commuters (which reduce the size of the floating solids) (Tchobanoglous et al. 2004; McGhee & Steel 1991).

Primary treatment removes a portion of suspended solids together with part of the organic load. This is typically achieved using simple sedimentation tanks or fine screens (Tchobanoglous et al. 2004; McGhee & Steel 1991).

Secondary treatment processes are mainly intended to apply a controlled biological treatment to the primary treated wastewater (Tchobanoglous et al. 2004; McGhee & Steel 1991). This biological treatment enhances the activity of the available microorganisms, that degrades and removes the organic material from the wastewater. Biological treatment process can be classified according to the unit design into attached growth and suspended growth processes (Tchobanoglous et al. 2004; McGhee & Steel 1991). In the attached growth techniques, the bacteria grow attached to a fixed bed of media (rock or plastic) which floats on the water surface (Shammas & Wang 2010a). Whereas in the suspended growth techniques, the bacteria is in suspension by continuous mixing and turbulence induced through an aeration device (activated sludge) (Shammas & Wang 2010b) or through mechanical mixers (anaerobic digesters) (Lyberatos & Pullammanappallil 2010). They can also be classified according to the type of bacteria into aerobic and anaerobic processes (Tchobanoglous et al. 2004).

Tertiary treatment, which is sometimes termed advanced treatment receives the effluent from the secondary treatment processes, and applies techniques related to suspended solids removal, ammonia, nitrogen (total or organic), phosphorus, refractory organics, and dissolved solids reduction so as to increase the quality of the treated wastewater (Tchobanoglous et al. 2004; McGhee & Steel 1991). Tertiary treatment may also apply disinfection techniques to control the pathogens available in the wastewater before their disposal (Tchobanoglous et al. 2004).

The level of treatment for the wastewater is generally governed by the applicable regulations (McGhee & Steel 1991; El-Gohary et al. 1998). However, the selection of the treatment processes that are used is constrained by the initial and running costs, the land availability for the installation, the complexity of the operation and maintenance of the units, (El-Gohary et al. 1998) or the environmental conditions which might deem some processes unsuitable (like the use of anaerobic treatment in cold climate).

Aeration in wastewater treatment plants is an essential process for the effectiveness of aerobic treatment units. Aerobic treatment units are widely used in wastewater treatment for their high efficiency in removal of organic load in terms of Biological Oxygen Demand (*BOD*), and the possibility of nutrient removal together with the removal of *BOD* and Total Suspended Solids (TSS) (Chan et al. 2009). The aerobic treatment units rely on the presence and activity of aerobic

bacteria (aerobes) within the unit to degrades the organic matter in presence of oxygen into biomass and CO_2 (Chan et al. 2009).

2.2. Mass Transfer Principals

Aeration of water and wastewater is a mass transfer process governed by Fick's law of molecular diffusion. During the aeration process, oxygen from gas phase, which is in high oxygen concentration, transfers to the water, which is of low oxygen concentration. Thus the driving force is the concentration gradient (Howe et al. 2012; Bird et al. 2007).

Based on Fick's law of molecular diffusion, the driving force for the mass transfer process is the concentration gradient (Howe et al. 2012; Bird et al. 2007; Tchobanoglous et al. 2004). Any constituent tends to transfer from the zone of high concentration to the zone of low concentration until both zones reach an equilibrium state with similar concentrations as illustrated in Figure 2.1. The rate of mass transfer of a constituent per unit area is termed the mass flux (J) and is estimated using Equation (2.1) (Howe et al. 2012; Bird et al. 2007; Tchobanoglous et al. 2004)

$$J = \frac{dm}{Adt} = \frac{d(CV)}{Adt} = \frac{V}{A}\frac{dC}{dt} = K_L(\Delta C) \quad \text{.....Equation (2.1)}$$

where (K_L) is the mass transfer coefficient in m/sec, (C) is the concentration of the constituent of interest in mg/L; (ΔC) is the difference in concentration between the two zones in mg/L; (t) is the time in sec; (A) is the interface area in m^2; (V) is the volume of water in m^3 over which (C) and (A) are measured; (C_S) is the saturation concentration of the gas in water in mg/L, and is equal to the partial pressure of oxygen in water divided by Henry's law constant; and (a) is the specific area in m^2/m^3, which is equal to the ratio between the interface area and the liquid volume. The value of (C_S) depends on the water temperature, barometric pressure and water salinity. It is obtained from published data and tables (USGS 2015).

It appears form Equation (2.1) that J increases as ΔC increases. So, the maximum J occurs when C in the zone of low concentration (liquid phase in Figure 2.1) is zero, as in Figure 2.1(a). The evaluation of the mass transfer coefficient K_L in aeration processes shall be discussed in subsequent sections.

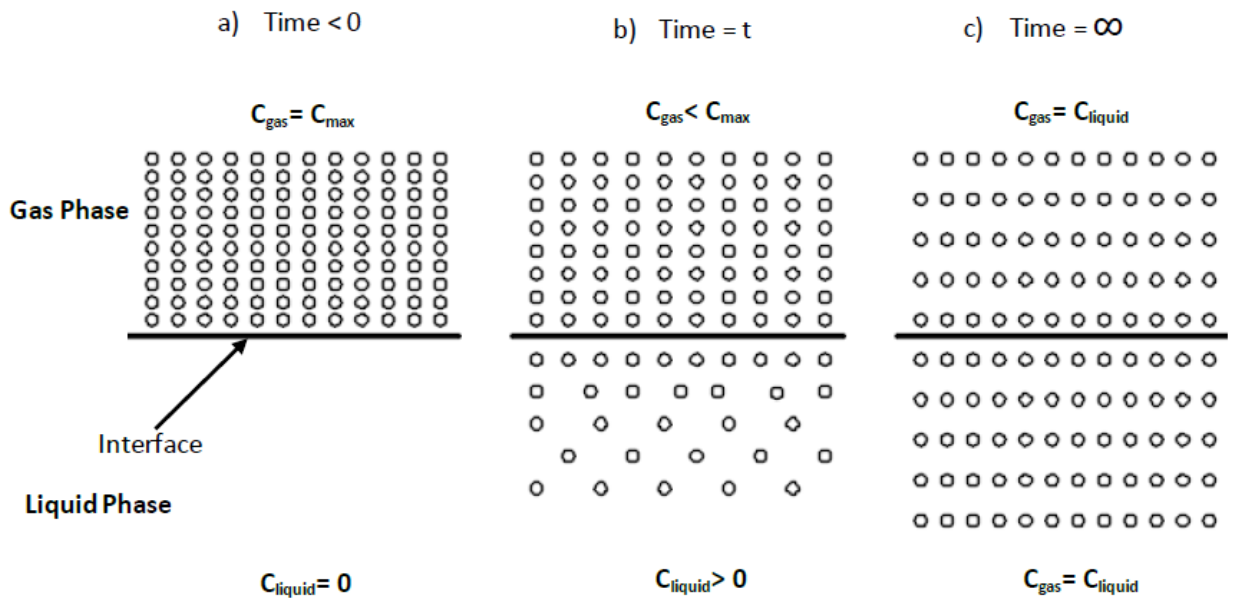

Figure 2.1 Schematic illustration of Fick's law of diffusion. a) condition before diffusion b) condition during diffusion c) condition at equilibrium

When diffusion occurs without the impact of any external forces, it is termed molecular diffusion (Howe et al. 2012). In molecular diffusion, the constituent transfers from the region of high concentration to the region of low concentration solely due to the internal energy of the constituent, while the fluid is at rest (Howe et al. 2012; Tchobanoglous et al. 2004). Other transfer modes are advection, turbulent diffusion and dispersion. Advection occurs when the fluid is in motion, and the constituent of interest transfers from one point to another with the moving fluid, in the absence of diffusion (Howe et al. 2012). If the fluid is mixed in the control volume with no flow, the diffusion is termed turbulent diffusion. The term dispersion is an inclusive term accounting for the advection, molecular diffusion, and turbulent diffusion (Tchobanoglous et al. 2004). The molecular diffusion is illustrated in Equation (2.2)

$$J = -D_m \frac{dC}{dz} \quad \text{.....Equation (2.2)}$$

where (D_m) is the molecular diffusion coefficient of the constituent. Values of D_m depend on the diffusing constituent, as well as the fluid it diffuses from or to. It is a function of the temperature. For oxygen diffusing into water at 25°C, the value of D_m is equal to 2.42×10^{-5} cm^2/sec (CRC 2016).

Through equating Equation (2.1) and Equation (2.2), the rate of oxygen transfer to water across an air-water interface can be described with Equation (2.3) (Wójtowicz & Szlachta 2013; Bird et al. 2007; Gulliver & Rindels 1993).

$$\frac{dC}{dt} = K_L \frac{A}{V}(C_S - C) = K_L a (C_S - C) \quad \text{.....Equation (2.3)}$$

2.2.1. Mass Transfer Coefficient (K_L)

The mass transfer coefficient (K_L), indicated in Equation (2.1) is a measure of gas flux per unit concentration gradient, and has the dimensions of velocity. Extensive effort has been made by several researchers to derive equations that can be used to estimate the value of K_L, however, there is no single equation that fits for all types of reactors or aerators (Garcia-Ochoa & Gomez 2009). Some of those equations are empirical and based on experimental work, while others are theoretical based. The theoretical models that predict K_L are based either on the assumption of a rigid interface surface indicated in the two film theory (Garcia-Ochoa & Gomez 2009; Bird et al. 2007; Tchobanoglous et al. 2004; Chapra 1997; Lewis & Whitman 1924; Whitman 1923), or the assumption of surface renewal concept (Garcia-Ochoa & Gomez 2009; Bird et al. 2007; Tchobanoglous et al. 2004; Chapra 1997), indicated in either the penetration theory (Higbie 1935), or the surface renewal theory (Danckwerts 1951). Some models are based on a combination of the two assumptions (Garcia-Ochoa & Gomez 2009).

The reciprocal of the mass transfer coefficient ($1/K_L$) is an indicator of resistivity, and is the summation of the resistivity from the gas side ($1/HK_g$) and the resistivity from the liquid side ($1/K_l$) (Tchobanoglous et al. 2004; Liss & Slater 1974) as indicated in Equation (2.4)

$$\left(\frac{1}{K_L}\right) = \left(\frac{1}{HK_g}\right) + \left(\frac{1}{K_l}\right) \quad \text{.....Equation (2.4)}$$

where (H) is Henry's Law constant, (K_g) is the gas side mass transfer coefficient; (K_l) is the liquid side mass transfer coefficient. In Equation (2.4), it should be noted that if Henry's Law constant is large, then the liquid side resistivity dominates, and the overall mass transfer coefficient is approximately equal to the liquid side mass transfer coefficient, and vice versa (Tchobanoglous et al. 2004; Liss & Slater 1974).

From the literature, K_L is proportional to the molecular diffusion raised to the power ranging between 0.5 (penetration and surface renewal theory) and 1 (two film theory) (Chapra 1997; Hsieh et al. 1993). Furthermore, K_L is found to have a dynamic value which is a function of the degree of turbulence of the two interacting fluids (Jamnongwong et al. 2010; Tchobanoglous et al. 2004), the chemical reactivity of gases (Wójtowicz & Szlachta 2013; Tchobanoglous et al. 2004; Liss & Slater 1974), physical properties of gas and liquid, operational conditions, and geometrical parameters of the reactor (Garcia-Ochoa & Gomez 2009; Tchobanoglous et al. 2004). Moreover, K_L changes with the change in water temperature (Tchobanoglous et al. 2004).

As the value of K_L is sensitive to the temperature variation, Equation (2.5) describes the correction of K_L at any temperature ($K_{L(T)}$) by knowing the value of K_L at 20°C ($K_{L(20)}$) (Tchobanoglous et al. 2004)

$$K_{L(T)} = K_{L(20)}\theta^{(T-20)} \quad \text{.....Equation (2.5)}$$

where θ is the temperature correction coefficient, ranging from 1.015 to 1.04, with typical value of 1.024 (Tchobanoglous et al. 2004).

Due to the difficulty of estimating K_L alone, most of the values reported in the literature are for the volumetric mass transfer coefficient (K_La), which characterizes the mass transport for a studied reactor operating under defined operating conditions and for specific constituents (Garcia-Ochoa & Gomez 2009; Bird et al. 2007; Thacker et al. 2002; Hsieh et al. 1993; Nakasone 1987; Kavanaugh & Trussell 1980). Among the limited number of reported values for air-water K_L is the proposed mean value between air and sea water $K_L=5.5x10^{-5}$ *m/sec*(Liss & Slater 1974). That value shall be used in the mathematical model in chapter 3 only to test the model, and will be corrected in chapter 4 after conducting the experimental work.

2.2.2. Aeration Overview

Some indicators are used to evaluated and compare between different aeration techniques and/or different operating conditions for the aerator. Those indicators are Oxygen Transfer Rate (*OTR*), Standard Oxygen Transfer Rate (*SOTR*), deficit ratio (*r*), and aeration efficiency(η).

The *OTR* is defined as "the quantity of oxygen transferred per unit time to a given volume of water for equivalent conditions (temperature and chemical composition of water, depth at which air is introduced, etc…)" (ASCE 2007; Tchobanoglous et al. 2004; Mueller et al. 2002). *OTR* is equivalent to Equation (2.3) multiplied by the water volume as indicated in Equation (2.6).

$$OTR = V\frac{dC}{dt} = VK_L a\left(C_S - C\right) \quad \text{.....Equation (2.6)}$$

The *SOTR* is defined as "the quantity of oxygen transferred per unit time into a given volume of water and reported at standard conditions (20°C, 1.00atm, and taking *DO* equal to zero)" (ASCE 2007; Mueller et al. 2002). The *SOTR* provides an indicator for the maximum driving force for the gas transfer. The *SOTR* is calculated according to Equation (2.7).

$$SOTR = VK_L a_{20^oC} C_{S_{20^oC}} \quad \text{.....Equation (2.7)}$$

Deficit ratio r is an indicator for the ratio of the oxygen deficit in the water prior to the aeration device to the oxygen deficit after the aeration device as indicated in Equation (2.8) (Baylar et al. 2007; Nakasone 1987). For any aeration device, this indicator will have a value greater than one.

$$r = \frac{C_S - C_{US}}{C_S - C_{DS}} \quad \text{.....Equation (2.8)}$$

η is a ratio between *DO* added through the aeration device to the *DO* deficit prior to the aeration device (Sabry et al. 2010; Moulick et al. 2010; Toombes & Chanson 2005; Gulliver & Rindels 1993). η is considered as the complementary to the inverse of *r* as indicated in Equation (2.9). Higher values of η indicate more oxygen transfer and higher aeration performance.

$$\eta = \frac{C_{DS} - C_{US}}{C_S - C_{DS}} = 1 - \frac{1}{r} \quad \text{.....Equation (2.9)}$$

2.3. Aeration Systems

Scott (1955) classified aeration of water into falling water aerators and diffused-air aerators. Falling water aerators depends on dropping water through the process, hence the energy used is the potential energy stored in the form of water head (Scott et al. 1955), while the diffused-air aerators depend on forcing compressed air or pure oxygen through water using submerged orifices

or diffuser. (Scott et al. 1955; Tchobanoglous et al. 2004). Other aeration systems are mechanical aerators, in which wastewater is agitated mechanically to boost the solution of air from the atmosphere (Tchobanoglous et al. 2004).

Different types of passive aerators, which are commonly used in treatment units are illustrated in Table 2.1 and detailed in subsequent sections.

Table 2.1 Aeration technologies

Aeration technology	**Feature**	**Reference**
Spray Aerator	Large specific area Low contact time Large installation area Not suitable for freezing weather Energy needed to compress water	(Scott et al. 1955; Sabry et al. 2010)
Cascade aerator	Thin film aeration and air bubbles entrainment High exposure time Large installation area No energy requirements	(Moulick et al. 2010; Baylar et al. 2007; Toombes & Chanson 2005; Scott et al. 1955; Sabry et al. 2010)
Multiple tray aerator	Thin film aeration and falling water Large specific area Small installation area No energy requirements	(Scott et al. 1955)

2.3.1. Spray Aerators

In Spray aerators, pressurized water flows through a pipe distribution grid and exit from fixed nozzles into the air as in a fountain. This process leads to formation of fine water droplets at the exit, with diameters depending on the nozzle exit diameter and design. The formed water droplets take a trajectory path and finally fall into a collection basin underneath the aerator. The aeration concept of spray aerators lays in diffusing the water into small droplets with high interfacial area to volume ratio (*A/V*), which leads to increase of mass transfer rate. As the water droplet exits from the nozzle in a trajectory motion, the contact time for each water droplet is relatively small (around

2 secs for a jet operating under a head of 6 meters), and hence the overall aeration efficiency is not better than other types (Scott et al. 1955).

Other drawbacks of the spray aerators are their large installation area, they are not suitable during freezing weather, and the nozzles have to be range from 25.4mm (1") to 38.1mm (1.5") to prevent clogging (Scott et al. 1955). Figure 2.2 below illustrates the spray aerators.

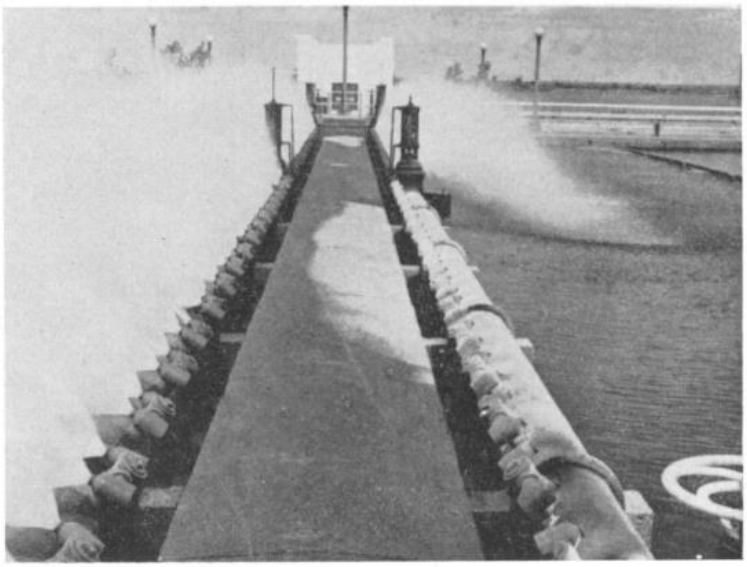

Figure 2.2: Spray aerators (Courtesy: (Scott et al. 1955)*)*

2.3.2. Cascade Aerators

Cascade aerators, resemble an open channel flow with a series of discrete steps among the invert. In their simplest form cascade aerators consist of a concrete step structure over which water spreads and flow from one level to another in thin films. Figure 2.3 indicates the cascade aerators at its various flow conditions.

The aeration efficiency in cascade aerators can reach up to 90% using 14 steps, at a slope of $\tan\theta = 0.351$ and a hydraulic loading rate of 0.009 m2/sec under nappe flow conditions (Moulick et al. 2010), where the nappe flow was previously defined by Bayler (2007) as a series of free-falling jets with nappe impact on the downstream step with an air cavity forming upstream of each step as illustrated in Figure 2.3. The drawback of the cascade aerator is the large space and height needed for the installation (Tchobanoglous et al. 2004).

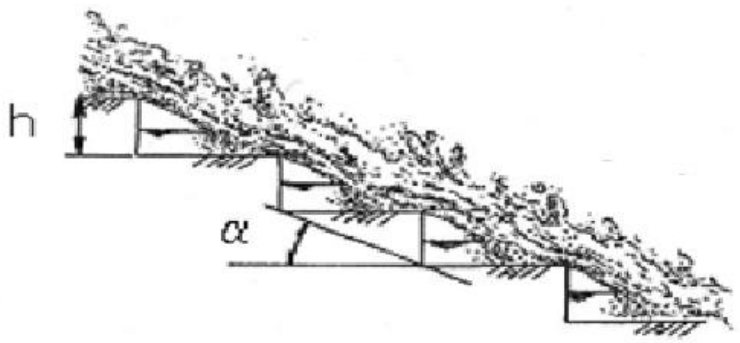

Figure 2.3: Cascade aerators Nappe flow (Courtesy (Ohtsu et al. 2001)*)*

2.3.3. Multiple Tray Aerators

The tray aerator is like a column in which water is supplied from the top, and flows under gravitational forces over a series of horizontal perforated plates below each other. This arrangement allows for the formation of thin water films above each tray, and water falls from tray to the subsequent tray in the form of water jets or water droplets. The large area to volume ratio of the thin films and falling water jets or droplets, together with the high retention time of water, result in an increase in the mass transfer from air to water (Tchobanoglous et al. 2004; Scott et al. 1955).

Multiple tray aerators, are a series of consecutive trays with perforated bottoms over which water falls from one tray to the next until it reaches a collection basin at the bottom as illustrated in Figure 2.4. Tray aerators are ideally designed to enhance the formation of thin water film above the trays which triggers aeration of water, and water falls from one tray to another through the holes in the perforated tray in the form of water droplets which ensures a large area to volume ratio between the air and water, and hence improves the aeration mass transfer. As the trays are installed above each other, the aeration area is achieved in the vertical direction, and high performance can be reached with small installation area.

Tray aerators were studied by different researchers. Scott et al. (1955) discussed the use of multiple tray aerators in water treatment plants for the purpose of removal of iron and manganese minerals with the use of coarse media above the trays to increase the turbulence and surface area of water exposed to the atmosphere, and thus increasing the oxidation of the minerals. Furthermore, they mentioned that the coarse media become coated with films which enhance the oxidation of

minerals and cause their precipitation. In their work, they referred to an empirical equation relating the CO_2 removal to the number of trays and a kinetic constant.

Figure 2.4: Tray Aerator (Courtesy (Lekang 2013)*)*

La Motta (1995) derived a model for the kinetic constant from Scott's work for the removal of CO_2 as a function of tray spacing (*SP*) and hydraulic Loading Rate (*HLR*) for the water. From the data he tested, La Motta concluded that the height of water film above the tray (*h*) was not statistically significant for the value of the kinetic constant, and did not have remarkable impact on the CO_2 removal.

Later, La Motta and Chinthakuntla (1996) studied the impact of other parameters on the kinetic constant for CO_2 stripping; namely, the effect of tray spacing (*SP*), Hydraulic Loading Rate (*HLR*), water temperature (*T*), wind speed (*WS*), initial water quality parameters (calcium concentration, alkalinity and *pH*). From the results they obtained from experimental runs, the *WS* turned out to be insignificant for the tested range (0.22-4.3 $m/\sec$).

Duranceau and Faborode (2012) investigated the use of tray aerators for the removal of sulfides from the ground water. Their work was based on data collected from three *WTPs* incorporating tray aerators in their process. A nonlinear regression analysis for the prediction of the kinetic constant was developed as a function of tray area (*A*), *pH*, flow rate (*Q*), *T*, and *DO*. From their analysis, Duranceau and Faborode (2012) reported that the sulfides removal using tray aerators are

inversely proportional to the number of free protons (H^+) and the *HLR*, and directly proportional with *A*.

3. Phase I - Mathematical Model

3.1. Introduction

In any research work, modelling is the tool utilized by the researchers to interpret different phenomena (response) into simple mathematical expression. Those expressions provide qualitative and quantitative understanding of the phenomena (Heinz 2011). Modelling is either through mathematical modelling, or experimental modelling. Mathematical modelling is mainly based on theory, in which different mathematical expressions are solved simultaneously to develop a formula that describes the response. Following mathematical modelling, experimental work is needed to verify the developed mathematical model.

Among the main benefits of the mathematical modelling, is that the mathematical modelling assist in predicting the input parameters which potentially impact the response, visualize the sensitivity of the response to the change in those parameters, and provide guidance to the levels of test conditions that need to be considered in the experimental modelling.

In the current chapter, the equations governing the mass transfer are considered as the basis for developing the model. The literature review highlights the different flow regimes for the free falling water through the tray holes, and the thresholds for each regime. The methodology describes the procedure to develop a mathematical model that predicts the aeration performance from tray aerators. The model is developed using MATLAB software. The results section shows the results obtained from the model under different test conditions, as well as the impact of changing each input parameter on the response of the aeration performance. The discussion section, draws a comparison between the developed aeration model and other air striping models for tray aerators that were developed in previous works.

3.2. Methodology

For this phase, a set of equations governing the flow and mass transfer for water in the tray aerators were derived from the basic equations. This set of equations (which are shown later in this section) were compiled in a MATLab - Mathworks function file to be used as a mathematical model for designing the tray aerators.

In deriving the mathematical model for *DO* concentration in the effluent from tray aerators, the model considered first a system of one aeration tray other than the distribution tray. Later, the model is expanded to consider more than one tray. Water entering the distribution tray shall exhibit two subsequent flow modes until it reaches the aeration tray; namely thin film formed above the distribution tray and free falling water between the distribution and aeration trays. Each mode is analyzed separately in the next sections.

3.2.1. Flow Regimes

Water exiting from nozzles or holes can attain several flow regimes, that are defined as periodic dripping, dripping faucet, or jetting regimes as illustrated in Figure 3.1. In dripping regime, regular spherical drops of constant mass detach from the nozzle or hole at a constant frequency (periodic dripping) or variable mass drops are formed in a random way (dripping faucet) (Clanet & Lasheras 1999). Dripping regime occurs when Weber number (*We*), a dimensionless parameter is less than a critical Weber number (We_c) defined by Clanet & Lasheras (1999) for any Newtonian fluid, as illustrated in Equations (3.1-3.3)

$$We = \frac{\rho v_1^{\,2} D_1}{\sigma} \qquad \text{Equation (3.1)}$$

$$We_c = 4\frac{BO_o}{BO}\left[1 + kBO_o BO - \left(\left(1 + kBO_o BO\right)^2 - 1\right)^{0.5}\right]^2 \qquad \text{Equation (3.2)}$$

$$BO = \left[\frac{\rho g d^2}{2\sigma}\right]^{0.5} \qquad \text{Equation (3.3)}$$

where *We* is the dimensionless Weber number, which is the ratio between the inertia force and the surface tension force; (ρ) is the density of the liquid; (v_1) is the initial exit velocity from the nozzle, which will be defined in section 2.3.2; (D_1) is the initial water diameter exiting the hole; (σ) is the surface tension of liquid; (BO_o) is the Bond Number based on the outside diameter (the wetting diameter) of the nozzle; (*BO*) is the Bond Number based on the inside diameter of the nozzle; (*k*) is a constant which is equal to 0.37 for water injected in air; (*g*) is the acceleration due to gravity; and (*d*) is the hole diameter. Above We_c, the falling flow transits to the jetting regime.

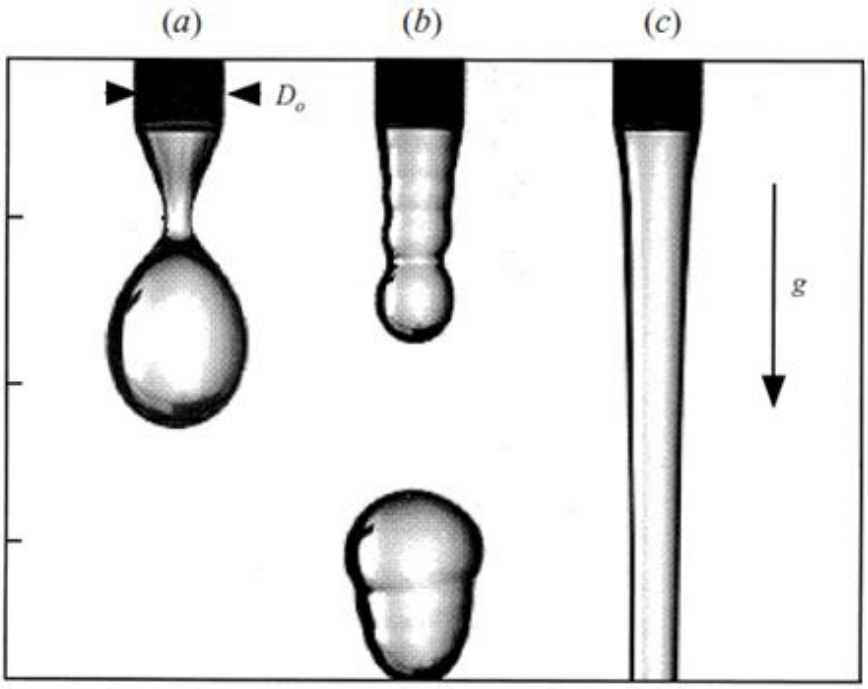

Figure 3.1 Free falling water regimes (a) Periodic dripping (b) Dripping faucet (c) Jetting (adopted from ((Clanet & Lasheras 1999)*)*

In the work of Clanet & Lasheras (1999), the model indicated in Equations (3.1-3.3) was verified using tubes which had a small thickness, allowing for the water exiting the tube to wet the tube thickness. This was the reason the model included the outside diameter (wetting diameter) and the inside diameter.

To model the water falling through holes in a tray aerator, Equations (3.1-3.3) are used with the assumption that the outside nozzle diameter is equal to the inside nozzle diameter and both are equal to the hole diameter. This research focuses on the jetting regime for the practical difficulties of achieving uniform dripping regime from all the holes of a tray. Furthermore, the jetting regime can be achieved using less number of holes, and consequently smaller tray area requirements.

To assure that the studied conditions include only the jetting regime, the model included a conditional loop that check *We* relative to the We_c, and adjusts the number of holes per tray to guarantee jetting conditions.

3.2.2. *Hydraulic Design*

The procedure for developing the hydraulic design equations is illustrated in Figure 3.3. For free falling water exiting from tray holes under gravitational forces, holes act as nozzles, and under steady state flow conditions, a thin water film of height (h) forms over the tray as illustrated in Figure 3.2. The initial exit velocity from the nozzle (v_1) can be estimated by knowing (h) using nozzle equation (Lienhard 1984; Scott et al. 1955) as illustrated in Equation (3.4)

$$v_1 = C_v\sqrt{2gh} \quad \text{.....Equation (3.4)}$$

where (C_v) is the coefficient of velocity through nozzles, and is assumed to be equal to 0.99 (Lienhard 1984); and (h) is the desired film height.

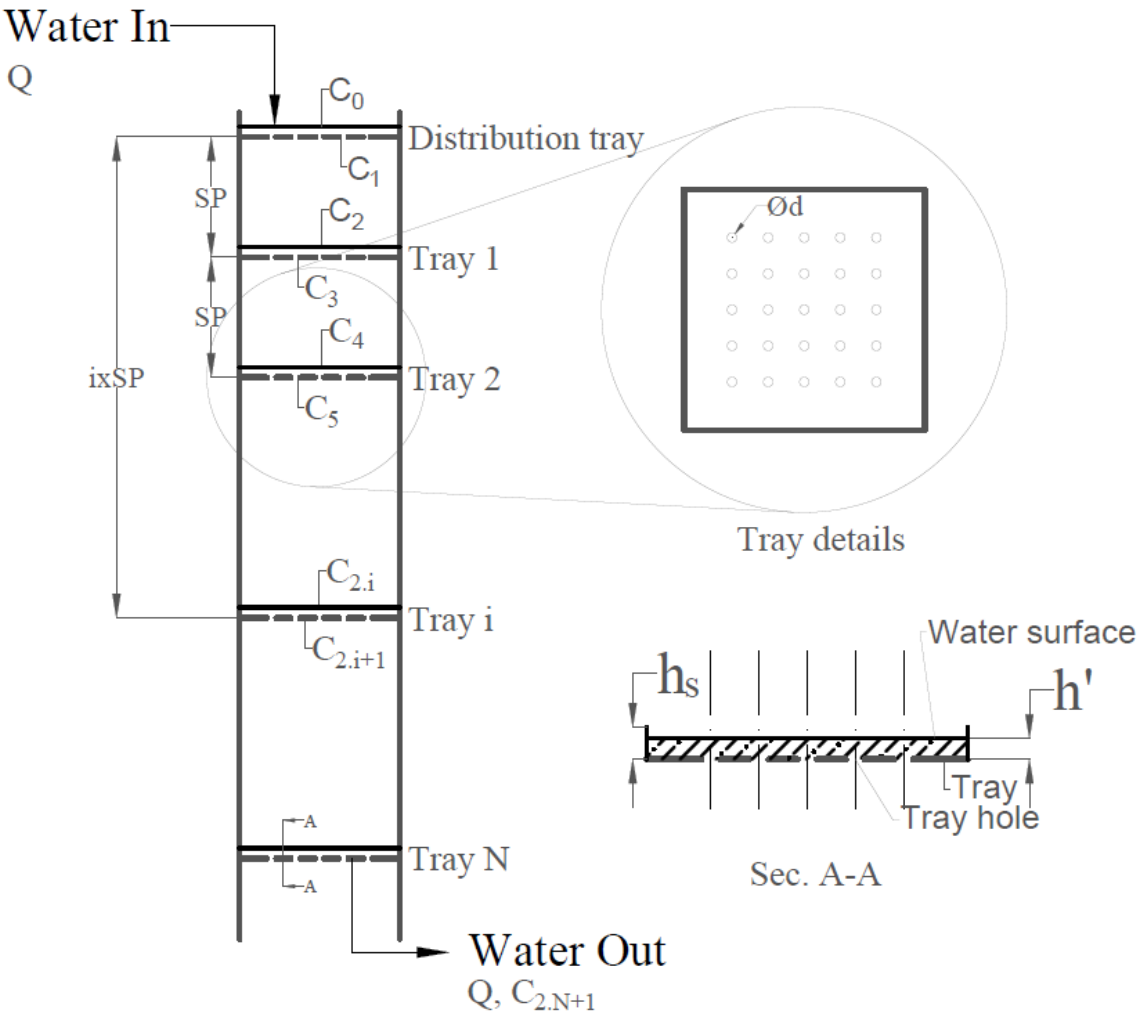

Figure 3.2 Schematic tray aerator setup

In the case of jetting regime, the water jet exiting the hole has an initial diameter (D_1) that is estimated as indicated in Equation (3.5), and the number of holes per tray needed to achieve a desired film height is estimated as indicated in Equation (3.6)

$$D_1 = d.\sqrt{\frac{C_d}{C_v}} \quad \text{.....Equation (3.5)}$$

$$n = \frac{Q}{\frac{\pi}{4} v_1 D_1^{\,2}} \quad \text{.....Equation (3.6)}$$

where (C_d) is the coefficient of discharge through nozzles, and is assumed to be equal to 0.6 (Lienhard 1984); (Q) is the total flow rate; and (n) is the number of holes per tray.

As the n should be an integer, the value obtained from Equation (3.6) is rounded to the nearest integer (n'), and then the initial water velocity (v_1'), and the film height (h') are recalculated as indicated in Equations (3.7-3.8)

$$v_1' = \frac{Q_{hole}}{A_j} = \frac{Q}{n' \frac{\pi}{4} D_1^{\,2}} \quad \text{.....Equation (3.7)}$$

$$h' = \frac{(v_1'/c_v)^2}{2g} \quad \text{.....Equation (3.8)}$$

where (v_1') is the corrected initial exit velocity from the nozzle; (Q_{hole}) is the flow rate per hole; (A_j) is the cross section area of the water jet; (n') is the corrected number of holes per tray; and (h') is the corrected film height.

In order to avoid overflow of water from the tray sides, if the corrected film height h' exceeds the tray side height (h_s) the corrected number of holes is increased by one hole until h' is less than h_s. The iterations for n', v_1' and h' continue till all conditions are satisfied, however the final film height shall differ from the desired film height.

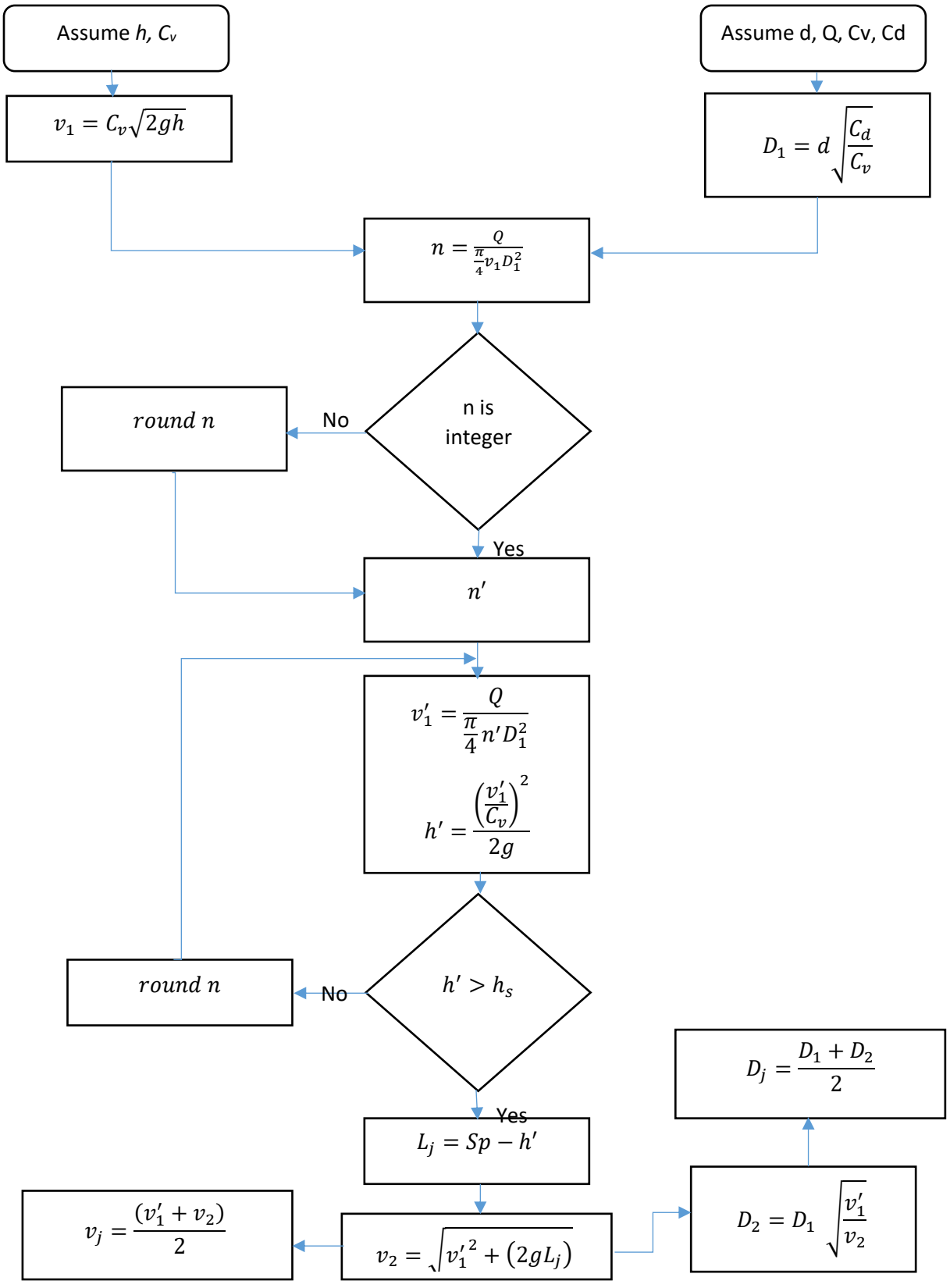

Figure 3.3 Flowchart of hydraulic design

The jet velocity increases as the water travels downwards due to the gravitational acceleration, resulting in a decrease in the jet diameter to satisfy the continuity equation. The parameters characterizing the water jet are calculated as indicated in Equations (3.9-3.13)

$$L_j = SP - h' \quad \text{Equation (3.9)}$$

$$v_2 = \sqrt{(v_1')^2 + (2gL_j)} \quad \text{Equation (3.10)}$$

$$D_2 = D_1\sqrt{\frac{v_1'}{v_2}} \quad \text{Equation (3.11)}$$

$$D_j = \frac{D_1 + D_2}{2} \quad \text{Equation (3.12)}$$

$$v_j = \frac{v_1' + v_2}{2} \quad \text{Equation (3.13)}$$

where (L_j) is the jet length; (SP) is the spacing between trays; (v_2) is the jet velocity reaching the subsequent tray; (D_2) is the jet diameter reaching the subsequent tray; (D_j) is the mean jet diameter; and (v_j) is the mean jet velocity.

3.2.3. Mass Transfer

For the tray aerator system, Equation (2.3) can be manipulated and integrated across the limits of time from zero to t, and the concentration from the initial concentration (C_0) to the concentration at time t (C_t), to reach the form illustrated in Equation (3.14).

$$\ln\left(\frac{C_S - C_t}{C_S - C_0}\right) = -K_L a t \quad \text{Equation (3.14)}$$

For wastewater effluent from an anaerobic system, C_0 is generally equal to zero (El-Gendy et al. 2012; Tchobanoglous et al. 2004); hence, this parameter is uncontrollable in the design.

It appears in Equation (3.14) that rate of aeration is directly proportional to C_S, C_0, K_L, a, and t (Scott et al. 1955). Therefore, as the only controllable parameters in Equation (3.14) are a and t, they are the main design parameters, which shall be increased to achieve better aeration.

3.2.4. *Thin Film Aeration*

The thin film is modelled to be uniform over the tray area, and would have a volume equal to the tray area multiplied by the film height. Since the specific area is equal to the ratio between the interface area and the liquid volume, the thin film specific area (a_f) is calculated as illustrated in Equation (3.15)

$$a_f = \frac{A}{V_f} = \frac{A}{A.h'} = \frac{1}{h'} \quad \text{.....Equation (3.15)}$$

where (A) is the interface area of the thin film, which is equal to the tray area; (V_f) is the liquid volume over the tray, which is equal to the tray area multiplied by the film height (h').

For the aeration time, the time for water to be aerated while it travels from point C_0 to point C_1 indicated in Figure 3.2, which are at a distance h' apart can be estimated as indicated in Equation (3.16)

$$t_f = \frac{V_f}{Q} = \frac{Ah'}{Q} = \frac{h'}{HLR} \quad \text{.....Equation (3.16)}$$

where (t_f) is the thin film aeration time; and (HLR) is the hydraulic loading rate (the flow rate per unit area).

Using Equation (3.14), and substituting a, and t by Equation (3.15), and Equation (3.16) respectively, the DO of water at the exit from the tray indicated as C_1 in Figure 3.2 can be calculated as illustrated in Equation (3.17).

$$C_1 = C_S - (C_S - C_0)e^{-K_L * \frac{1}{h'} * \frac{h'}{HLR}} = C_S - (C_S - C_0)e^{\frac{-K_L}{HLR}} \quad \text{.....Equation (3.17)}$$

3.2.5. *Water Jet Aeration*

Using the same approach of estimating the specific area and aeration time for the thin film, the specific area of water jet is estimated as indicated in Equation (3.18). As indicated in Equation (3.12), the jet diameter decreases as the jet travels downwards, the jet will assume an inverted cone shape rather than a perfect cylinder. However; as a simplification of the calculations, the jet is

modelled as a cylinder having a diameter of *Dj*, travelling with a velocity of *vj*, and a length of L_j. The aeration time is estimated as indicated in Equation (3.19)

$$a_j = \frac{A_j}{V_j} = \frac{\pi D_j L_j}{\frac{\pi}{4} D_j{}^2 L_j} = \frac{4}{D_j}$$

.....Equation (3.18)

$$t_j = \frac{L_j}{v_j}$$

.....Equation (3.19)

where (a_j) is the specific area of the jet; (D_j) is the mean jet diameter; (V_j) is the volume of water within the jet; and (t_j) is the jet aeration time.

Equation (3.14) is used to calculate the *DO* reaching the aeration tray by substituting *a* by a_j from Equation (3.18), and *t* by t_j from Equation (3.19), as illustrated in Equation (3.20) where (C_1) and (C_2) are the *DO* concentration at the exit point from the distribution tray, and the point reaching the next aeration tray respectively as illustrated in Figure 3.2.

$$C_2 = C_S - (C_S - C_1)e^{-K_L . a_j . t_j}$$

.....Equation (3.20)

3.2.6. Overall Aeration Through a Single Tray

For the estimation of the overall aeration occurring over a single tray other than the distribution tray, Equation (3.17), and Equation (3.20) are combined to account for the two aeration regimes; namely the thin film above the tray and the water jetting from the tray, as illustrated in Equation (3.21).

$$C_2 = C_S - (C_S - C_0)e^{-K_L (\frac{1}{HLR} + a_j . t_j)}$$

.....Equation (3.21)

3.2.7. Number of Trays

Now considering the case where there is a number of (*N*) consecutive trays arranged beneath each other below the distribution tray, with a constant spacing between trays equal to (*SP*) as illustrated in Figure 3.2. The influent *DO* to the (i^{th}) tray is denoted as (C_{2i}), where (*i*)=1: *N* is the number of tray including the distribution tray. Water reaching the i^{th} tray experience *i-1* thin film above the

tray and *i-1* falling water regimes. Thus Equation (3.21) can be generalized to include the tray number as indicated in Equation (3.22)

$$C_{2(i-1)} = C_S - (C_S - C_0)e^{-K_L.(i-1).(\frac{1}{HLR}+a_j.t_j)} \quad \text{.....Equation (3.22)}$$

where ($C_{2(i-1)}$) is the influent *DO* to the (i-1^{th}) tray; and (i) is the number of tray including the distribution tray.

3.2.8. Model Assumptions

The current model is split into two parts. The first part studies the flow regime for water falling from trays. It investigates the threshold for achieving the jetting regime at various hole diameter and flow rate. The second part investigates the effect of different design parameters on the aeration performance for a tray aerator system that is operating in the jetting regime conditions.

To simplify solving the model equations, the following set of assumptions are made:

1- The flow is at steady state conditions

2- The trays are perfectly horizontal

3- All trays are square with a cross section area (*A)*.

4- All trays have the same number of holes and hole diameters, and are installed with constant spacing (*SP*) between each other

5- The maximum allowable height for the thin film (h_s) is 25×10^{-3} m, otherwise, the tray would overflow.

6- The velocity distribution is uniform along the cross section of jets and the thin film.

7- The value for oxygen mass transfer coefficient (K_L) between air and water is 5.5×10^{-5} m/sec (Liss & Slater 1974).

8- The coefficient of discharge through holes (C_d) is equal to 0.6 (Lienhard 1984), and the coefficient of velocity through holes (C_v) is equal to 0.99 (Lienhard 1984).

9- The inlet dissolved oxygen concentration (C_0) to the system is zero

3.2.9. Model Equations

Two function files are developed using MATLab R2013b (8.2.0.701); the first file aims at illustrating the threshold for the jetting regime, whereas the second file predicts the effluent *DO* from a tray aerator system that is installed at a distance (*SP*) above the water surface in the receiving tank. The receiving tank acts as the (*Nth*+1) tray. Both codes are based on the equations derived in the methodology section, and are included in Annex I for reference. The model was tested for the conditions indicated in Table 3.1.

Table 3.1 Values of mathematical model input parameters

Parameter	Unit of Measurement	Value
Flow rate *Q*	$x10^{-5}$ m^3/sec (m^3/day)	1.157(1), 1.736(1.5), 2.315(2), 2.894(2.5), 5.208(4.5)
Tray Area *A*	m^2	0.15x0.15, 0.2x0.2, 0.25x0.25
Number of trays *N*	Dimensionless	1, 2, 3, 4, 5, 6, 7, 8, 9, 10
film height *h*	$x10^{-3}$ m	2, 3, 5, 10, 15, 20
Diameter of hole *d*	$x10^{-3}$ m	3, 4, 5, 6
Overall System height *H*	m	1
Temperature	^oC	24
Oxygen mass transfer coefficient K_L	m/sec	5.5x10-5 (Liss & Slater 1974)

3.3. Results

3.3.1. Flow Regime

The first function file solves Equations (3.1-3.3) proposed by Clanet & Lasheras (1999) to get the maximum number of holes among which water is uniformly distributed in a tray before it transits from jetting to dripping for the set of tested diameters and flow rates. Results are illustrated in Figure 3.4 where the maximum number of holes, for jetting regime, increases with the increase in the total flow rate. Furthermore, the increase in the hole diameter results in a decrease in the maximum number of holes. The maximum number of holes is not affected by the tray area.

Figure 3.4 can be used as a design chart for any application involving falling water through holes or nozzles to define the threshold for the falling water regime, by using the design flow rate, and desired hole diameter.

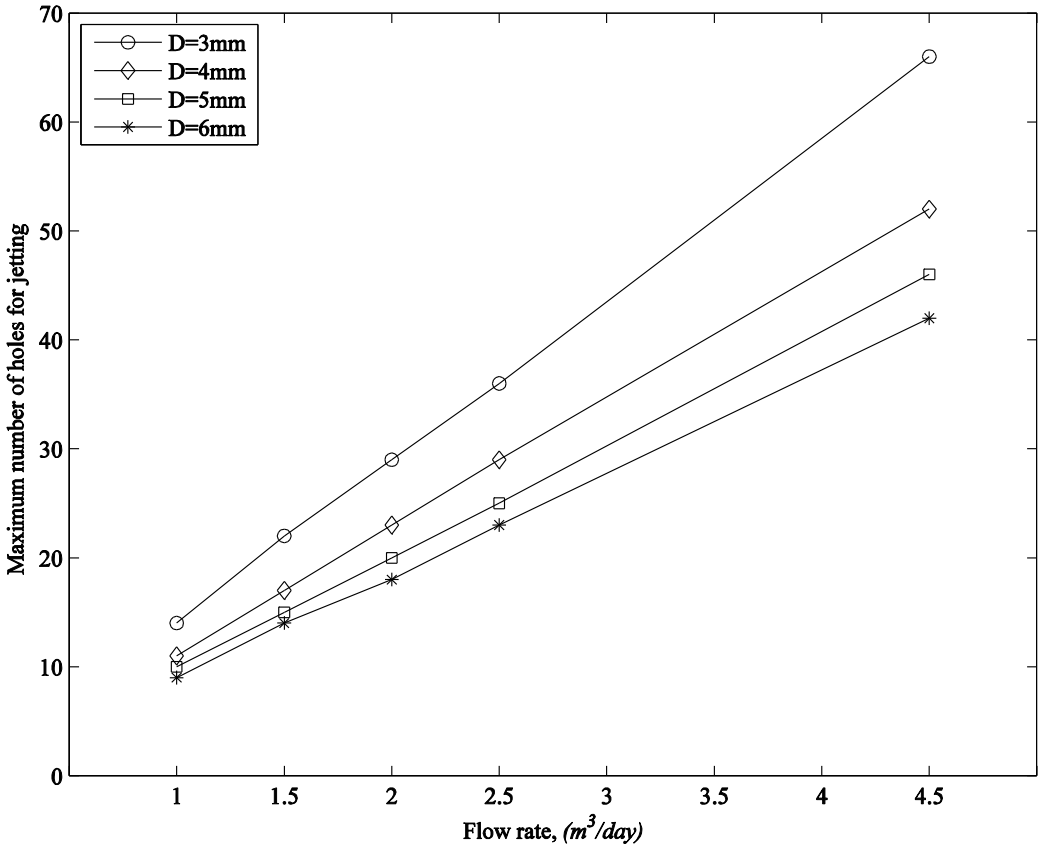

Figure 3.4 Maximum number of holes for jetting flow regime at different flow rates

3.3.2. Hydraulic Design

As illustrated earlier in the hydraulic design section, *n'* for each *d* was estimated using a loop that optimizes *h'* as close as possible to *h*. Table 3.2 shows *n'* and the corresponding *h'* for each of the tested diameters and flow rates. The data show that *n'* decreases with the increase in *d* for the same *Q* and *h*. It is worth noting that *h'* is not possible to equate *h* and is different among different diameters. The increase in *Q* leads to an increase in *n'*. Smaller *d* allows more possibilities of changing *n'*, resulting in higher flexibility in achieving different values of *h'*.

Table 3.2 Test conditions for fixing the jet area

Q x10^{-5} (m^3/sec)	h (mm)	d				d			
		3mm	4mm	5mm	6mm	3mm	4mm	5mm	6mm
		n’				h’ (mm)			
1.157	2	14	8	5	3	1.94	1.88	1.97	2.64
	3	11	6	4	3	3.14	3.34	3.07	2.64
	5	9	5	3	2	4.67	4.80	5.47	5.93
	10	6	3	2	1	10.54	13.34	12.30	23.72
	15	5	3	2	1	15.18	13.34	12.30	23.72
	20	4	3	2	1	23.72	13.34	12.30	23.72
1.736	2	21	12	8	6	1.94	1.88	1.73	1.48
	3	17	10	6	4	2.96	2.70	3.07	3.33
	5	13	7	4	3	5.05	5.51	6.92	5.93
	10	9	5	3	2	10.54	10.81	12.30	13.34
	15	8	5	3	2	13.34	10.81	12.30	13.34
	20	7	4	3	2	17.43	16.89	12.30	13.34
2.315	2	28	16	10	7	1.94	1.88	1.97	1.94
	3	22	12	8	6	3.14	3.34	3.07	2.64
	5	17	10	6	4	5.25	4.80	5.45	5.93
	10	12	7	4	3	10.54	9.80	12.30	10.54
	15	10	6	4	3	15.18	13.34	12.30	10.54
	20	9	5	3	2	18.74	19.22	21.86	23.72

Table 3.2 (continued) Test conditions for fixing the jet area

Q x10^{-5} (m^3/sec)	h (mm)	d				d			
		3mm	4mm	5mm	6mm	3mm	4mm	5mm	6mm
		n’				h’ (mm)			
2.894	2	34	19	12	8	2.05	2.08	2.13	2.32
	3	28	16	10	7	3.03	2.93	3.07	3.03
	5	22	12	8	6	4.90	5.21	4.80	4.12
	10	15	8	5	3	10.54	11.73	12.30	16.47
	15	13	7	4	3	14.03	15.32	19.21	16.47
	20	11	6	4	3	19.60	20.85	19.21	16.47
5.208	2	62	35	22	15	2.00	1.98	2.06	2.13
	3	51	29	19	13	2.95	2.89	2.76	2.84
	5	39	22	14	10	5.05	5.02	5.08	4.80
	10	28	16	10	7	9.80	9.5	9.96	9.80
	15	23	13	8	6	14.53	14.39	15.57	13.34
	20	20	11	7	5	19.21	20.10	20.33	19.21

3.3.3. Performance of Tray Aerator

The aeration model was run to investigate the effect of the change in *Q*, *A*, *N*, *n*, *d*, and *SP* on the water aeration performance over the tray aerator. Results are shown in the following sections.

3.3.4. Effect of Changing the Hole Diameter and Number of Holes

Typical results in Figure 3.5 illustrate the influent *DO* to the second tray from a single aeration tray system versus the change in the hole diameter and number of hole as per the values illustrated in Table 3.2. Presented results are for a flow rate of 1.0 m^3/day of water having initial *DO* of zero, and the trays placed at spacing of 0.2 m, with a tray area of 0.2x0.2 m^2. The *DO* influent to the second tray appears to decrease with the increase in both *n’* and *d*. However, the magnitude of that

change in *DO* is not significant among the tested conditions of *n'* or *d*. The values of *n'* and *d* are important in defining the free falling flow regime.

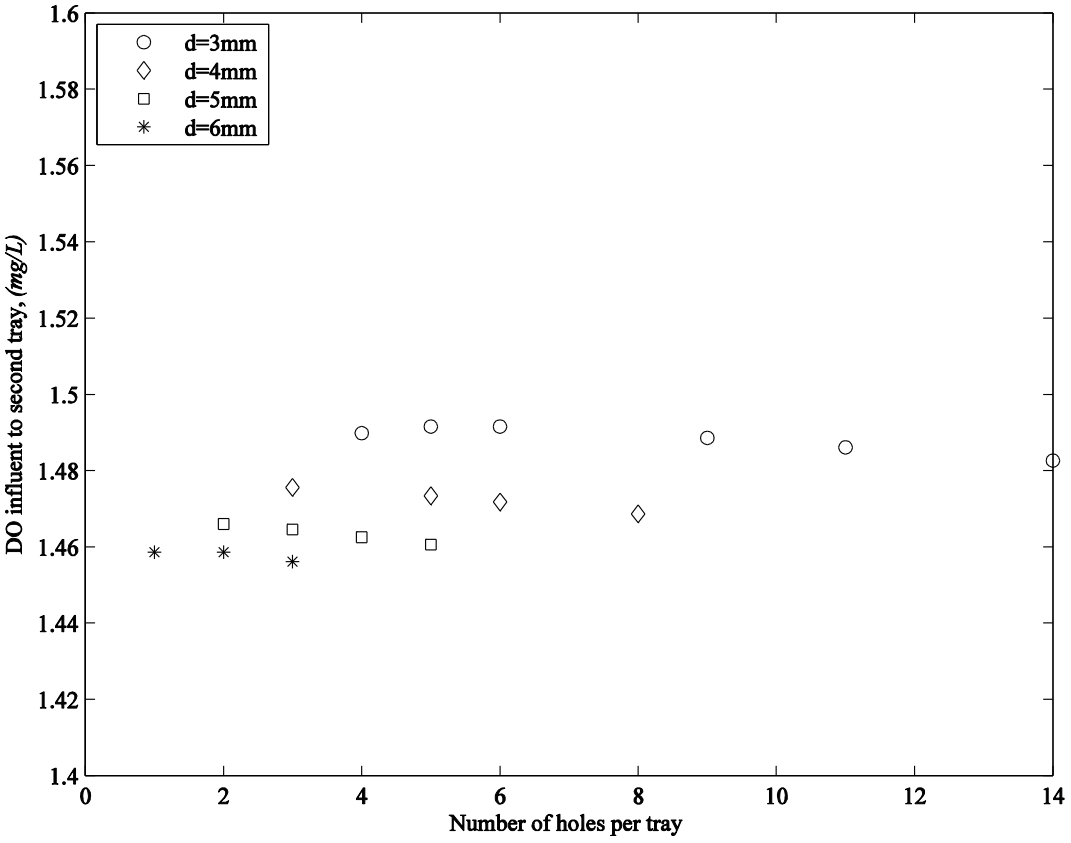

Figure 3.5 Typical change in DO resulting from changing the number of holes per tray and diameter of holes. Results are for a single tray at Q = 1.157 m³/sec of water, DO_0= zero, SP = 0.2 m, A=0.2x0.2 m²

3.3.5. Effect of Changing the Spacing Between Trays

Through running the model while varying the tray spacing, it is illustrated in Figure 3.6 that the aeration through a single tray increases with the increase in the spacing between trays. This increase is postulated to be mainly due to the increase in the jet length, which leads to more aeration time over the water jets. On the other side, with the increase of the jet length, the volume of water jet increases, resulting in a decrease in the a_j as the jet area is constant. Regarding the sensitivity of the *DO* to the change of *SP*, it can be concluded that the change in *SP* has limited impact on the *DO*.

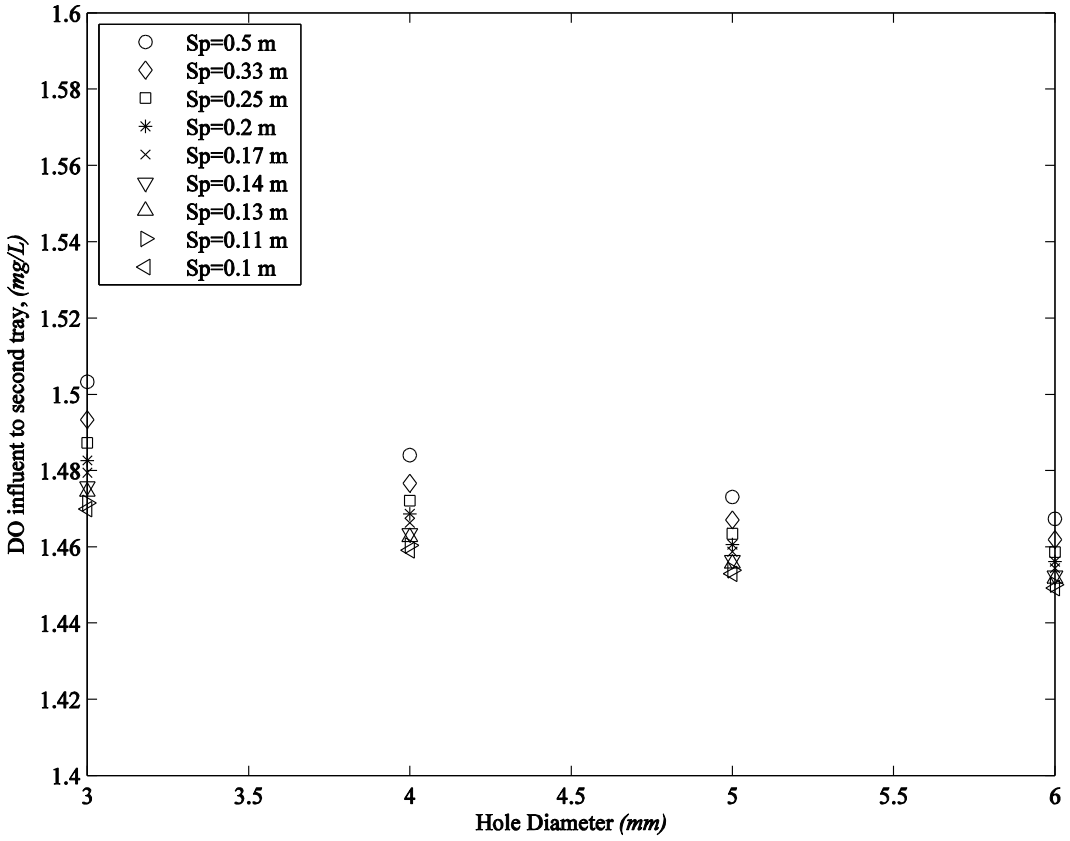

Figure 3.6 Typical change in DO resulting from changing the spacing between trays and diameter of holes. Results are for a single tray at Q = 1.157 m^3/sec of water, DO_0= zero, h = 2 mm, A=0.2x0.2 m^2.

3.3.6. Effect of Increasing the Number of Trays

In the design of tray aerators, the available height for the installation acts as a constraint on the maximum number of trays that can be installed. Thus, Figure 3.7 illustrates a typical change in the *DO* resulting from the simultaneous change in the number of trays and tray spacing to adopt the system for an overall height of 1m, where the overall height is calculated as illustrated in Equation (3.23)

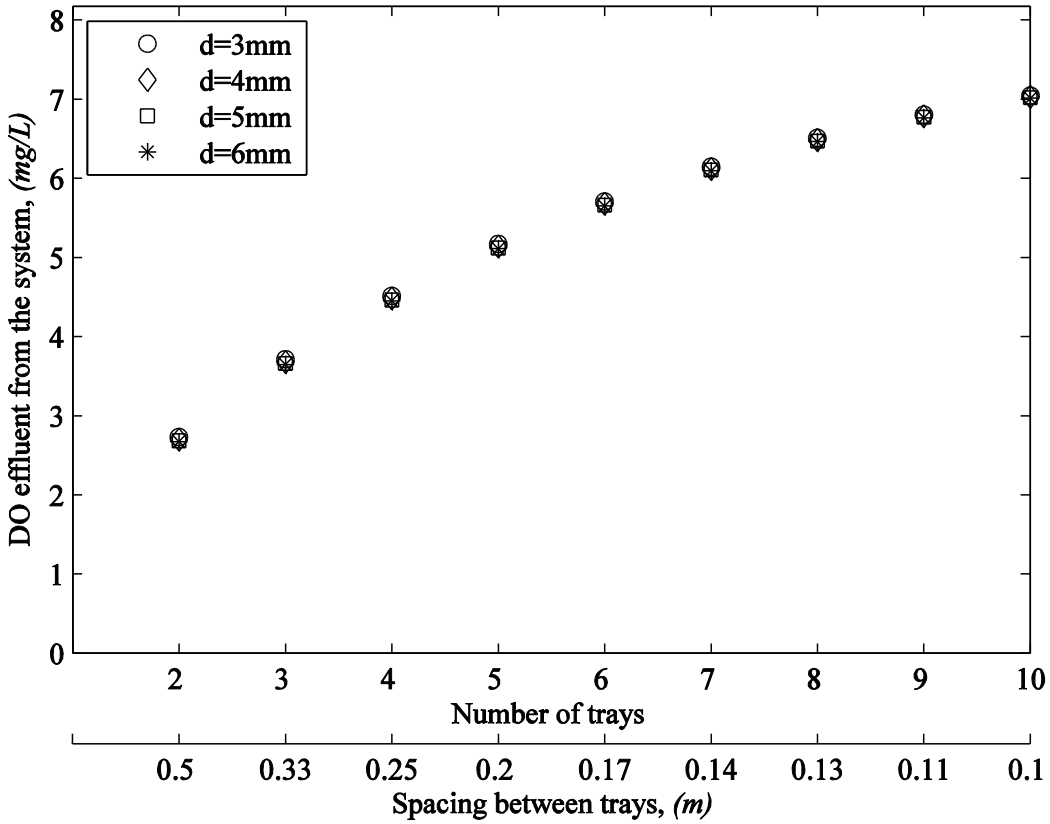

Figure 3.7 Typical change in DO from the system resulting in change in tray spacing and number of trays at different hole diameters. Results are for Q = 1.157 m^3/sec of water, DO_0= zero, SP = 0.2 m, A=0.2x0.2 m^2

$$H = SP * N \quad \text{.....Equation (3.23)}$$

Where (H) is the overall system height. It appears from Figure 3.7 that the increase in the number of trays highly increases the *DO*. This is due to the formation of more thin films, which increases the aeration.

3.3.7. Effect of Changing the Tray Area and Flow Rate

Increasing A results in a decrease in the *HLR*, and thus an increase in $a_f t_f$ for the thin film, which is reflected in higher *DO*. The effect of increasing A is illustrated in Figure 3.8, in which the increase in A results in offsetting the curve towards higher *DO*. Figure 3.8 also illustrates that the increase in Q for the same A results in a decrease in the *DO*. This decrease results mainly from the increase in the *HLR*.

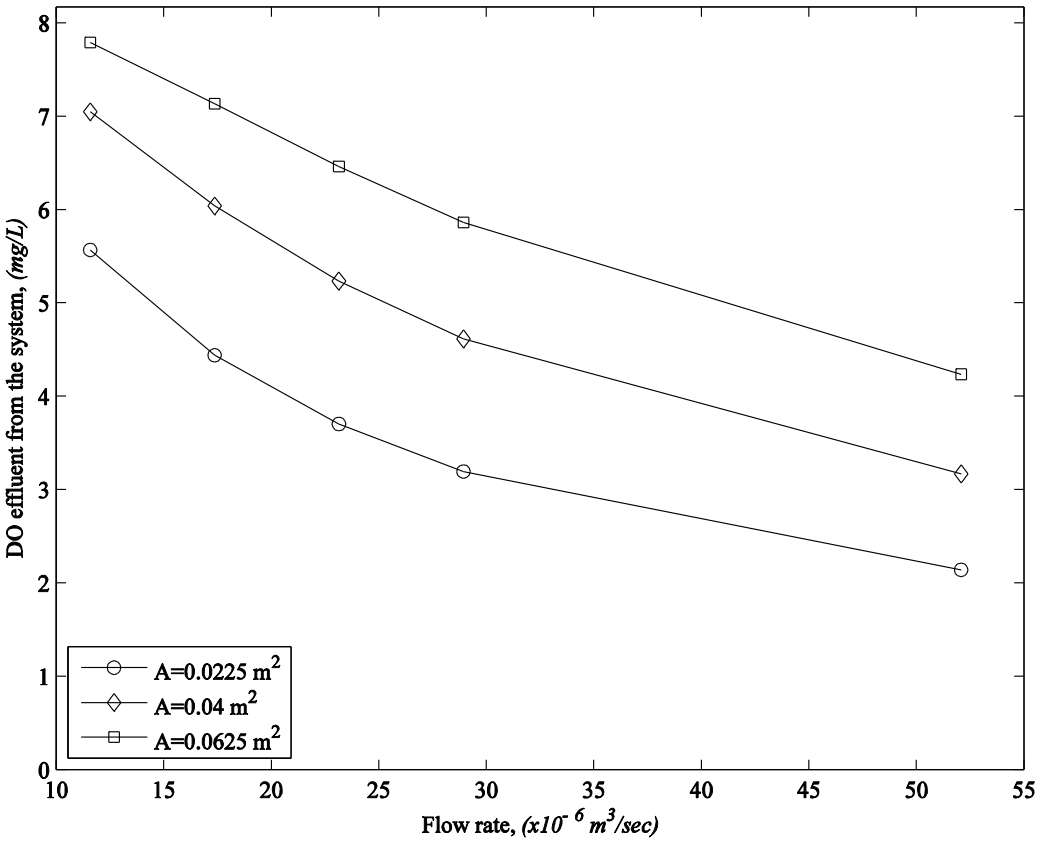

Figure 3.8 Typical change in DO from the system resulting from change in flow rate and tray area. Results are for N=10 trays, DO_0= zero, SP = 0.1 m, h = 2 mm, A=0.2x0.2 m^2

3.4. Discussion

The first part of the analysis illustrates different flow regimes that can be achieved for the water falling from trays; most commonly dripping and jetting regimes. Even though the dripping regime is thought to have higher mass transfer than the jetting regime for the larger specific area of drops over jets, it is difficult to achieve dripping regime with uniform water distribution among tray holes. Moreover, jetting regime can be achieved using less number of holes per tray, resulting in smaller area requirements. Hence the analysis deals only with the jetting regime. The threshold for achieving the jetting regime is dependent on the hole diameter, number of holes and the flow rate as per Equations (3.1-3.3) proposed by Clanet and Lasheras (1999). Their equation was applied to the water setup from tray aerators, and design charts were obtained for any application involving

falling water through holes or nozzles to define the threshold for the falling water regime, by using the design flow rate, and desired hole diameter.

The second part of the study analyzed the hydraulic design of the tray aerators and the parameters that might affect the aeration performance of tray aerators. The analysis addressed the estimation of *a*, and *t* which are the design parameters for Equation (2.3). Those two parameters are dependent on the *d*, *Q*, *N*, *n*, *SP*, and *A*. The impact of each parameter on the effluent *DO* was investigated separately.

Changing *d* defines the flow regime into jetting or dripping, with minor effect on the effluent *DO*. This slight impact of *d* on the *DO* is seen from Equation (3.18), where the value of a_j is inversely proportional with D_j, which is a function of *d*, *SP*, *Q*, and *n*. However, in order to limit the flow regime to the jetting regime for a given *Q*, *n* changed accordingly to assure that *We* is greater that We_c to satisfy Equation *(3.1-3.3),* mitigating the impact of changing *d*. Changing *Q* is inversely proportional with the *DO*, and as a result has *a* high impact on its value., and is inversely proportional. Increasing *Q* results in an increase in *HLR*, which in turn results in a decrease in t_f *as* illustration in Equation (3.16). Similarly, increasing *A* results in an increase in *DO* due to the decrease in *HLR*. The *DO* increased slightly with the increase in *SP*, which was interpreted to be due to the increase in L_j (Equation (3.10)), which led to the increase in v_2 and v_j, and a decrease in D_2 and D_j according to Equation (3.11-3.14). As a result, a_j decreased (Equation (3.18)) and t_j increased (Equation (3.19)) resulting in higher mass of oxygen diffusing into the falling water. Increasing *N* results in an increase in the number of thin films and water jets within the tray aerator system, leading to an increase in *DO*. The exponential trend of increase in *DO* with the increase in *N* (Figure 3.6) is the result of approaching the saturation level for *DO*.

These results when compared to the results achieved by La Motta for CO_2 stripping (La Motta 1995; La Motta & Chinthakuntla 1996) appeared to be comparable. The empirical equation derived by La Motta (1995) revealed that the effluent concentration is proportional to the tray spacing, number of trays and the hydraulic loading rate, while the updated formula indicated by La Motta and Chinthakuntla (1996) shows that the effluent concentration is proportional to the tray spacing, hydraulic loading rate, temperature , number of trays and initial water quality parameters.

3.5. Conclusion

This phase investigates analytically the design parameters of passive aeration technique. This technique is suitable as an intermediate stage after anaerobic treatment to enhance the performance of the subsequent aerobic unit. A key benefit from tray aerators lies in the fact that they do not require energy input for aeration in its operation, and hence sustains the natural resources and is suitable for installation in rural areas.

The design equations for the tray aerator are introduced in this chapter, and were tested mathematically to evaluate the sensitivity of the performance to the change in the design parameters. Based on the current work, the aeration performance of the system for water falling under jetting flow regime is mainly controlled by the thin film aeration, which is controlled by the hydraulic loading rate. The number of holes, and hole diameters controls the flow regime to fall within the jetting or dripping regime. They further control the height of the thin film to assure that no overflow would occur from the tray sides.

From the limitations of the developed model is the value of C_d, which was assumed to be equal to 0.6 (Lienhard 1984). Several formulae were developed in published work for C_d. Jan et al. (2010) presented an empirical formula for C_d from a bottom orifice of a conical hopper, where they found that C_d is inversely proportional to the ratio between the water head to the hopper diameter, and the ratio between the orifice diameter to the hopper diameter. Their results could not be adopted in the current research as the range of validity for their results is for a minimum diameter of 11 mm, and a minimum water head of 300mm, which is much larger than the range of application for tray aerators. Swamee & Swamee (2010) developed another explicit equation for C_d as a function of the kinematic viscosity, orifice diameter, and water head. That explicit equation was missing the units for each parameter; thus could not be utilized to verify C_d values.

Achieved results need to be followed by experimental work to introduce correction factors to verify the equation results.

4. Phase II – Laboratory Study

4.1. Introduction

Experiments are considered as a powerful modelling technique. They are utilized by researchers in almost all fields of inquiry to answer a question of interest regarding the response of a system to a set of varying parameters or input parameters (Montgomery 2001). In the current research, a set of experiments are conducted to test the aeration performance (the response) of tray aerators as a result of varying the input parameters, which are the hole diameter, the number of holes per tray, the spacing between trays, the water flow rate, and the spacing between trays.

Experimental work differs from the mathematical modelling in that the mathematical modelling deals with the solution of mathematical equations to predict an expression for the response of the system, whereas the experimental work observes the response of the system to the change in the input parameters. The main purpose of splitting the current work into mathematical model and experimental model is to develop the design equation in the mathematical model, which are then verified using the experimental model.

In this chapter, a tray aerator module is designed and built at the Environmental Laboratory of the American University in Cairo. That module is tested using deoxygenated water. The literature review section shows the previous studies on the aeration technologies. It also discusses the methods used in preparing deoxygenated water. The methodology describes the procedure and material used to prepare the deoxygenated water, as well to examine the tray aerator system. The results section shows the output charts from the model under different test conditions, as well as the impact of changing each input parameter on the response of the aeration performance. The discussion section draws a contrast for the experimental results with the mathematical model.

4.2. Material and Methods

In the current research, laboratory experimental runs were conducted to test the aeration performance of tray aerators under different operating conditions. All the laboratory experiments were designed and conducted in the Environmental Engineering Laboratories of the American University in Cairo. The laboratory experimental work was divided into three subsequent steps; preparing deoxygenated water, arrange the laboratory setup, and conducting the experiments as illustrated in Figure 4.1

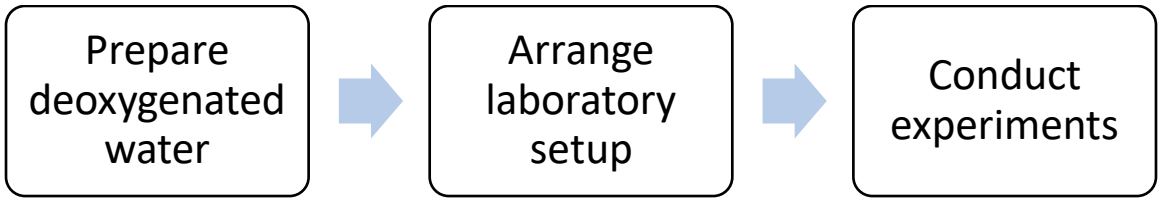

Figure 4.1 Phases of laboratory modelling

4.2.1. Preparing Deoxygenated (Synthetic) Water

4.2.1.1. Methods of Preparing Deoxygenated Water

Preparing deoxygenated water is common practice in conducting experiments that study the water mass transfer, and aeration performance. The procedure recommended by the ASCE for measurement of Oxygen Transfer in Clean water involves the deoxygenation of tap water using Sodium Sulfite (Na_2SO_3) to deoxygenate the water followed by re-oxygenation to near saturation level. The volumetric mass transfer coefficient is then obtained through recording and analyzing the *DO* values at different time intervals during the re-oxygenation duration (ASCE 2007).

Published works show the possibility of preparing deoxygenated water either through nitrogen bubbling, or by adding Na_2SO_3 with a catalyst (Garcia-Ochoa & Gomez 2009; Özbek & Gayik 2001; Liu et al. 1972). In the gassing out method, nitrogen is bubbled through the water to strip out the *DO*, whereas in the Na_2SO_3 method, Na_2SO_3 reacts with the oxygen in the presence of a cobalt or copper cation to form Na_2SO_4. Both nitrogen bubbling method and Na_2SO_3 method produce comparable results in terms of achieving completely deoxygenated water as well as in the values of oxygen mass transfer coefficient (Ghaly & Kok 1988).

The theoretical concentration of Na_2SO_3 required to deoxygenate 1 mg/L of the *DO* is around 7.88 mg/L of Na_2SO_3 (ASCE 2007); however, an excess to that theoretical concentration is usually added in experiments. Ghaly & Kok (1988) used Na_2SO_3 equivalent to double the theoretical dose, with cobalt chloride ($CoCl_2$) with a concentration of 0.2mg/L, to study the oxygen mass transfer coefficient. Adding Na_2SO_3 at a concentration of 14 mg/L for each mg/L of *DO*, which is equivalent to an excess of about 77% from the theoretical dose, with $CoCl_2$ as a catalyst at concentration less than 0.5mg/L to fresh tap water results in zero *DO* water (Hsieh et al. 1993). In their experiment, Hsieh, Ro and Stenstrom mentioned that the common practice in preparing

deoxygenated water for laboratory work relies on an excess of 50% to 100% from the theoretical Na_2SO_3 dose to reach complete deoxygenation. This excess dose was further explained to account for the time needed by the system to uniformly distribute the Na_2SO_3 dose (Wójtowicz & Szlachta 2013). ASCE guideline (ASCE 2007) indicate that the Na_2SO_3 excess dose could vary from 20% to 250% of the theoretical dose, depending on the transfer rate system, with the low range for the low rate systems, and the high range for the high rate systems.

The second method, gassing out, is conducted by passing pure nitrogen gas (oxygen free) through water leading to oxygen stripping. (Liu et al. 1972). (Özbek & Gayik 2001) introduced nitrogen at a rate of 0.6L/min into 1L of distilled water for 30 minutes in order to reduce the water DO. (Schladow et al. 2002; Lee 2002) used pure nitrogen bubbling for 6 hours through the water tank to purge the oxygen from the water.

The tray aerators studied in this research are intended to aerate oxygen deficit wastewater. For the laboratory work to mimic the operating conditions of the tray aerators, deoxygenated water was needed. The method of adding Na_2SO_3 with $CoCl_2$ as a catalyst was selected to prepare the deoxygenated water for its simplicity and the availability of the chemicals in the local market. Furthermore, the gassing out method required long lead time reaching up to 6 hours as per the studies of (Schladow et al. 2002) and (Lee 2002) which was not practical for the number of experimental runs.

Laboratory experiments were conducted in duplicates to estimate the optimum dose of Na_2SO_3. For each experiment, *DO* values were recorded each 30 second, for a total duration of 1 hour. The procedure involved the preparation of stock solution of Na_2SO_3 and $CoCl_2$, then testing the different doses of Na_2SO_3 in order to verify the suitable concentration that will be used in testing the tray aerator system.

4.2.1.2. Preparing Sodium Sulfite Stock Solution

Na_2SO_3 with 20g/L concentration stock solution is prepared through adding 5g of Na_2SO_3 to 250ml of distilled deionized water as per the following procedure.

Weight 5 g of Na_2SO_3 over an aluminum sheet using an Analytical balance KERN ALS 220-4 (Readability (d) 0.1mg, Linearity ±0.2mg), then pour the weighed Na_2SO_3 into a glass beaker, and

use a washing bottle filled with distilled deionized water to wash out any Na_2SO_3 sticking to the aluminum sheet to the beaker. Then distilled deionized water is added to the beaker to completely cover the powder. The solution is poured into a 250ml volumetric flask. The beaker is then washed several times using the washing bottle and the solution is poured to the volumetric flask to assure that all the 5g are contained within the flask. The solution in the flask is completed to the 250ml level. A magnet is placed into the flask, then the flask is closed with a stopper and put on a magnetic stirrer set to rotate on gentle speed for 30 minutes to mix the Na_2SO_3 in the water.

4.2.1.3. Preparing Cobalt Chloride Stock Solution

$CoCl_2$ with 1g/L concentration stock solution is prepared through adding 0.25g of $CoCl_2$ to 250ml of distilled deionized water as per the following procedure.

Weight 0.25g of $CoCl_2$ over an aluminum sheet using an Analytical balance KERN ALS 220-4 (Readability (d) 0.1mg, Linearity ±0.2mg), then pour the weighed $CoCl_2$ into a glass beaker, and use a washing bottle filled with distilled deionized water to wash out any $CoCl_2$ sticking to the aluminum sheet to the beaker. Then distilled deionized water is added to the beaker to completely cover the powder. The solution is poured into a 250ml volumetric flask. The beaker is then washed several times using the washing bottle and the solution is poured to the volumetric flask to assure that all the 0.25g are contained within the flask. The solution in the flask is completed to the 250ml level. A magnet is placed into the flask, then the flask is closed with a stopper and put on a magnetic stirrer set to rotate on gentle speed for 30 minutes to mix the $CoCl_2$ in the water.

4.2.1.4. Testing the Optimum Dose

In running the experiment, different concentrations from Na_2SO_3 are tested. The reaction of Na_2SO_3 with the *DO* is governed by Equation (4.1)

$$Na_2SO_3 + 0.5O_2 \xrightarrow{CoCl_2} Na_2SO_4 \quad \text{.....Equation (4.1)}$$

Where the molecular weight of Na_2SO_3 is 126.042 g/mol; ($0.5O_2$) is oxygen atom, which has a molecular weight of 16 g/mol; and (Na_2SO_4) is sodium sulfate, which has a molecular weight of

142.042 g/mol. From stoichiometry, to reduce the *DO* by 1mg/L, it is required to add 126.042/16 mg/L of Na_2SO_3 (approximately 7.9mg/L).

$CoCl_2$ is to be added as a catalyst at a concentration of 0.2mg/L (Ghaly & Kok 1988).

- Required tools are:
    - Stock solution 1g/L $CoCl_2$
    - Stock solution 20g/L Na_2SO_3
    - Glass beaker 500ml
    - HACH HQd30 meter equipped with *DO* measurement probe (LDO101)
    - 1000microliter micropipette
- Procedure:
    - Calibrate the *DO* meter using the manufacturer's recommended procedure
    - Fill a specified volume of tap water, and pour to the beaker, record the water height in the beaker.
    - Measure the *DO* in the used water
    - Set the *DO* meter for interval measurements according to the desired time step and duration, start the measurement to record the *DO*, and duration.
    - Add the desired concentration of $CoCl_2$ from the stock solution according to Equation (4.2)

$$V(microliter) = 250ml * \frac{0.2\frac{mg}{L}}{1\frac{mg}{L}} \quad \text{.....Equation (4.2)}$$

    - Add the desired concentration of Na_2SO_3 from the stock solution according to Equation (4.3)

$$V(microliter) = 250ml * \frac{7.9\frac{mg}{L} * DO(initial)\frac{mg}{L}}{20\frac{mg}{L}} * \%required \quad \text{.....Equation (4.3)}$$

    - Keep the measurement running for at least one hour to reach steady increase in DO.

- Repeat the above steps according to the test conditions illustrated in Table 4.1

Table 4.1 Test conditions for Na_2SO_3 Optimization runs

Parameter	**Unit of Measurement**	**Test range**
Excess Na_2SO_3	%	50, 75, 100
Water volume	mL	200, 250, 300

4.2.2. Experimental Setup

A laboratory scale tray aerator setup was designed and fabricated at the Environmental Lab. The setup is illustrated in Figure 4.2, and is composed of four threaded steel rods each of 8mm diameter and 1 m length. The four rods are fixed on steel supports using hexagonal nuts to hold the rods vertically and at 1 m above the ground. Trays are made from polycarbonate sheets of 0.2m length, and 0.2m width, having holes drilled according to the desired number of holes and hole diameter. Figure 4.3 illustrates the tray manufacturing with the locations of the holes for an 8-hole tray. The polycarbonate sheets are fixed on rectangular frames using antibacterial silicone. The rectangular frames are fabricated from steel angles of 0.3mX0.3m legs as illustrated in Figure 4.4, and detailed in Figure 4.5. Each rectangular frame with the polycarbonate sheet resemble a single tray which is installed through the threaded rods and fixed in the desired position using hexagonal nuts. The spacing between trays is adjusted through tightening or losing the nuts, and the trays horizontality is adopted by spirit level and fine tuning of the nut location. In installing the polycarbonate sheets over the rectangular frames, the sheets are rotated to assure that the holes from subsequent trays will not fall above each other. This allows for more residence time for the water over the trays, and potentially provides higher aeration.

A plastic cylindrical bucket of 45 L capacity is used as the test water tank. A 1” hole is drilled at the center of the bucket base, and 1” pipe is fitted through that hole. The pipe was connected to a 90-degree elbow followed by another pipe, a water valve, and a centrifugal radial pump. The pump had an operating discharge of 2L/min, at a head of 1m. The centrifugal pump delivered the test water to the top of the tray aerator setup through flexible 1/8” pipe. The electrical connection of

the pump is fitted with a variable frequency switch to adjust the discharge flow through reducing the rotating speed of the pump motor. A second pump is used in the experiment, which is a submersible pump. The submersible pump is used to circulate the water in the feed bucket to assure the uniform distribution of the Na_2SO_3 and $CoCl_2$ solutions among the test water until the water *DO* starts to increase, and is then switched off to avoid any eddies in the water.

Na_2SO_3 solution was prepared using pure Na_2SO_3 powder. The concentration of Na_2SO_3 in the solution was calculated with an excess of 30% to completely deoxygenate the *DO* from the test water according to Equation (4.4).

$$Dose\ (g) = test\ water\ volume * \frac{7.9\frac{mg}{L} * DO(initial)\frac{mg}{L}}{1000\frac{mg}{g}} * 130\% \quad \text{.....Equation (4.4)}$$

The procedure of preparing the solution is by getting a 1L capacity flask, and put a magnet inside it, then 1L of water from the feed bucket is withdrawn to the flask, then weighing the dose of Na_2SO_3 on an aluminum sheet using KERN ALS 220-4 analytical balance. Na_2SO_3 dose is then added to the water flask, and the flask top is sealed with parafilm.

The flask is then put on a magnetic stirrer and left under gentle mixing speed for 15 minutes for the Na_2SO_3 to be completely dissolved in the water. Then the parafilm is removed from the flask and the solution is poured to the feed bucket.

$CoCl_2$ stock solution of 1g/L concentration is prepared using the same procedure indicated in the previous section, a specified volume from the $CoCl_2$ stock solution was added to the test water to have a concentration of 0.2mg/L $CoCl_2$ in the test water.

Number	Description
1	Feed Bucket
2	Feed pump
3	Threaded rods
4	Steel frames
5	Polycarbonate sheet
6	Feed pipe

Figure 4.2 Experimental Setup

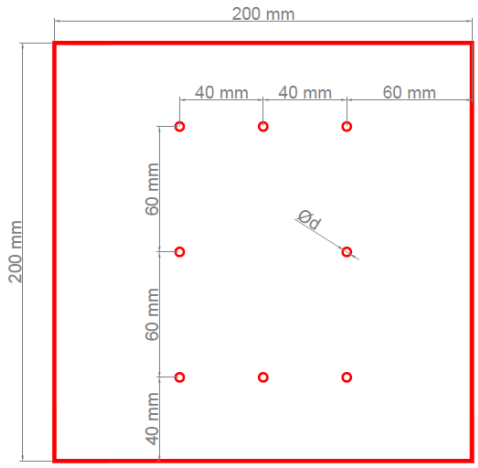

Figure 4.3 Holes location on tray

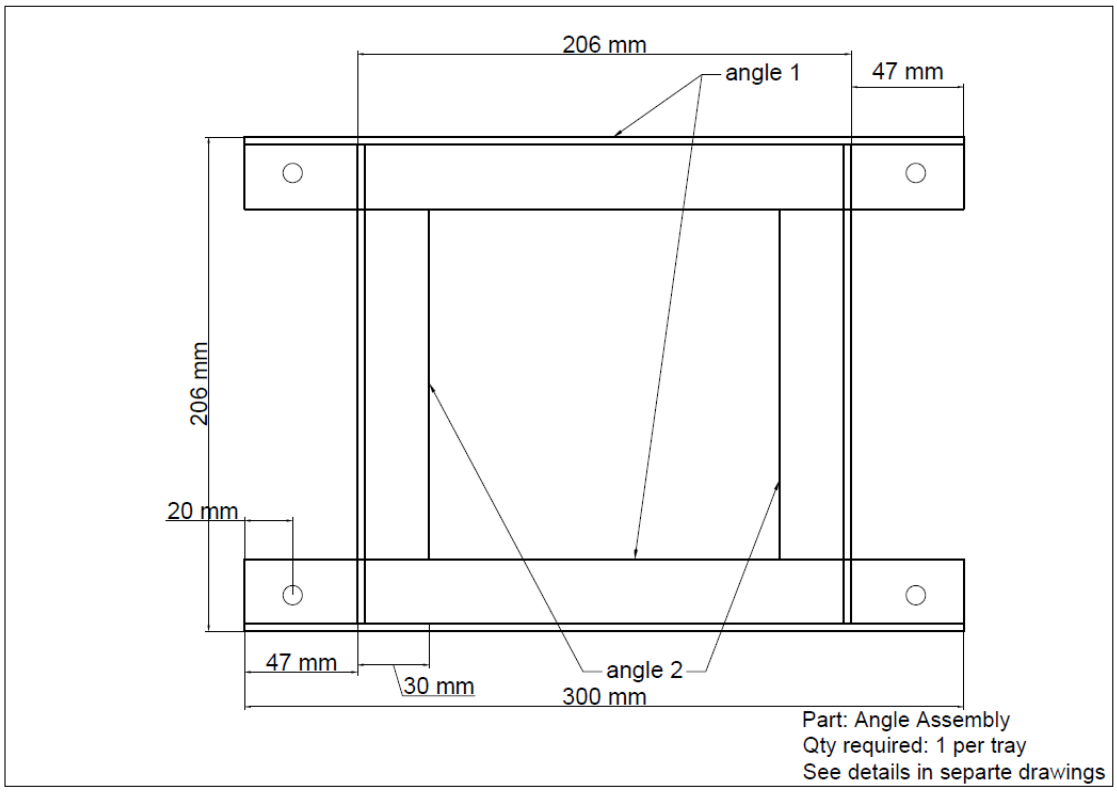

Figure 4.4 Tray frame assembly

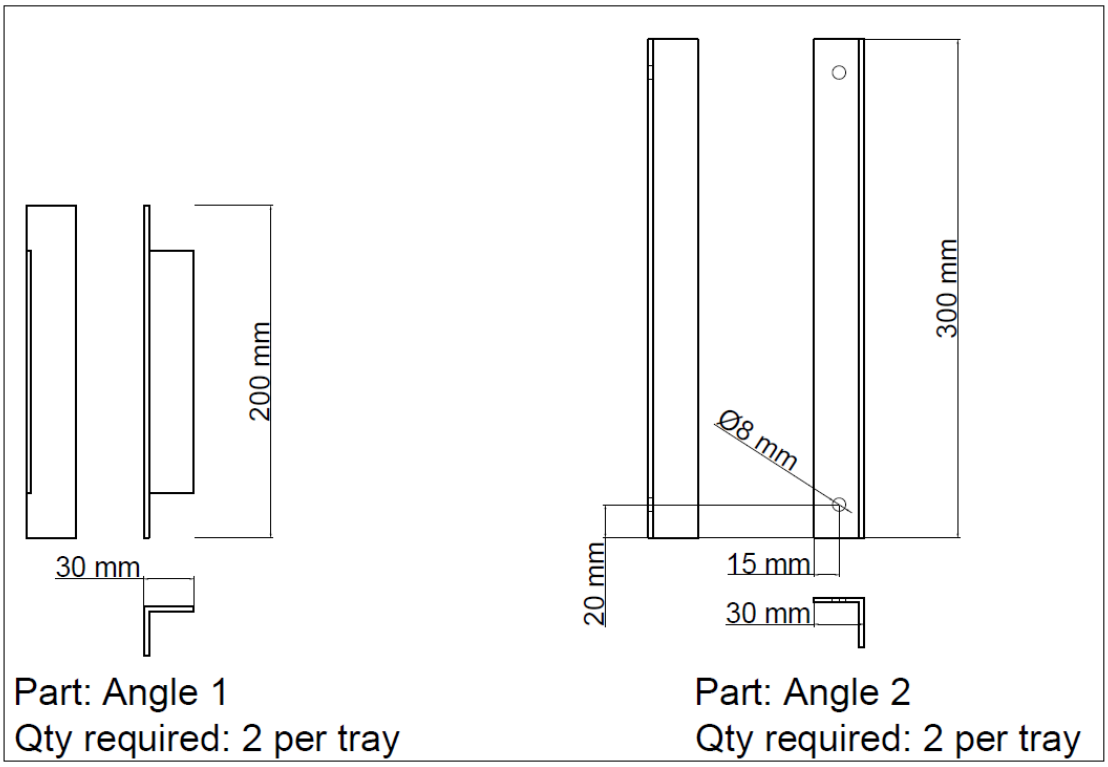

Figure 4.5 Tray frame – Angles Details

4.2.3. Experimental Procedure

- Fill the feed bucket with tap water up to 30 L
- Measure the initial *DO* in the water using HACH HQd30 meter equipped with *DO* measurement probe (LDO101).
- Prepare the Na_2SO_3 solution as indicated earlier
- Add $CoCl_2$ to the test water from the $CoCl_2$ stock solution (1g/L concentration) using 100-1000 microliter micropipette to achieve a concentration of 0.2mg/L in the test water
- Add the Na_2SO_3 solution to the test water
- Switch on the submersible pump to circulate the water and uniformly distribute both the Na_2SO_3 and $CoCl_2$ solutions among the test water.

- Continuously measure the *DO* in the feed bucket during the deoxygenation phase, and until the *DO* starts to increase. This implies that all Na_2SO_3 is consumed by the water.
- Switch off the submersible pump.
- Turn the valve at the feed bucket bottom into fully open position, and switch on the discharge pump.

Two water samples are collected to assure that the Oxygen Uptake by the distribution tray is not consumed by Na_2SO_3 traces. The sampling location is right above the distribution tray at point (C_0) in Figure 3.2 and right above the first tray at point (C_2) in Figure 3.2. Samples are collected in 50 ml glass beakers, and analyzed using HACH HQd30 meter equipped with *DO* measurement probe (LDO101).

Water flow rate is calculated through collecting the discharge water before it enters the distribution tray into a pre-weighed flask for a defined duration, then re-weigh the flask. The weight difference represents the water weight in the defined duration, which is multiplied by the water density and divided by the duration to get the flow rate. The duration is measured using a stop watch.

The experiment is conducted for the conditions illustrated in Table 4.2

Table 4.2 Experimental test conditions

Parameter	Unit of measurement	Test levels
Diameter of holes	mm	3, 4, 6
Number of holes per tray		6, 8
Spacing between trays	m	0.15, 0.2, 0.25, 0.3
Flow rate	L/min	0.6, 0.773, 1.153, 1.295, 1.614, 1.959

Water samples are collected in 50 ml glass beakers from the top of each tray in an upward manner; i.e. samples are first collected from the (N^{th}) tray at point (C_{2N}), followed by the one above at point ($C_{2(N-1)}$), until it is collected from the distribution tray at point (C_0). The reason for this sequence

is to avoid the disturbance in the water flow which will result from reducing the tray exit flow during the sample collection.

Once collected, the *DO* and temperature of the water samples are measured using the *DO* meter. After collecting the sample from the distribution tray, the water flow rate is remeasured to assure that it didn't vary during the run. When the run is finished, the test conditions are changed to test condition first through changing the flow rate, until all flow rates are tested, then changing (*SP*), then other trays are installed to test different diameters. This arrangement served in reducing the experimental time.

4.3. Results and Discussion

4.3.1. Preparing Deoxygenated (Synthetic) Water

Following charts illustrate the results obtained for the water *DO* for the tested excess doses of Na_2SO_3 and water volume. The truncated duration from each run represent the time taken from adding the Na_2SO_3 dose till the *DO* reaches the minimum concentration. Figure 4.6 illustrates the response of the *DO* at different Na_2SO_3 doses for a water volume of 300 ml in the beaker, which corresponds to a water height of 54mm. It appears from the results that all the tested doses were sufficient to completely deoxygenate the water. Increasing the dose of Na_2SO_3 resulted in increasing the duration before the *DO* starts to increase. Similar conclusion can be concluded from Figure 4.7 for a water volume of 250 ml. However, testing water volume of 200 ml, the 50% excess dose was not enough to totally deoxygenate the water as shown in Figure 4.8.

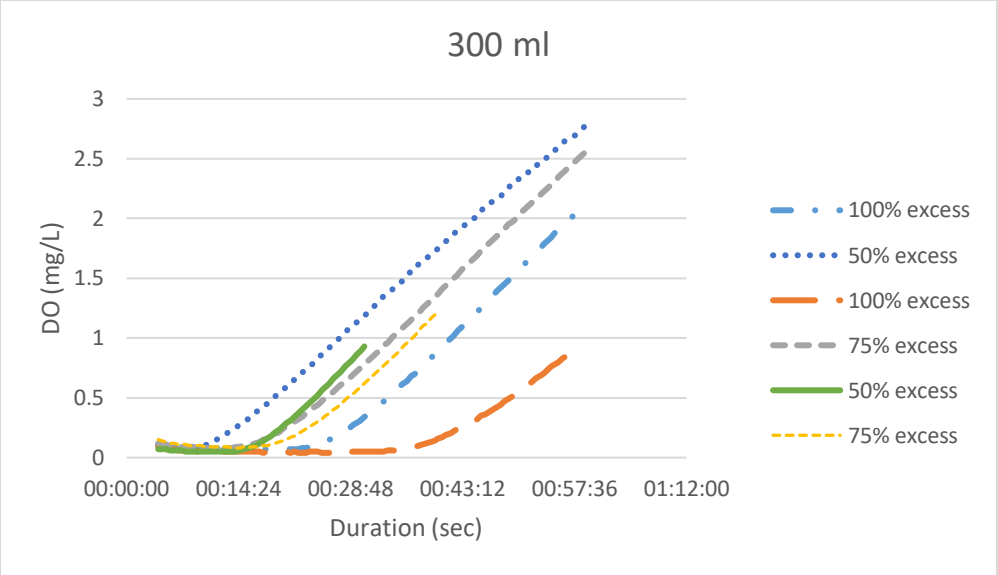

Figure 4.6 DO concentration response to different Na_2SO_3 doses at water volume of 300 ml

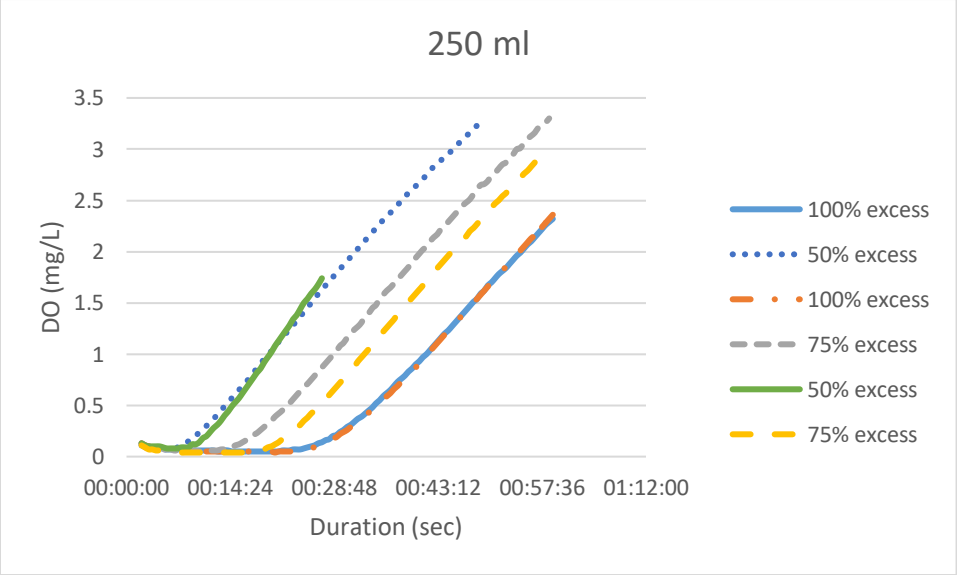

Figure 4.7 DO concentration response to different Na_2SO_3 doses at water volume of 250 ml

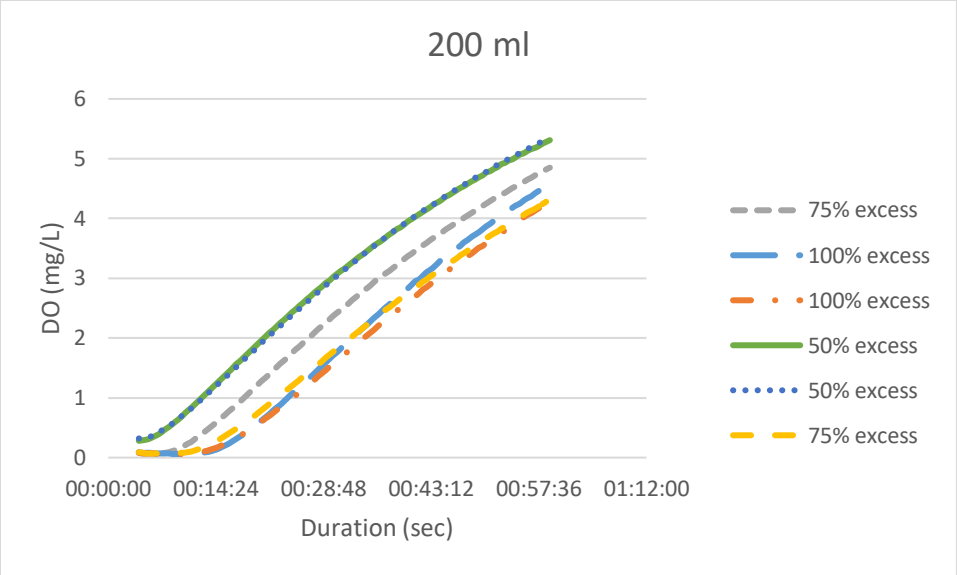

Figure 4.8 DO concentration response to different Na_2SO_3 *doses at water volume of 200 ml*

Thus, it can be concluded that an excess dose in Na_2SO_3 over the theoretical is needed to fully deoxygenate the water. This conclusion is coping with the suggestion stated by Stukenberg et al. to use an excess Na_2SO_3 of 1.5-2 times the theoretical dose (Ghaly & Kok 1988), and the range indicated in the ASCE guidelines of using an excess of 1.2-2.5 times the theoretical dose of Na_2SO_3 (ASCE 2007).

Regarding the time taken from the addition of the Na_2SO_3 dose till the water *DO* starts to increase, a linear regression analysis was made using *Microsoft Excel 2016 MSO (16.0.6925.1018) 32-bit* built in data analysis toolbox. The parameters that were thought to affect the minimum time were taken as the excess Na_2SO_3 dose and the specific area. The regression analysis yielded a strong correlation between the two parameters and the time before the *DO* increases with an adjusted R^2 value of 0.799. the developed equation is indicated in Equation (4.5) below

$$time(\text{min}) = 0.268*(\%\ \text{excess sodium sulfite})-1.1854*(a)+20.83853 \quad \text{.Equation (4.5)}$$

This equation implies that increasing the excess Na_2SO_3 results in an increase in the time taken till water *DO* starts to increase, while increasing the specific area results in a decrease in that time.

The time calculated using Equation (4.5) represents the minimum duration after adding the Na_2SO_3 to the feed water in the laboratory experiment, after which the experiment can be started to assure that there is no trace of Na_2SO_3 which can affect the *DO* measurements during the experiment.

4.3.2. *Laboratory Scale Test for Tray Aerator*

When the experiments were conducted, the influent *DO* to the tray aerator system was not recorded to be an absolute zero, the water entering the system was ranging from 0.01mg/L to 1.56mg/L for some runs. Full data of recorded *DO* in the experimental work is tabulated in Annex II for reference. For the purpose of fair comparison, all the recorded *DO* concentrations are converted into aeration efficiency relative to the influent concentration based on the general equation of aeration efficiency provided in section 2.2.2 (Equation (2.9)), however, the nomenclature of Equation (2.9) is modified to suite the current experiment as indicated in Equation (4.6) below

$$\eta_{2i} = \frac{C_{DS} - C_{US}}{C_S - C_{US}} = \frac{C_{2i} - C_0}{C_S - C_0} \text{ , (i=1:N)} \quad \text{.....Equation (4.6)}$$

Where (η) is the aeration efficiency, (C_{DS}) is the downstream *DO* concentration; (C_{US}) is the upstream *DO* concentration; (i) is the tray number, (C_{2i}) is the *DO* concentration entering tray (i), (C_0) is the initial *DO* concentration entering the distribution tray, (C_S) is the saturation *DO* at the recorded water temperature, and (N) is the total number of examined trays. Following sections present the effect of the different parameters on the aeration efficiency.

4.3.2.1. *Effect of Changing the Spacing Between Trays*

In order to study the impact of changing the spacing between trays, the results from each hole diameter, from different hole diameters, of aeration efficiency obtained after the first tray at different flow rates and spacing between trays, while fixing other parameters at 8 holes per tray, and 20cmx20cm tray system are illustrated in Figure 4.9**Error! Reference source not found.**.

The aeration efficiency obtained from the results in Figure 4.9 (a), (b), and (c) are compared together. The increase in tray spacing from 15cm to 20cm, or from 20cm to 25cm, while maintaining other parameters fixed (diameter, number of holes, flow rate, tray area, and number of trays) results in an increase in aeration efficiency. However, the rate of increase in the aeration efficiency when the spacing increased to 20cm is noted to be higher than when the spacing was increased to 25cm. Therefore, the aeration efficiency is concluded to be directly proportional with the tray spacing in an exponential form.

4.3.2.2. Effect of Changing the Hole Diameter

The general trend describing the impact of increasing the hole diameter among the tested diameters in noted to slightly increase the aeration efficiency. Figure 4.10(a) is for the 15 cm tray spacing. This spacing was tested for the 3mm and 4mm diameters only. The results show that the 3mm holes provide higher aeration efficiency over the 4mm holes with the low and high flow rates, while the 4mm diameter yields higher aeration efficiency for the medium flow rate. The overall difference resulting from the change in hole diameter is within 5% difference.

The 20 cm spacing as illustrated in Figure 4.10(b) also shows that the difference in aeration efficiency resulting from changing the hole diameters is inconsistent, where the 6mm diameter is higher than the 3mm and the 4mm diameters for the high and low flow rates, and almost similar to the 4mm diameter for the medium flow rate. The 3mm diameter gives the lowest aeration efficiency with the low and medium flow rates, whereas the 4mm diameter results in the lowest aeration efficiency with the high flow rate. The change in efficiency is also within 8%.

The 25 cm spacing was tested for the 4mm and the 6mm diameters only as illustrated in Figure 4.10(c) the aeration efficiency for both diameters is almost identical for the medium and high flow rates, while for the low flow rate the 6mm holes result in an aeration efficiency around 4% higher than the 4mm diameter.

The inconsistent trend for the impact of changing the hole diameters on the aeration efficiency is thought to be due to the limited effect of the change in diameter over the aeration efficiency, as was illustrated in the mathematical model.

4.3.2.3. Effect of Changing the Flow Rate

Through inspecting the results illustrated in Figure 4.10, the aeration efficiency is seen to be affected by the flow rate. The values of the aeration efficiency demonstrate the decrease in aeration efficiency resulting from the increase in the flow rate. Results postulate that there is an inversely exponential relation between the flow rate and the aeration efficiency as illustrated in Figure 4.10(b), and Figure 4.10(c).

4.3.2.4. *Effect of Changing the Number of Trays*

The increase in number of trays in a tray aerator system results in an exponential increase in the aeration efficiency, as illustrated in Figure 4.11 for 1 to 4 tray aerator systems. This increase is thought to be due to the increase in number of thin films with the increase in number of trays. Moreover, increasing the number of trays result in an increase in the time of exposure of water to air due to the damping of the water fall speed. This result is strongly coping with the results obtained from the mathematical model for the increase in number of trays.

4.1. *Discussion and Model Verification*

The results obtained from the laboratory work are compared to the expected results that were produced using the mathematical model for similar operating conditions. Those results are illustrated in Figure 4.12. The error in the predicted values from the measure is notably high, with a mean error of -32% and a standard deviation of 15%. Another remark is that all the predicted values are less than the measured ones. This implies that the actual value of (K_L) is higher than the assumed value in the analytical model, of 20cm/hr.

The development of the value of K_L was made using the equations developed for the analytical model section, with changing their order. The known parameters are the values of *DO* that were obtained from the laboratory experimental work, together with *Q*, *SP*, *n*, *A*, and *d*. *HLR* is estimated as indicated in Equation (4.7), while $a_f t_f$ is estimated as per Equation (4.8).

$$HLR = \frac{Q}{A} \quad \text{.....Equation (4.7)}$$

$$a_f t_f = \frac{1}{HLR} \quad \text{.....Equation (4.8)}$$

$a_j t_j$ are estimated using equations (3.5, 3.7 - 3.13, 3.18, and 3.19), and Equation (3.21) was rearranged as in Equation (4.9) to calculate K_L from each tray.

$$K_L = \frac{\ln(\frac{C_S - C_{US}}{C_S - C_{DS}})}{a_f t_f + a_j t_j} \quad \text{.....Equation (4.9)}$$

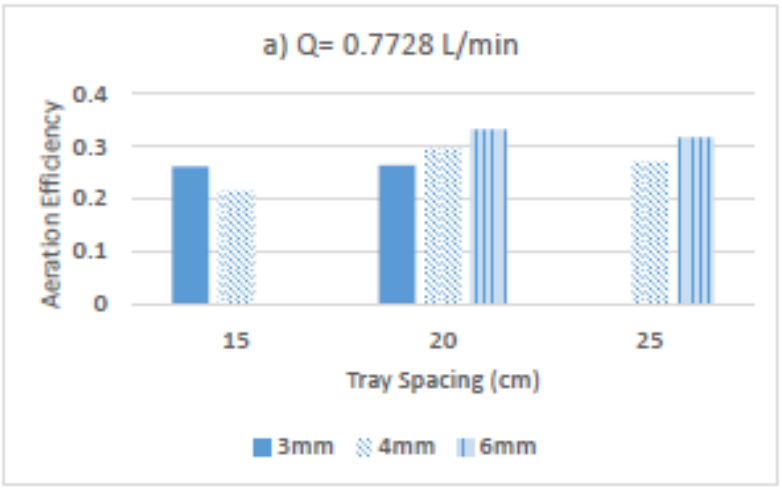

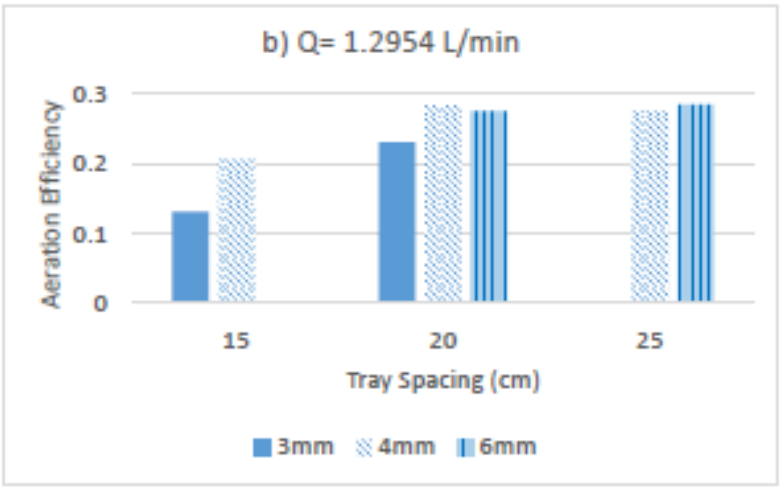

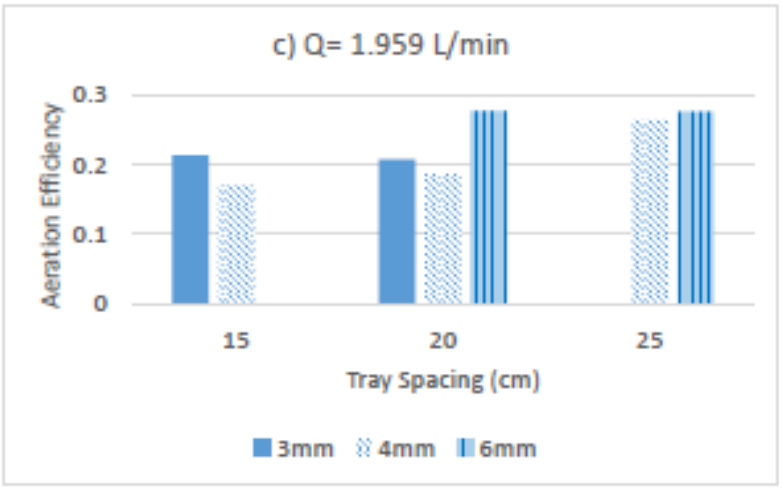

Figure 4.9 Aeration efficiency from single tray at different hole diameters for 8 holes per tray, 20cmx20cm tray area a) Q=0.7728 L/min b) Q=1.2954 L/min c) Q=1.959 L/min

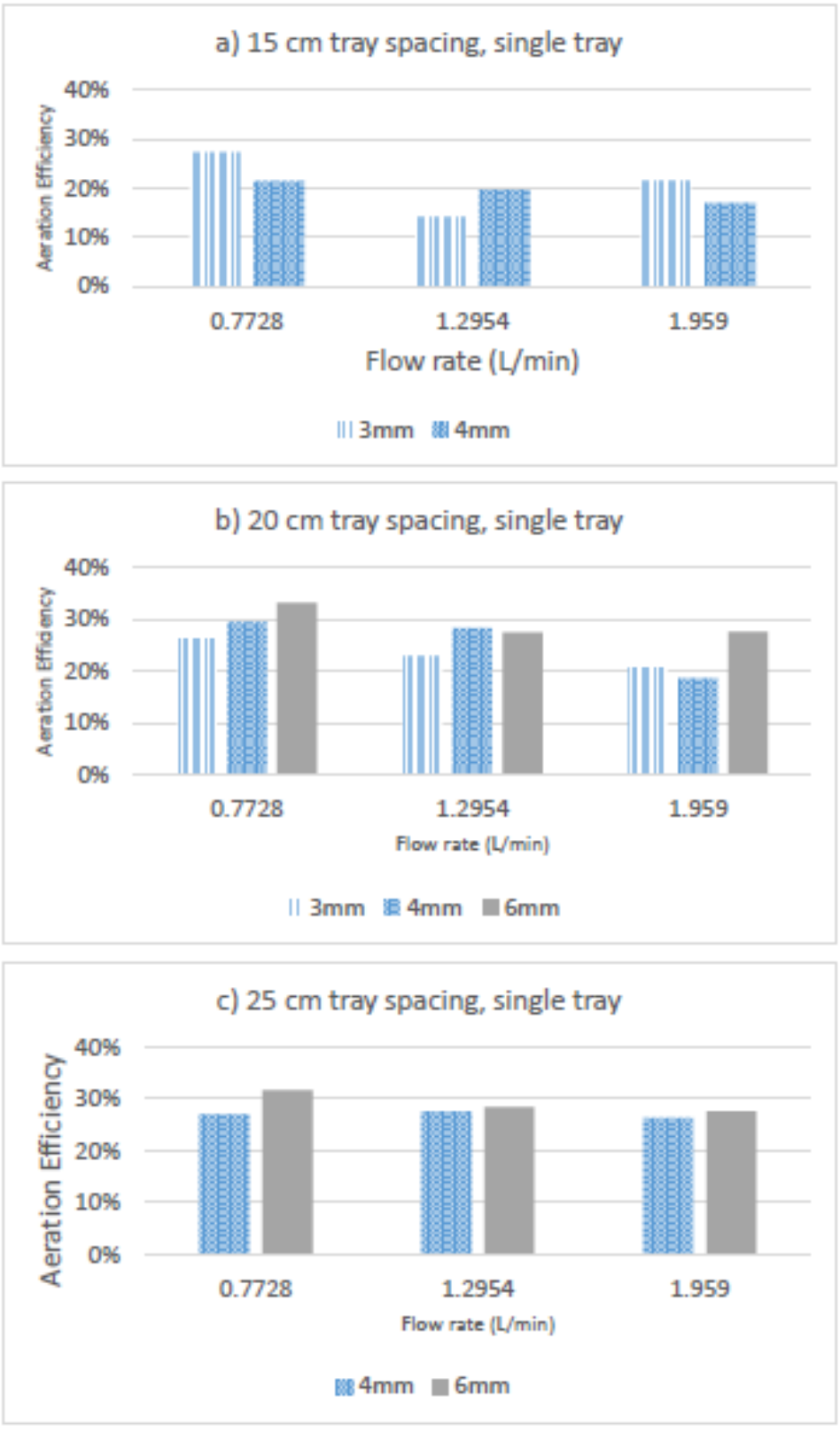

Figure 4.10 Aeration efficiency from single tray at different hole diameters for 8 holes per tray, 20cmx20cm tray area a) 15 cm tray spacing b) 20 cm tray spacing c) 25 cm tray spacing

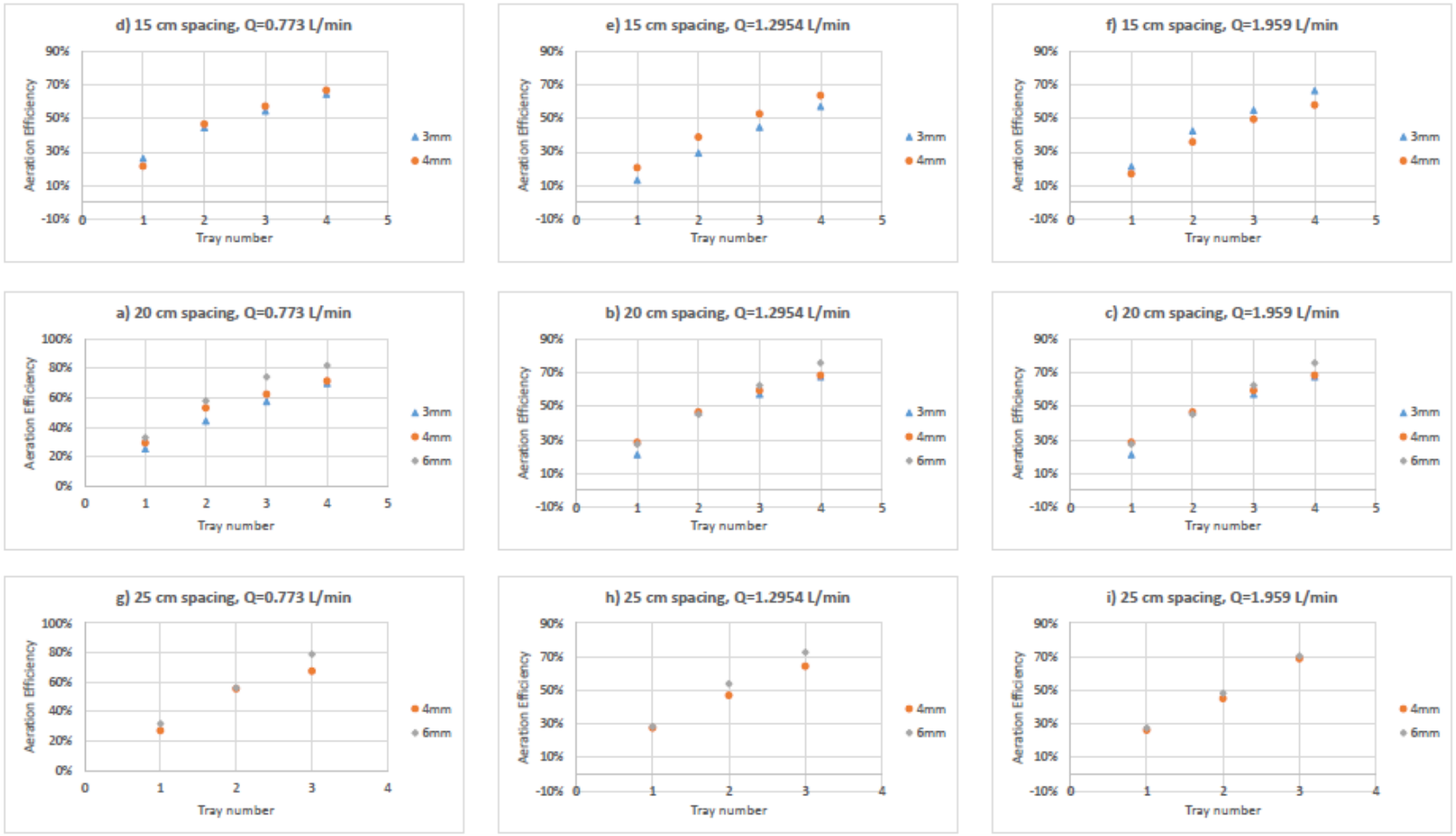

Figure 4.11 Aeration efficiency at different hole diameters for 8 holes per tray, 20cmx20cm tray area

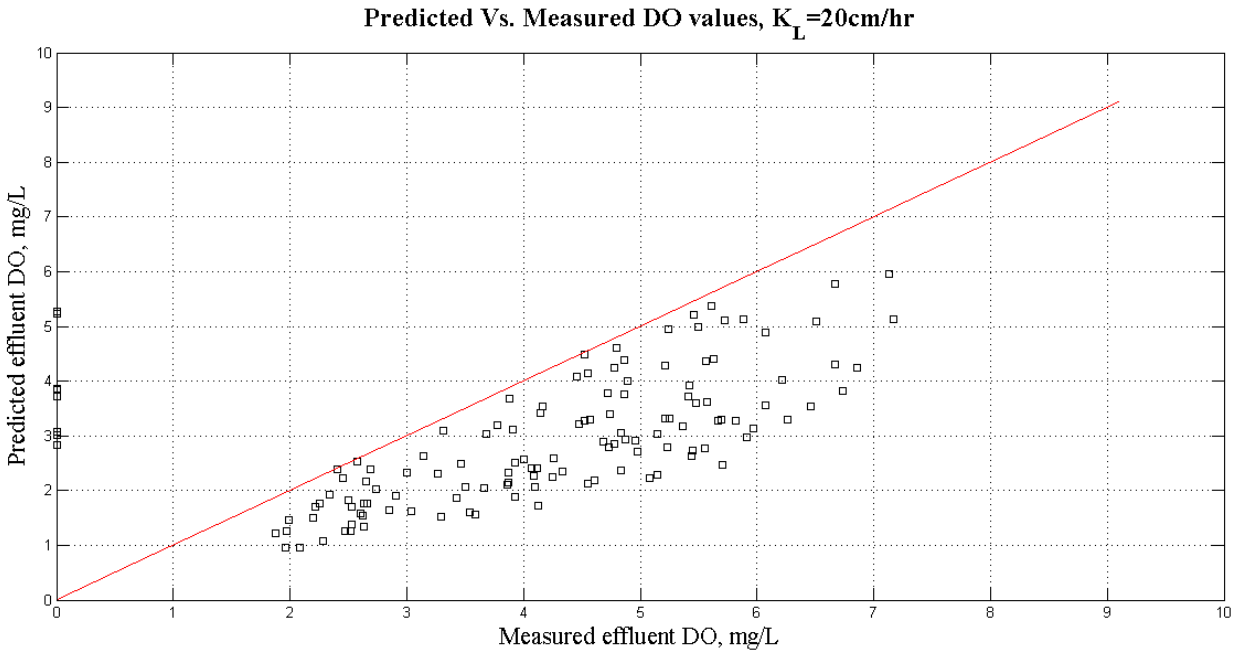

Figure 4.12 Predicted DO from Analytical Model Vs. Laboratory Measured DO, KL=20cm/h (Liss & Slater 1974)

The geometric average of the K_L value obtained from each run is calculated to represent the run conditions, and several methodologies were tested to estimate K_L. The first approach is to average all the values of K_L from the different runs which resulted in a mean K_L of 41.8cm/h. By substituting this value in the model equation, the error was decreased to have a mean of 5%, with a standard deviation of 23% as illustrated in Figure 4.13.

The second approach was to develop a regression model between K_L and the potential parameters which might have impact on K_L; those are Q, SP, n, area of holes A_h, and d. The area of holes is calculated as illustrated in Equation (4.10). As both n and d are considered in A_h, they were removed from the regression analysis, and the only tested parameters were Q, SP and A_h. The regression model of those parameters, resulted in an adjusted R2 value of 0.966, and the model equation should be as illustrated in Equation (4.11) and illustrated in Figure 4.14

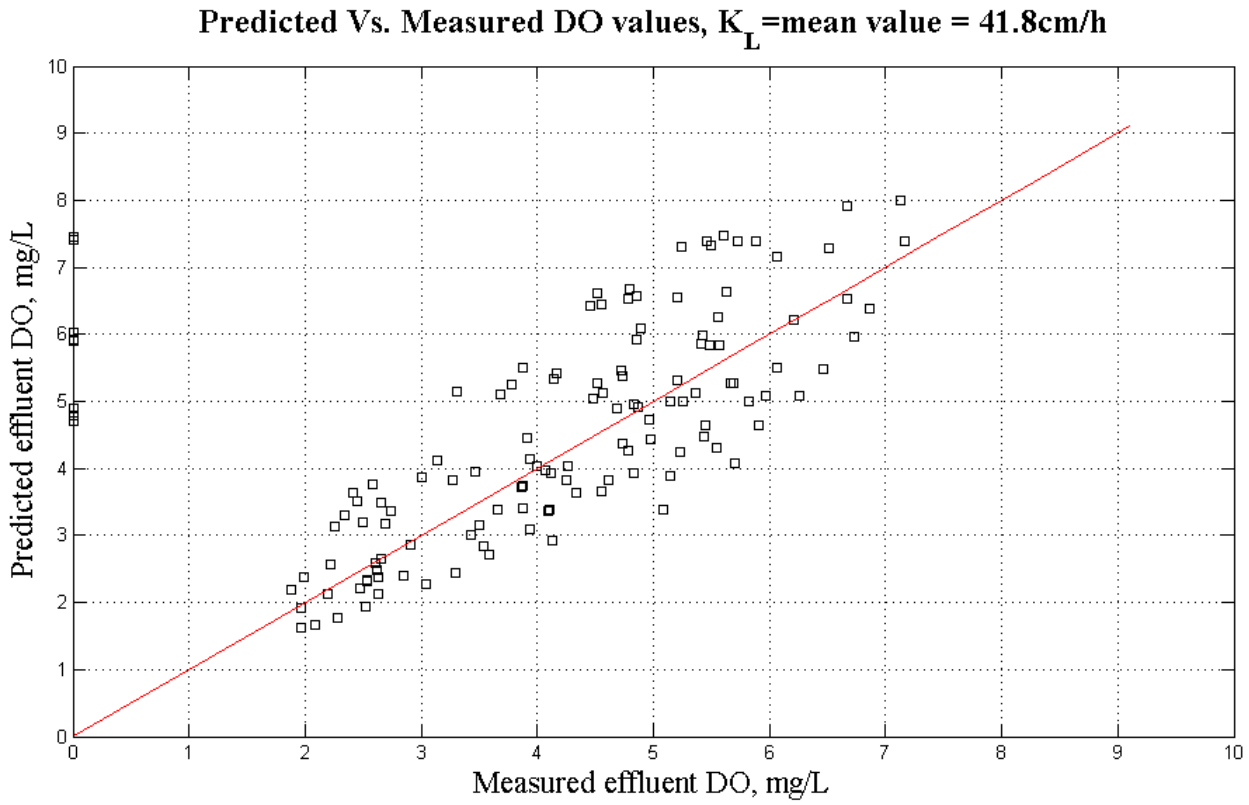

Figure 4.13 Predicted DO from Analytical Model Vs. Laboratory Measured DO, K_L =41.8cm/h

$$A_h = n * \frac{\pi}{4} * d^2$$

.....Equation (4.10)

$$K_{L_{model}} = -4.55623\text{E-}05 + 4.1231 * Q(m3/\sec) + (0.000328 * SP(m)) + (5.64E-8 * A_h(mm2))$$

.....Equation (4.11)

Equation (4.11) was used to check the error between the measured and the predicted values of the effluent *DO* from the tray aerator system. The Equation was introduced to the model, and the error was decreased to have a mean value 0.4% and a standard deviation of 6% as illustrated in Figure 4.15.

	A	B	C	D	E	F	G	H	I
1	SUMMARY OUTPUT								
2									
3	*Regression Statistics*								
4	Multiple R	0.984417778							
5	R Square	0.969078362							
6	Adjusted R Square	0.965879572							
7	Standard Error	7.25619E-06							
8	Observations	33							
9									
10	ANOVA								
11		*df*	*SS*	*MS*	*F*	*Significance F*			
12	Regression	3	4.78533E-08	1.59511E-08	302.9515278	5.57893E-22			
13	Residual	29	1.52692E-09	5.26523E-11					
14	Total	32	4.93802E-08						
15									
16		*Coefficients*	*Standard Error*	*t Stat*	*P-value*	*Lower 95%*	*Upper 95%*	*Lower 95.0%*	*Upper 95.0%*
17	Intercept	-4.55623E-05	6.1786E-06	-7.374208932	4.00009E-08	-5.81989E-05	-3.29256E-05	-5.81989E-05	-3.29256E-05
18	ah	5.63741E-08	2.43507E-08	2.315091314	0.027884888	6.57132E-09	1.06177E-07	6.57132E-09	1.06177E-07
19	Q1 (m3/sec)	4.123065316	0.160211459	25.7351462	1.60442E-21	3.795396091	4.45073454	3.795396091	4.45073454
20	sp(m)	0.000327813	3.15363E-05	10.39478157	2.72204E-11	0.000263314	0.000392312	0.000263314	0.000392312

Figure 4.14 Regression analysis for KL estimation

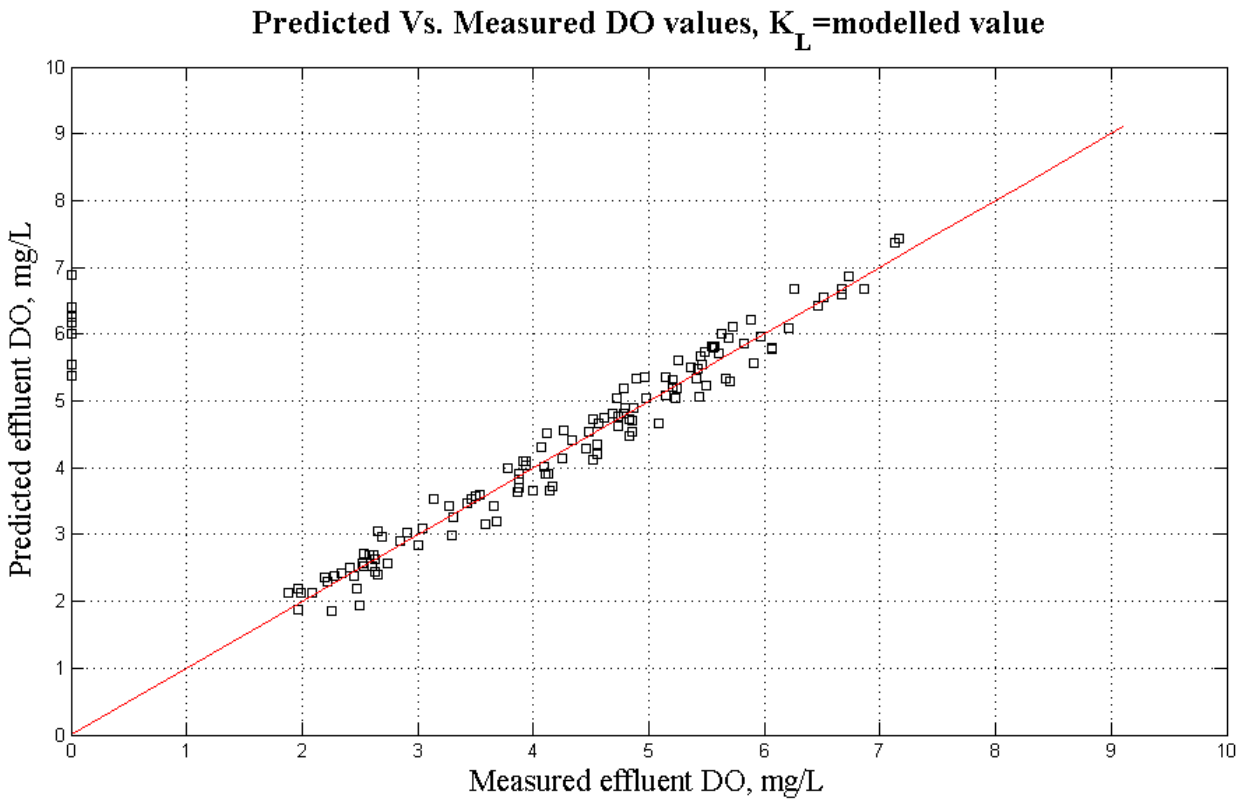

Figure 4.15 Predicted DO from Analytical Model Vs. Laboratory Measured DO, K_L from regression model

Following the previous analysis, few validation runs were conducted using the same methodology of testing the tray aerator, at different conditions for the test parameters to verify the validity of

the model. Results from those runs are summarized in Table 4.3, and the model validation is illustrated in Figure 4.16. It appears from Figure 4.16 that the error is uniformly distributed around the perfect fit line (red line), and the mean error is about 1.6%, with a standard deviation of 6%.

Table 4.3 Results of verification runs

Q (L/min)	d (mm)	n	SP (m)	C0	C2	C4	C6	C8
1.7142	6.00	6	0.20	0.06		3.09	4.71	5.287
1.14	3.00	8	0.20	0.71	2.4	4.13	5.43	6.39
0.63	3.00	8	0.20	1.84	3.56	5.28	6.29	7.08
0.7368	6.00	12	0.20	1.02	3.26	4.48	5.84	6.59
1.068	6.00	12	0.20	1.73	3.48	4.42	5.75	6.33
0.693	6.00	12	0.30	1.92	3.88	5.25	7.05	8.07
1.2672	6.00	12	0.30	1.73		5.94	6.85	7.03
1.1022	4.00	12	0.30	0.84	3.77	5.37	6.27	7.2

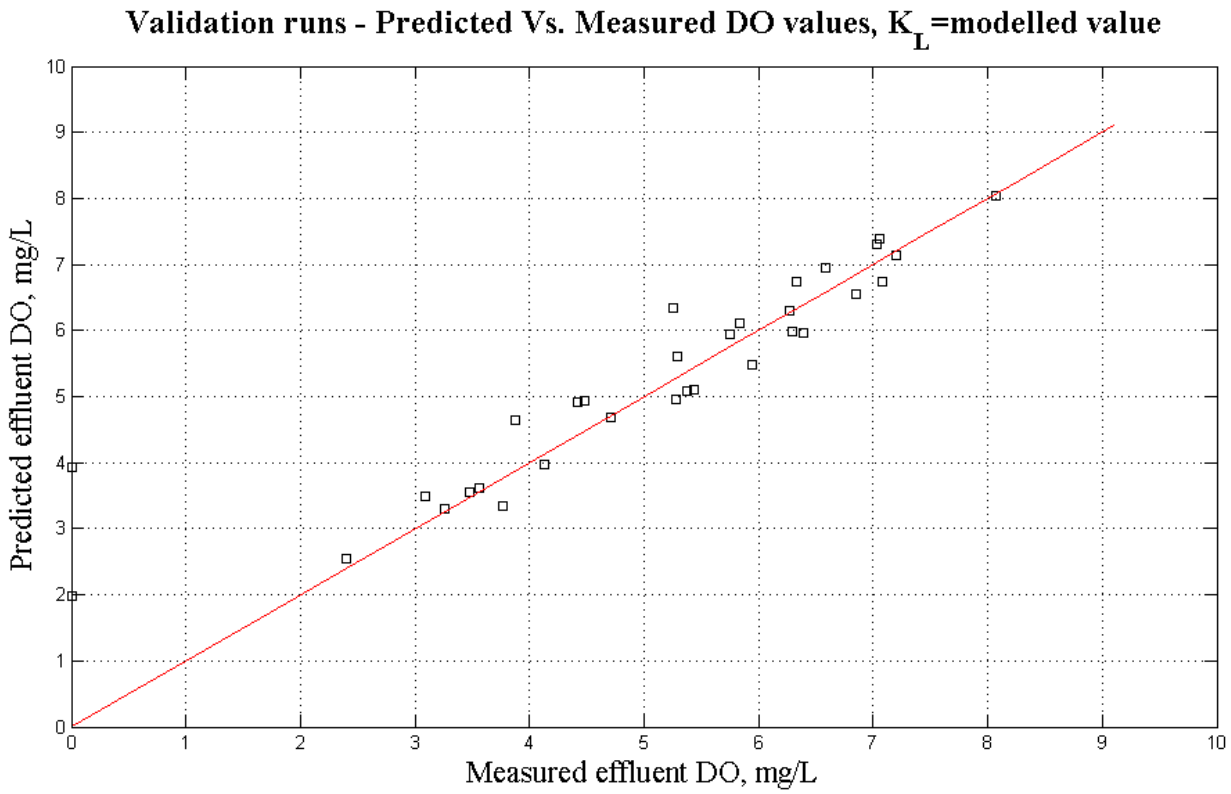

Figure 4.16 Predicted DO from Analytical Model Vs. validation runs Measured DO, K_L from regression model

4.2. Conclusion

In the laboratory experimental model for the tray aerators, Na_2SO_3 reduction of the *DO* from water was used to completely deoxygenate tap water. Several experiments were conducted to check the optimum dose of Na_2SO_3 needed to completely deoxygenate water. This method proved good results with the optimum dose to deoxygenate one mg/L of *DO* is equal to 130% of the stoichiometric value of 7.9mg/L of Na_2SO_3.

Through testing the performance of the tray aerators on laboratory scale, the results illustrated that the performance of the tray aerators is strongly affected by the number of trays used as well as the flow rate. The aeration efficiency is directly proportional with the spacing between trays in an exponential form, with the spacing of 20cm between trays considered as the optimum spacing beyond which the increase in efficiency associated with the increase in spacing is not significant. Changing the hole diameters didn't result in significant change in the aeration efficiency. This conclusion is in line with the results obtained from the mathematical modelling.

In the analysis of the results, an empirical equation for the mass transfer coefficient is developed using linear regression analysis. That equation is a function of the area of holes, flow rate and the tray spacing. The error in estimating the effluent *DO* through using this empirical equation was at 0.4% with a standard deviation of 6%.

The validation illustrated that the model is valid for number of holes, and flow rates other than those used in developing the model. Pilot scale application in next chapter shall be utilized to further validate the model with real wastewater.

5. Phase III - Pilot Scale Study

5.1. Introduction

Most studies and research work in the field of wastewater, if not all, starts by a mathematical modelling, followed by laboratory scale experimental studies, and ends by a scaling up pilot scale study. The main reason for conducting the scaling up pilot scale application is to investigate the performance of the research subject under the normal operating conditions in the field rather than the controlled conditions which characterize the laboratory experiments.

Furthermore, and specifically in water and wastewater oxygen transfer related work, some parameters vary in the full scale application from the small scale laboratory application. Those parameters are the oxygen saturation concentration value, and the oxygen mass transfer coefficient. For the oxygen saturation concentration, a correction factor termed (β) is multiplied to the published saturation values to account for the difference in saturation concentration between wastewater and clean water. This correction factor is due to the effect of other gases, organics, and salts as well as the difference in temperature and/or pressure of water from the tabulated values (Leung et al. 2006; Mueller et al. 2002).

Regarding the correction in the mass transfer coefficient, a correction factor termed (α) is multiplied to the mass transfer coefficient of clean water to account for different chemical and process parameters, including the chemical oxygen demand, surface tension, liquid temperature, presence of suspended solids, aeration methods and velocities (Leung et al. 2006; Mueller et al. 2002).

Another benefit from the pilot experiment is to investigate whether the tray holes will be clogged from the microbial growth over the trays, which might affect the aerator hydraulics and consume the added oxygen. If the clogging is to occur, the conclusion section shall propose a maintenance technique suitable for sustaining the aerator performance.

5.2. Material and Methods

A full scale sequential anaerobic-aerobic wastewater treatment plant termed Zero Energy Compact Unit (ZECU) was designed and built at Zawyat Al Karadsah wastewater treatment plant in Fayyoum Governorate, by a research team led by Dr. Tarek Ismail Sabry and Dr. Ahmed Shafik El-Gendy. The location of the plant is indicated in Figure 5.1. ZECU unit is composed of a three

stage anaerobic treatment unit, followed by a tray aerator unit, which discharges into a down-flow aerobic unit as illustrated in Figure 5.2. The three stage anaerobic treatment unit is composed of an up-flow anaerobic reactor, followed by a down-flow anaerobic packed-bed reactor, then an up-flow anaerobic reactor. the aerobic unit is composed of an aerobic biological filter packed with sponge media. The whole system is composed of two identical units, which have one influent downstream the grit removal chamber (preliminary treatment). The system design flow rate is 9m3/day equally distributed between the two units. The actual flow of the system during the experimental runs was approximately 4m3/day. ZECU treatment plant is selected to test the tray aerators as that system is already operating with tray aerators, which can be easily replaced with the test arrangements.

Four parallel tray trains were prepared at the American University in Cairo. Each train had 8 trays other than the distribution tray. Trays were fixed on steel frames of 20cmX20cm inner dimensions, which were fabricated using steel angles of 3cmX3cmX3mm dimensions as illustrated in Figure 4.4, and Figure 4.5. The only difference in the frames of the pilot scale arrangement from the those in Figure 4.5 is in the diameter of the fixation holes of Angle 2, which was increased in the pilot scale arrangement to 10mm instead of the indicated 8mm. This increase is to account for the larger diameter steel threads used in the pilot arrangement to withstand the weight of the 10 trays in each train.

In the pilot experiments, trays were made from 20cmX20cm polycarbonate sheets. Trays were cut and drilled at the American University in Cairo - Architectural Engineering computer laboratory using CNC laser cutting machine as illustrated in Figure 5.3 for the 3mm, 4mm, 5mm, and 6mm hole diameter. The number of holes per tray (35, 20, 12, and 8 holes per tray for the 3mm, 4mm, 5mm and 6mm hole diameter respectively) were selected according to the results indicated in Table 3.2 for the case of 2.5m3/day flow rate that would result in 2mm film thickness. Fabricated trays are fixed to the steel frames using antibacterial silicone to fill any voids of gaps between the tray edges and the steel frame sides.

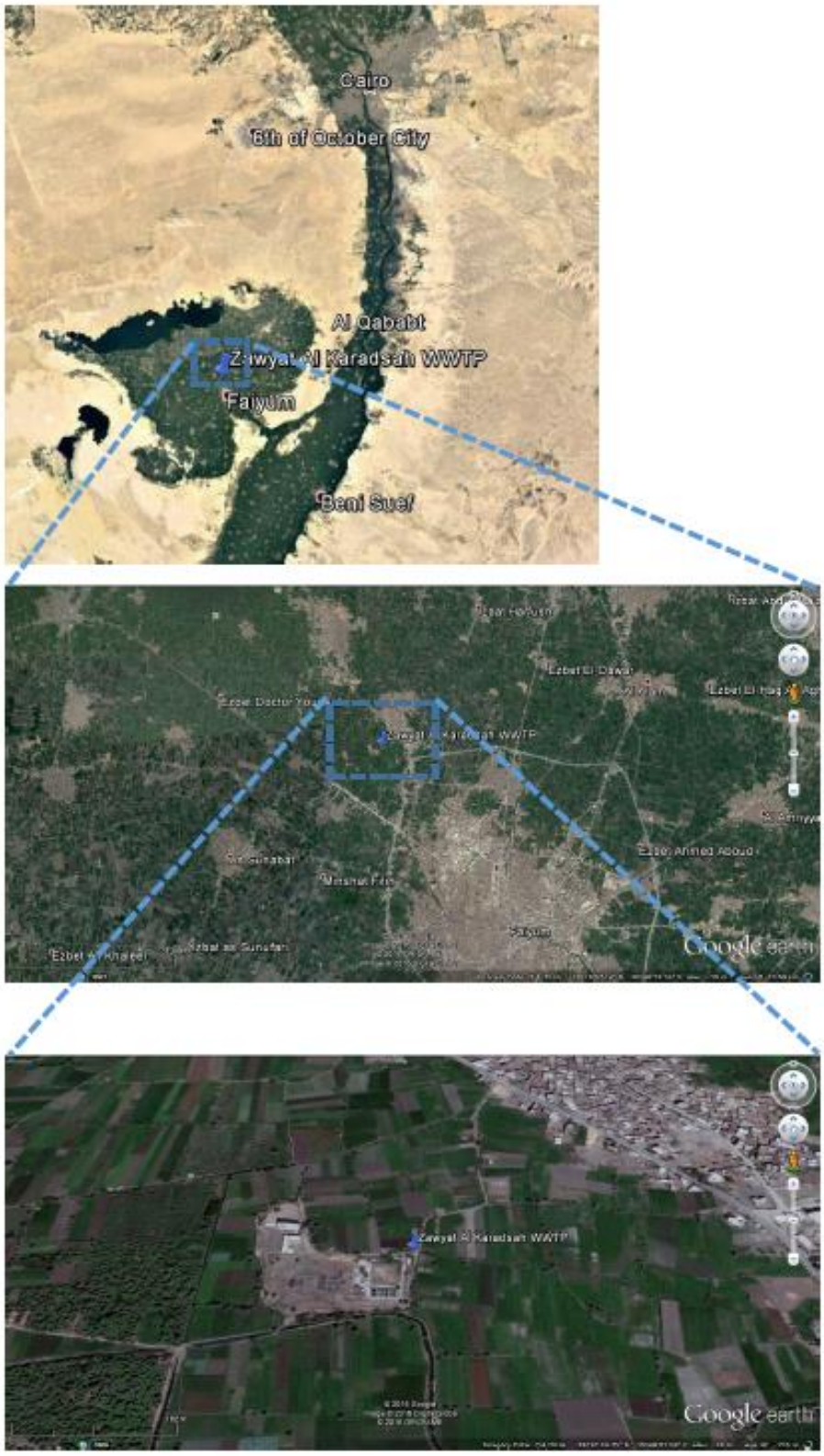

Figure 5.1 Zawyet Al Karadsah WWTP location

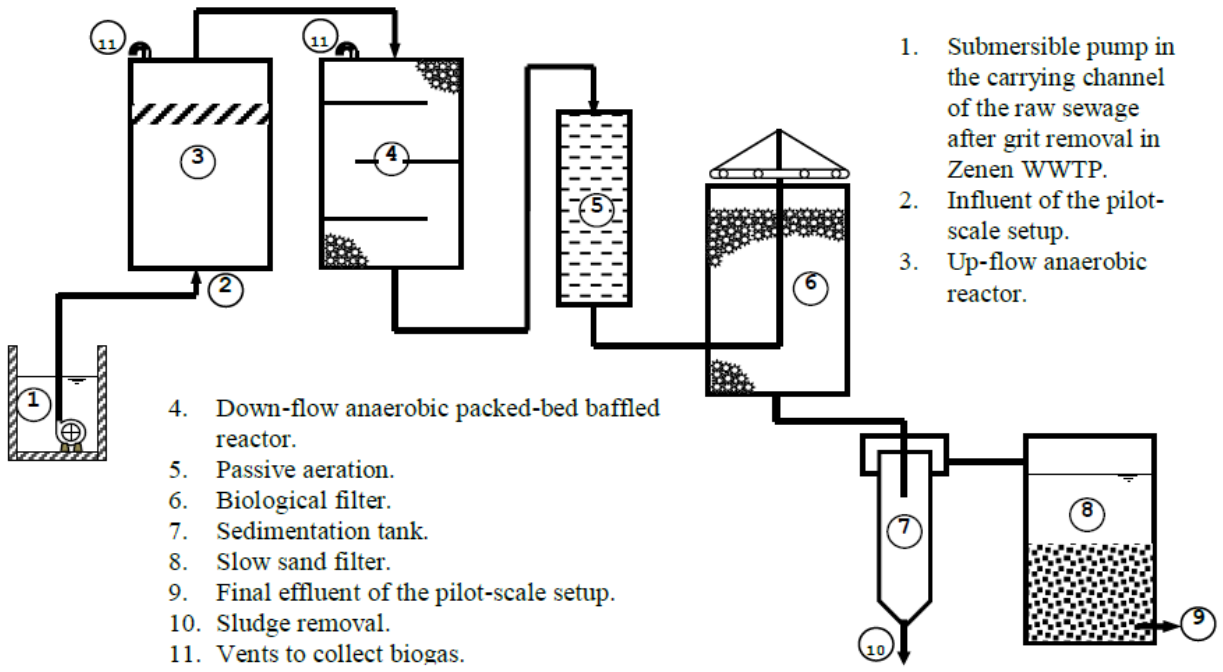

Figure 5.2 Schematic Diagram of the Full-Scale Setup (Sabry et al. 2011; El-Gendy et al. 2012)

Each rectangular frame with the polycarbonate sheet resemble a single tray which is installed through the threaded rods and fixed in the desired position using hexagonal nuts. The spacing between trays is adjusted to 20cm through tightening or losing the nuts, and the trays horizontality is adopted by spirit level and fine tuning of the nut location. The spacing of 20 cm was selected to permit the installation of more trays within the 2m length threaded rod, while maximizing the spacing between trays to achieve higher *DO* as illustrated in Phase I - Mathematical Model, and Phase II – Laboratory Study, that the *DO* is directly proportional with the with the tray spacing.

Two square steel beams of 5cmX5cmX4mm dimensions and 1.3m length each, are used as supporting frame to hold the four tray trains. The square beams were drilled at the positions of fixation of the steel rods. The drilled holes were of 12mm diameter to allow for 2mm tolerance to adjust the steel rods. The two square rods carrying the four tray trains were installed on top of the sedimentation tank of ZECU unit, and beside the existing trays as illustrated in Figure 5.5. Water effluent from the anaerobic stage was diverted toward the tested tray trains using T-connection and valves, delivering the water to a flexible hose of 1” diameter.

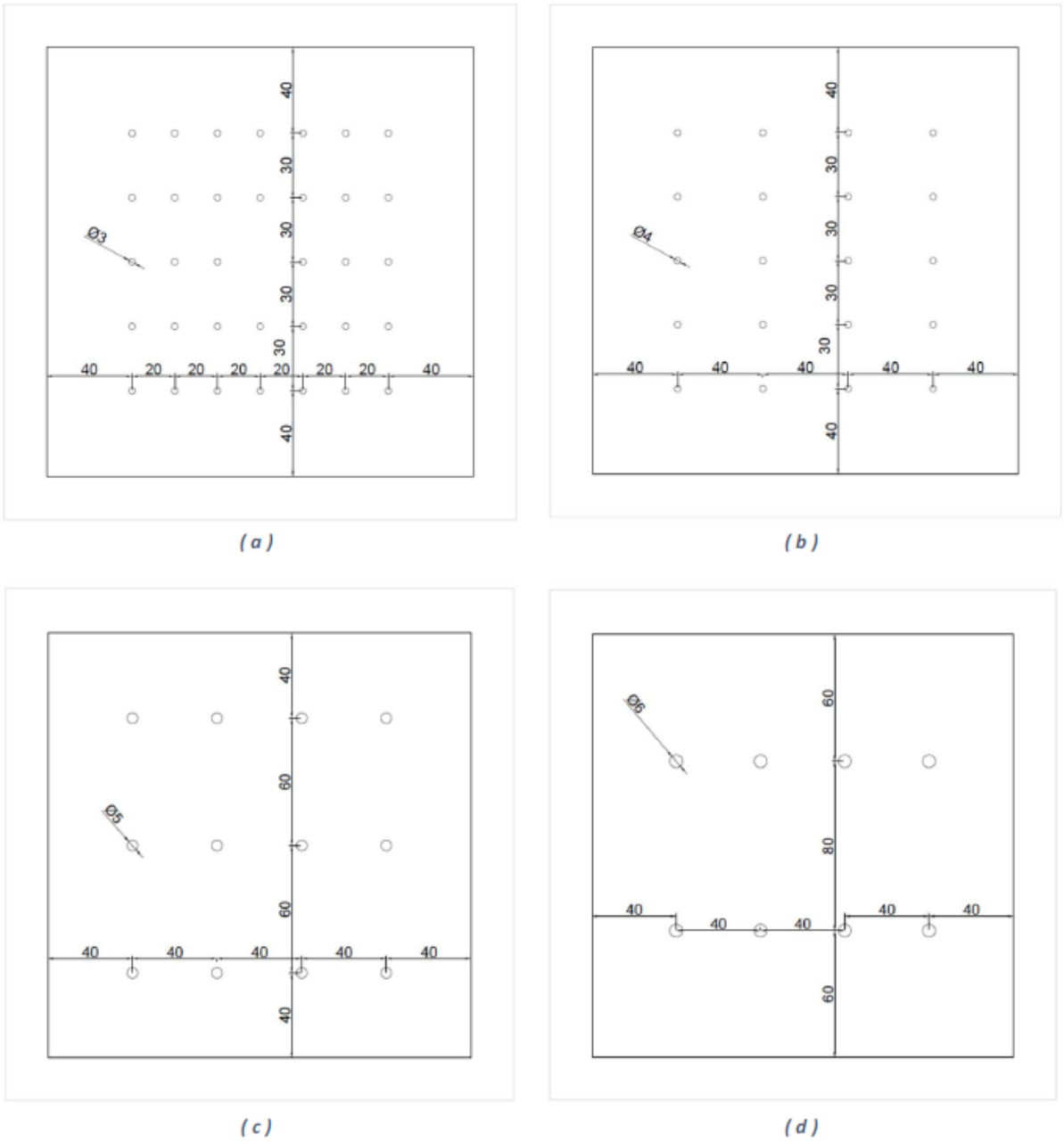

Figure 5.3 Tray dimensions – (a) 3mm hole diameter. (b) 4mm hole diameter. (c) 5mm hole diameter. (d) 6mm hole diameter.

Water flow rate to the system is controlled through the valve opening, and is measured through collecting the water from the flexible 1" hose in a 1L graduated cylinder for a defined time duration. The flow rate is calculated by dividing the collected volume over the duration of collection. The tested flow rates are 1L/min (1.44m3/day) and 1.8L/min (2.592m3/day).

Water samples are collected from top of each tray starting from the bottom tray followed by the one above until the distribution tray. Samples were collected in 120ml plastic beakers as indicated in Figure 5.4, and analyzed using HACH HQd30 meter equipped with *DO* measurement probe (LDO101). Each plastic beaker was used to collect a single sample, and they were thoroughly washed using diluted nitric acid, and rinsed by tap water and distilled water before reuse.

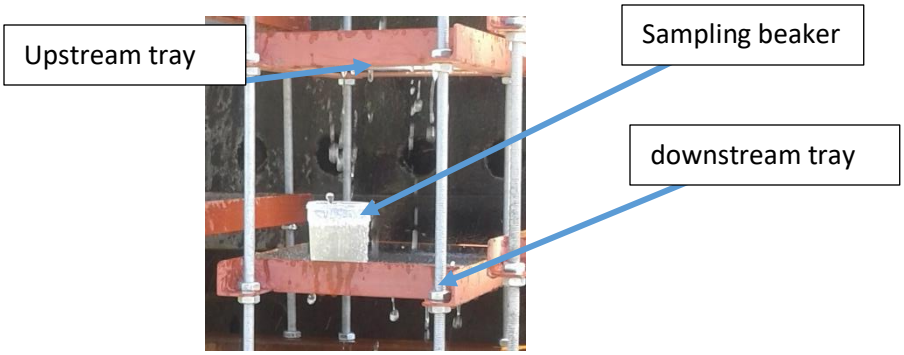

Figure 5.4 Water sampling

The *DO* meter was manually calibrated on site before the initial use according to the supplier's recommendation (Hach 2013), according to the following procedure:

- Connect the probe to the meter. Make sure that the cable locking nut is securely connected to the meter. Turn on the meter.
- Push Calibrate
- Push Methods. Select User Cal - 100%. Push OK.
- Rinse the probe cap with deionized water. Blot dry with a lint free cloth.
- Add approximately ¼ inch (6.4 mm) of reagent water to a narrow-neck bottle, such as a BOD bottle (a 500-mL Erlenmeyer flask is used in case of rugged probe).
- Put a stopper in the bottle and shake the bottle vigorously for approximately 30 seconds to saturate the entrapped air with water. Allow up to 30 minutes for contents to equilibrate to room temperature.
- Remove the stopper. Carefully dry the probe cap with a nonabrasive cloth. Put the probe in the bottle.

- Push Read. The display shows "Stabilizing" and a progress bar as the probe stabilizes. The display shows the standard value when the reading is stable.
- Push Done to view the calibration summary.
- Push Store to accept the calibration and return to the measurement mode. If a rugged probe, install the shroud on the probe.
- After each sample analysis, the *DO* probe was washed using clean water and dried by a clean paper tissue.

5.3. Results and Discussion

5.3.1. Effect of Changing the Hole Diameter

Changing the hole diameters together with the number of holes per tray, to achieve similar film height above the trays, is illustrated in terms of average aeration efficiency in Figure 5.6. The average aeration efficiency is calculated as the geometric average of the efficiency obtained from each tray using Equation (4.6), taking the *DO* value from the (*i-1*) tray as the upstream *DO*, and the *DO* value from the (i^{th}) tray as the downstream *DO*. It appears that there is no significant change in aeration efficiency resulting from changing the hole diameter while maintaining the film height constant for the 1L/min flow rate, however, as the flow rate increased to 1.8L/min, the aeration efficiency from the small diameters (3mm and 4mm) are higher than the aeration efficiency from the larger diameters (5mm and 6mm). The highest aeration efficiency is obtained from using 4mm diameter holes.

As the test conditions in the pilot scale experiment is different from the test conditions of the laboratory scale experiment, where in the pilot scale experiments both the diameter and number of holes per tray changed simultaneously, while in the laboratory scale experiments either the hole diameter or the number of holes was changing, therefore it is not possible to compare both results together.

5.3.2. *Effect of Changing the Number of Trays*

The results obtained from running the experiments are illustrated in Figure 5.7. It appears from the results that the *DO* increases exponentially with the increase in the number of trays for all tested diameters and flow rates. This is similar to the conclusion that was drawn from the analytical model and the experimental model of this work, as well as the models studied by other researchers (Duranceau & Faborode 2012; La Motta & Chinthakuntla 1996; La Motta 1995; Scott et al. 1955).

5.3.3. *Model Validation*

The empirical equation for K_L that is derived in Phase II – Laboratory Study is validated using the results obtained from the Phase III - Pilot Scale Study. This validation was conducted through running the model that was developed in Phase I - Mathematical Model using the same parameters tested in the pilot study, and then comparing the measured *DO* against the predicted values. Results are illustrated in Figure 5.8. Results illustrate that the model overestimates the *DO* values with a mean error of 20% and standard deviation of about 10%.

As the error in the estimate is linear, and the standard deviation in the error is only 4% higher than the standard deviation from the laboratory runs, this error is foreseen to be systematic error. Therefore, the model is deemed to be valid for the prediction of the *DO* effluent from tray aerators.

Possible sources of the systematic error might be due to the microbial activity in the real wastewater, which consumes a portion of the added oxygen. Therefore, through correcting the saturation concentration of oxygen in wastewater, by setting the value of β equal to 0.9 to account for the available organics (typical values of β range from 0.7 to 0.95 (Tchobanoglous et al. 2004), the error in the estimate is reduced to around 10% as illustrated in Figure 5.9.

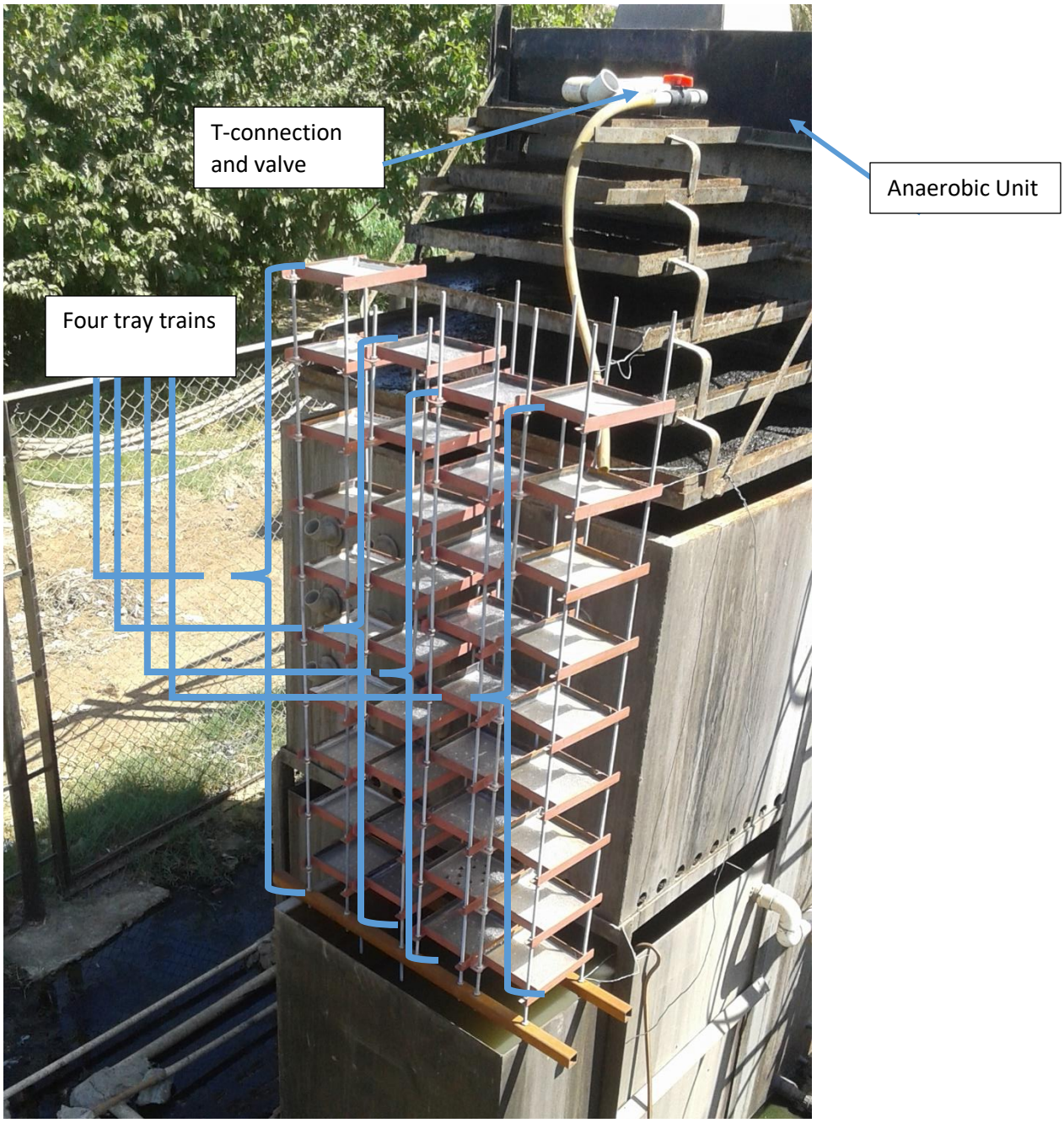

Figure 5.5 Pilot experiment setup

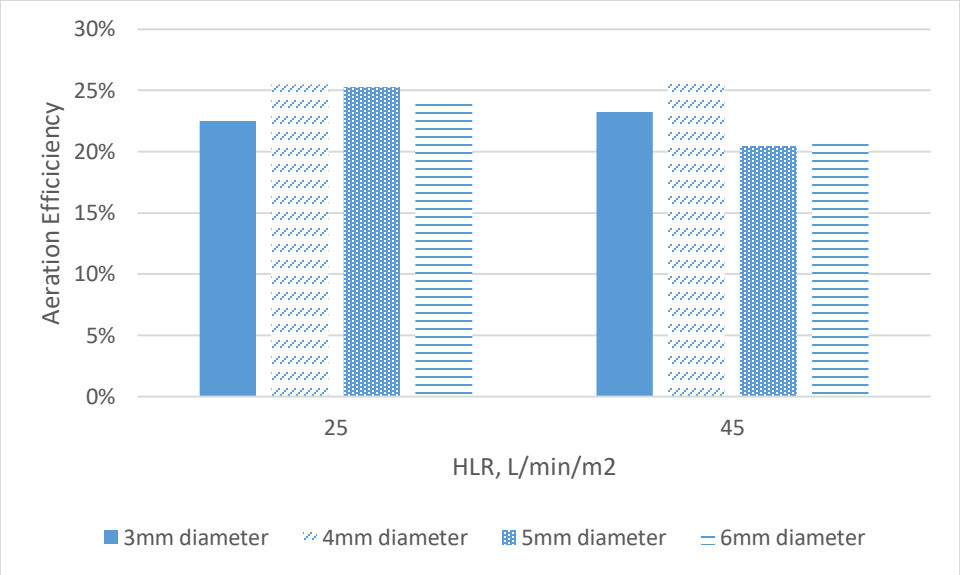

Figure 5.6 Average aeration efficiency of all trays Vs. flow rate for different hole diameters and flow rates

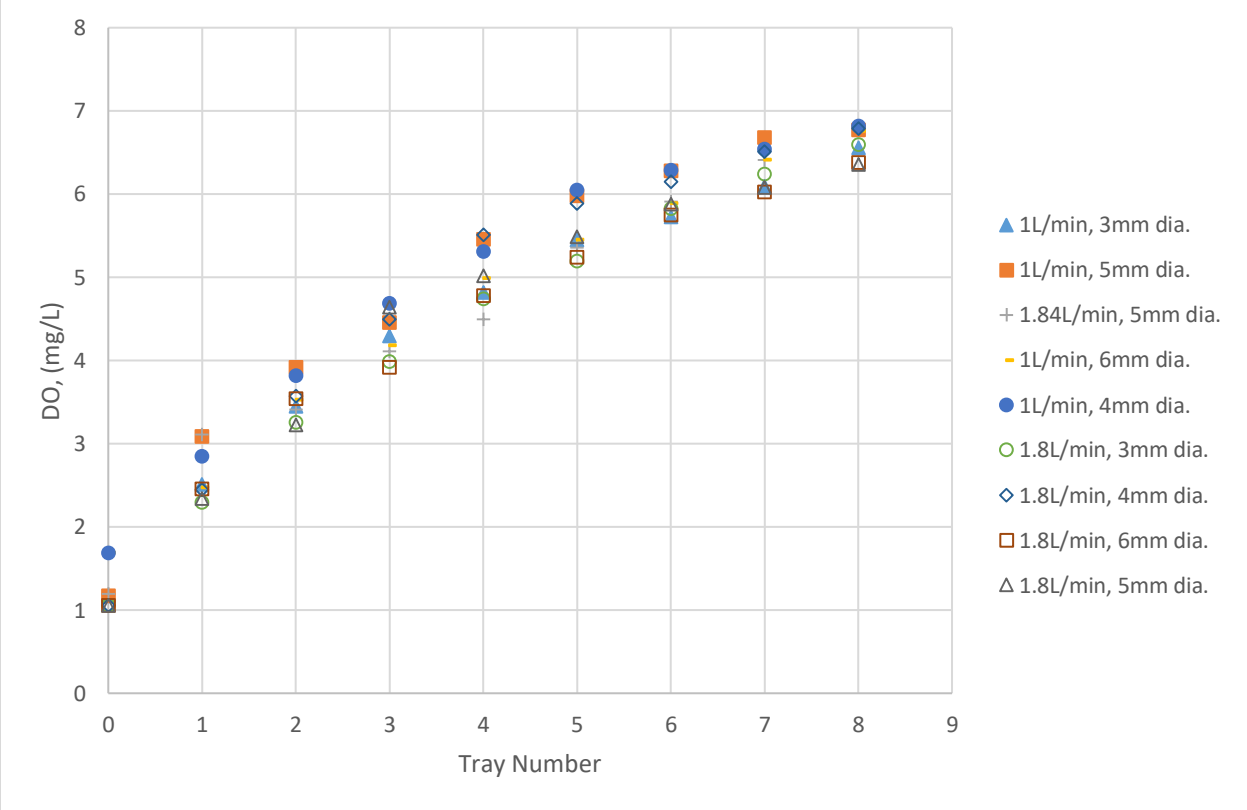

Figure 5.7 Pilot experiment results

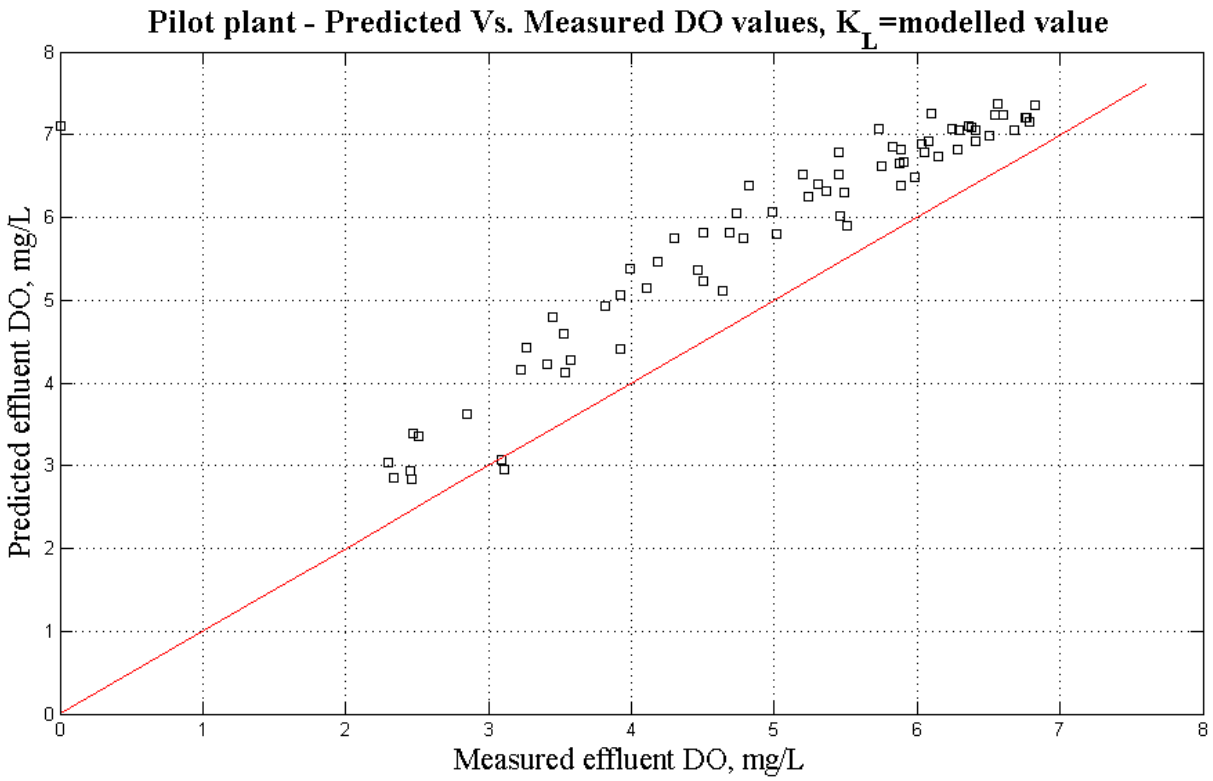

Figure 5.8 Predicted DO from Analytical Model Vs. Pilot Plant Measured DO, K_L from regression model

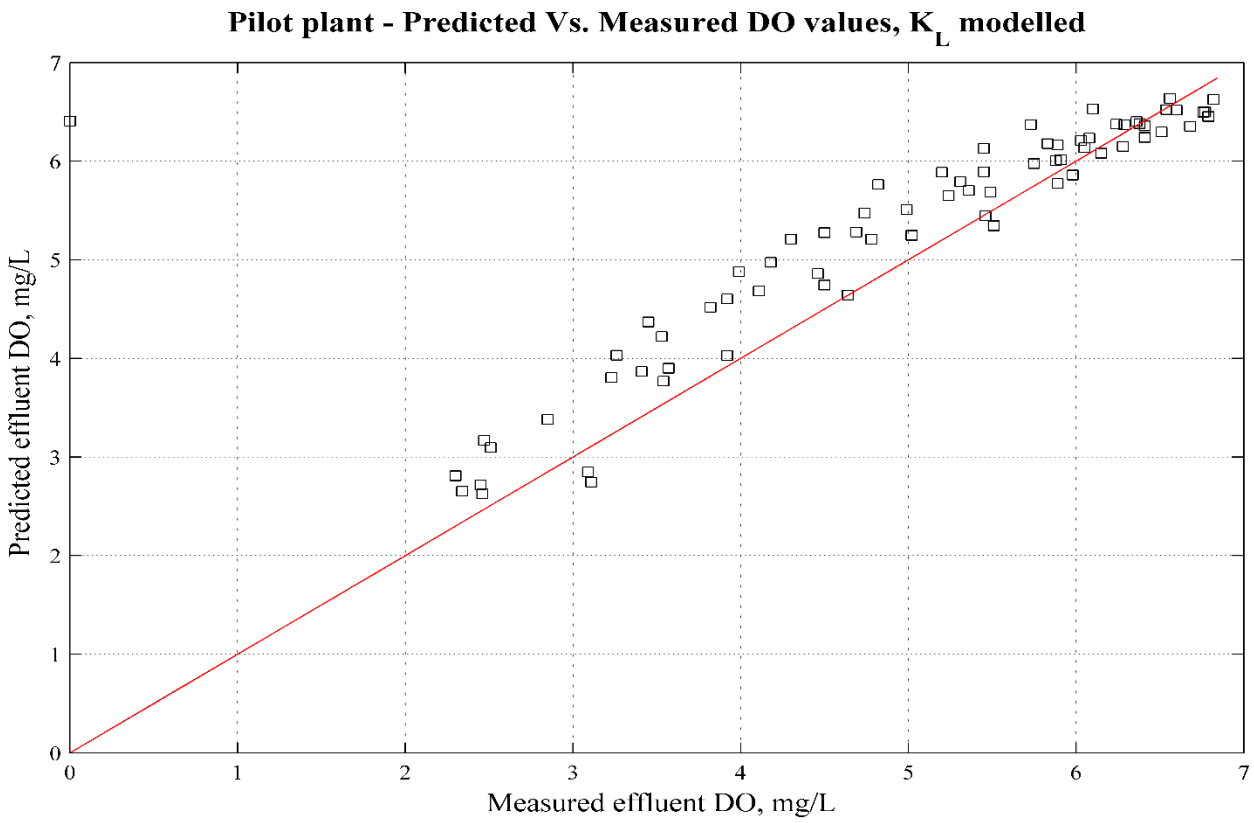

Figure 5.9 Predicted DO from Analytical Model with β=0.9 Vs. Pilot Plant Measured DO, K_L from regression model

5.4. Conclusion

In this phase, the use of the tray aerator in a pilot wastewater treatment plant was investigated. The results illustrate that the tray aerator performance is highly affected by the number of trays, and the hole diameter. Results highlights that the optimum number of trays is five trays other than the distribution tray, as the change in *DO* beyond the fifth tray was not significant.

The empirical formula for (K_L) that was developed in Phase II – Laboratory Study (Equation (4.11)) was validated for the pilot application. The error in the estimation was higher than the error from the Laboratory results, which is postulated to be resulting from the microbial activity in the real wastewater, which potentially consumed some of the added oxygen. Through setting β=0.9, that error was reduced to 10%, which is within an acceptable range, and implies that the model fits well for predicting the *DO* effluent from tray aerators operating on real wastewater.

6. General Discussion

Results from the developed equations illustrate that the aeration performance from tray aerators is strongly driven by *N* and *HLR*. Increasing *N* results in an increase in the aeration efficiency as was illustrated in Figure 3.7, Figure 4.11, and Figure 5.7. The three figures indicate that the effluent *DO* increases exponentially with the increase in *N*. This exponential relation is explained to be due to the decrease in the concentration gradient with the increase of the *DO*, resulting in a decrease in mass flux, according to Fick's law indicated in Equation (2.1). Similar dependence was observed for the tray aerators studied for CO_2 stripping (Scott et al. 1955; La Motta 1995; La Motta & Chinthakuntla 1996) as well as for sulfide stripping (Duranceau & Faborode 2012).

The effect of the *HLR* on the aeration performance is highlighted in the mathematical model results illustrated in Figure 3.8. Decreasing the HLR, which is either by increasing the tray area or decreasing the flow, rate results in an increase in the *DO*. Similar conclusion was drawn from Figure 4.10 for the laboratory study, however the results from the pilot scale application indicated in Figure 5.6 were not sufficient to proof or reject that hypothesis. This relation between the *DO* and the *HLR* is resulting from the increase of the interface time between water and air with the decrease in the HLR. La Motta realized the same conclusion but for CO_2 stripping, where the model equations he developed illustrated that the CO_2 stripping is inversely proportional with the *HLR* (La Motta 1995; La Motta & Chinthakuntla 1996). Similarly, Duranceau and Faborode reported that the sulfide stripping from tray aerators is inversely proportional with the *HLR* (Duranceau & Faborode 2012).

Regarding the tray spacing, apparently from the mathematical model, the change in tray spacing did not result in significant change in the aerator performance (Figure 3.6 and Figure 3.7), while the results from the laboratory investigation indicated the increase in the aerator performance with the increase of tray spacing (Figure 4.10). These contradicting conclusions were explained by the analysis of K_L. K_L is a function of the degree of turbulence of the two interacting fluids (Jamnongwong et al. 2010; Tchobanoglous et al. 2004). Since *SP* affects the jet velocity and diameter according to Equations (3.9-3.13), the change in *SP* result in a change in the degree of turbulence, and affects K_L. The relation between K_L and *SP* is indicated in Equation (4.11), in which K_L is proportional with *SP*. This analysis justifies the proportional relation of *DO* with *SP*. This conclusion is aligned with the conclusion for CO2 stripping (La Motta 1995; La Motta &

Chinthakuntla 1996), whereas Duranceau and Faborode did not address SP in their analysis for sulfide stripping (Duranceau & Faborode 2012).

Changing the hole diameter and/or the number of holes per tray did not have significant impact on the aeration efficiency. The results from the three phases of this study show that the impact of changing the hole diameter is limited and can be neglected if compared to the change of aeration efficiency resulting from changing *N*, *HLR*, and *SP*. Even though the variation in *d* affects the value of a_j and t_j as indicated in Equations (3.9-3.13, 3.18, & 3.19), the value of d changed with a step of unity, and is constrained by the studied conditions to a maximum change of 3mm (3mm≥d≥6mm) hindering the impact of changing *d* on the aeration performance. None of the published studies addressed the impact of *d* on the performance of tray aerators (La Motta 1995; La Motta & Chinthakuntla 1996; Duranceau & Faborode 2012).

Despite that *d* and *n* do not impact the aeration performance, they are important design parameters for the tray aerator from a hydraulic prospective. Those two parameters, together with *Q* define the flow regime over tray aerators. Underestimating the values of *d* and *n* for a design *Q* might result in decreasing the flow rate effluent from tray holes resulting in water overflow from tray sides, while overestimating *d* and *n* would necessitate larger *A*, and the flow of water would assume dripping regime rather than jetting regime. this was highlighted in section 3.2.1 of this thesis and illustrated in Figure 3.4. This needs to be verified in further works.

6.1. Design Procedure

In order to develop the design model for tray aerators, that can be used by engineers and consultants to design an effective passive aeration module, some parameters should be acquired or measured.

6.1.1. Input Parameters

- Design flow rate
- Operating temperature
- Influent DO

- Minimum desired effluent DO
- Maximum allowable height for system installation

6.1.2. Design Steps

The design procedure is indicated in the following steps:

- Number of modules

The studied tray aerators were all having a tray area of 20cmX20cm. This constant A was intentionally selected, so as to design the tray aerators in modules, depending on the expected flow rate. each module should have an area of 20cmX20cm, and can serve a maximum flow rate of 2.5m3/day (the maximum tested flow rate). In order to select the proper number of modules, the design flow rate should be divided among a number (n_{module}) of modules to assure that none of them would serve more than the maximum flow rate according to Equation (6.1)

$$n_{module} = \frac{Q_{design}(m^3/day)}{2.5(m^3/day)} \quad \text{.....Equation (6.1)}$$

And then the flow rate per module (Q_{module}) would be calculated as indicated in Equation (6.2)

$$Q_{module} = \frac{Q_{design}}{n_{module}} \quad \text{.....Equation (6.2)}$$

- Hydraulic Design

For each tray, the number and diameter of holes should be properly selected to assure jetting regime for water exiting from holes, and guarantees that no overflow would occur from tray sides. The hydraulic design is an iterative process. Three initial assumptions are made, *N=1* (other than the distribution tray), *d=3mm* and *n=1*. The assumption for *N* shall be corrected from the aeration design, which is illustrated in the next subsection. *SP* shall be calculated by knowing *H*, and *N* according to Equation 3.23.

The design of the number of holes for a selected diameter is an iterative process, in which an initial guess is made for *n=1*, for the diameter of 3mm. Then the iterations for D_1, v_1, and *h* are calculated

according to equations (3.5, 3.4, and 3.8). If h is greater than h_s, n will be increased by 1, and new iterations for v_1, and h calculated.

The next step is to assure that the water exiting the tray holes will assume jetting regime. this will be through estimating L_j, v_2, and D_2 using equations (3.9-3.11), and substituting in equations (3.1-3.3) to assure that We is greater than We_c. n is increased by 1, and iterations for v_1, h, L_j, v_2, D_2, and We are calculated, until We is less than We_c. n_{design} is equal to the last tested n-1.

The operating hydraulic parameters v_1, h, L_j, v_2, D_2, v_j, and d_j are calculated using n_{design}.

- Aeration design

Following the determination of n_{module}, Q_{module}, d, n_{design}, and for the assumed of N, Equations (3.22) is solved and if $C_{2(i-1)}$ is greater than or equal the desired $DO_{effluent}$, the iterations for that diameter is terminated. Else, $N=N+1$, and the whole iteration process is repeated. The same procedure will be made for other diameters.

6.1.3. Output Parameters

The aforementioned design procedure shall result in the definition of the following parameters

- Number of modules (n_{module})
- Flow rate per module (Q_{module})
- Number of holes per tray (n_{design})
- Diameter of holes (d)
- Number and Spacing between trays

7. Conclusion

Tray aerators, as a passive aeration unit, can increase the DO of effluent from anaerobic treatment for sewage treatment in small communities. An aeration efficiency over 75% can be achieved with a one meter drop in water height, utilizing five trays at 20cm apart.

The developed model equations (Equations 3.15, 3.16, 3.18, 3.19, and 3,22) illustrate that the *DO* is controlled by the number of trays used, the flow rate, and area of trays. The number of holes per tray, hole diameter, and flow rate define the flow regime into jetting regime or dripping regime. Furthermore, proper combination of those three parameters assure the uniform flow of water over the tray aerator system without the water overflow from the tray sides. Spacing between trays had limited impact on the *DO*.

In the laboratory study, the model equation was verified against measured *DO* values effluent from the tested tray aerator system. A correction to the model was introduced in the form of an empirical formula for K_L indicated in Equation (4.11). That empirical formula is developed from linear regression analysis for the measured K_L from various runs taking the area of holes, the flow rate and the spacing between trays as the drivers. The set of equations from the mathematical model were corrected with the empirical formula for K_L, and the error in estimate was validated from additional experimental runs.

The pilot scale study investigated the performance of the tray aerator system on anaerobically treated wastewater. The measured *DO* effluent form the system was analyzed using the model equations, and the error in estimate was recorded to be 20% ±10% for all the runs. Through including β=0.9, that error was reduced to 10%, which is within an acceptable range. This implied that the model is valid for real wastewater application, however further studies shall be conducted to investigate the accurate value for β in the wastewater to be treated.

This research can be considered as a first step towards the complete analysis and development of the tray aerators for passive aeration of wastewater. The developed model is validated for flow rates ranging from 1m3/day to around 2.6m3/day, diameters of holes of 3, 4, 5, and 6 mm, trays with an area of 0.2mX0.2m, and spacing ranging between 0.15m to 0.25m. The model could be tested at other conditions to validate them.

Another further step, which was beyond the scope of the current work, is to optimize the design parameters of the tray aerator system in order to achieve the highest possible aeration efficiency, while keeping the system area and overall height as small as possible.

References

ASCE, 2007. Measurement of Oxygen Transfer in Clean Water. *ASCE Standard*, ASCE/EWRI, pp.1–32. Available at: http://dx.doi.org/10.1061/9780784408483 [Accessed July 12, 2016].

Baylar, A., Bagatur, T. & Emiroglu, M.E., 2007. Prediction of oxygen content of nappe, transition, and skimming flow regimes in stepped-channel chutes. *Journal of Environmental Engineering and Science*, 6(2), pp.201–208. Available at: http://www.icevirtuallibrary.com/doi/10.1139/s06-048 [Accessed July 1, 2016].

Bird, R.B., Stewart, W.E. & Lightfoot, E.N., 2007. *Transport phenomena*, J. Wiley.

Chan, Y.J. et al., 2009. A review on anaerobic–aerobic treatment of industrial and municipal wastewater. *Chemical Engineering Journal*, 155(1–2), pp.1–18. Available at: http://linkinghub.elsevier.com/retrieve/pii/S1385894709004902 [Accessed June 17, 2016].

Chapra, S.C., 1997. *Surface water-quality modeling*, McGraw-Hill.

Clanet, C. & Lasheras, J.C., 1999. Transition from dripping to jetting. *Journal of Fluid Mechanics*, 383, pp.307–326.

CRC, 2016. Physical Constants of Organic Compounds W. M. Haynes, ed. *Handbook of Chemistry and Physics, 97th Edition (Internet Version 2017)*. Available at: http://hbcponline.com/faces/contents/ContentsSearch.xhtml;jsessionid=5C9FAA1780A47332E801A78C40222140 [Accessed August 28, 2016].

Danckwerts, P. V, 1951. Significance of liquid-film coefficients in gas absorption. *Industrial and engineering chemistry*, 43(6), pp.1460–1467.

Duranceau, S.J. & Faborode, J.O., 2012. Predictive modeling of sulfide removal in tray aerators. *American Water Works Association. Journal*, 104(2).

El-Gendy, A.S., Sabry, T.I. & El-Gohary, F.A., 2012. The Use of AN Aerobic Biological Filter for Improving the Effluent Quality of A Two-Stage Anaerobic System. *International Water Technology Journal (IWTJ)*, 2(4), pp.298–308.

El-Gohary, F.A. et al., 1998. Evaluation of wastewater treatment technologies for rural Egypt. *International Journal of Environmental Studies*, 54(1), pp.35–55. Available at: http://www.tandfonline.com/doi/abs/10.1080/00207239808711138 [Accessed June 14, 2016].

Garcia-Ochoa, F. & Gomez, E., 2009. Bioreactor scale-up and oxygen transfer rate in microbial processes: An overview. *Biotechnology Advances*, 27(2), pp.153–176.

Ghaly, A.E. & Kok, R., 1988. The effect of sodium sulfite and cobalt chloride on the oxygen transfer coefficient. *Applied Biochemistry and Biotechnology*, 19(3), pp.259–270.

Gulliver, J.S. & Rindels, A.J., 1993. MEASUREMENT OF AIR-WATER OXYGEN TRANSFER AT HYDRAULIC STRUCTURES. *Journal of Hydraulic Engineering*, 119(3), pp.327–349. Available at: http://ascelibrary.org/doi/abs/10.1061/(ASCE)0733-9429(1993)119:3(327) [Accessed June 2, 2016].

Hach, 2013. User Manual: Luminescent Dissolved Oxygen Probe - Model LDO10101, LDO10103, LDO10105, LDO10110, LDO10115 or LDO10130. *User Manual: Luminescent Dissolved Oxygen Probe - Model LDO10101, LDO10103, LDO10105,*

LDO10110, LDO10115 or LDO10130. Available at: http://mena.hach.com/intellical-standard-ldo-sensor-1m-cable/product-downloads?id=24759766760&callback=pf [Accessed August 15, 2016].

Heinz, S., 2011. *Mathematical modeling*, Berlin, Heidelberg: Springer. Available at: http://library.aucegypt.edu:2048/login?url=http://dx.doi.org/10.1007/978-3-642-20311-4 [Accessed July 24, 2016].

Hendrickson, T.P. et al., 2015. Life-Cycle Energy Use and Greenhouse Gas Emissions of a Building-Scale Wastewater Treatment and Nonpotable Reuse System. *Environmental science & technology*, 49(17), pp.10303–11. Available at: http://www.ncbi.nlm.nih.gov/pubmed/26230383 [Accessed October 2, 2016].

Higbie, R., 1935. The rate of absorption of a pure gas into still liquid during short periods of exposure. *Institution of Chemical Engineers*, 35, pp.36–60.

Howe, K.J. et al., 2012. *Principles of Water Treatment*, Somerset, US: John Wiley & Sons. Available at: https://books.google.com/books?hl=en&lr=&id=dSZHAAAAQBAJ&oi=fnd&pg=PT10&dq="Kerry+J.,+Hand,+David+W.,+and+Crittenden,+John+C..+Principles+of+Water+Treatment+(1).+Somerset,+US:+Wiley,+2012.+ProQuest+ebrary.+Web.+30+May"+"Kerry+J.,+Hand,+David+W.,+and [Accessed June 3, 2016].

Hsieh, C.-C., Ro, K.S. & Stenstrom, M.K., 1993. Estimating emissions of 20 VOCs. I: Surface aeration. *Journal of Environmental Engineering*, 119(6), pp.1077–1098. Available at: http://ascelibrary.org/doi/abs/10.1061/(ASCE)0733-9372(1993)119:6(1077) [Accessed June 8, 2016].

International Energy Agency, 2015. *Key World Energy Statistics*, Paris.

Jamnongwong, M. et al., 2010. Experimental study of oxygen diffusion coefficients in clean water containing salt, glucose or surfactant: Consequences on the liquid-side mass transfer coefficients. *Chemical Engineering Journal*, 165(3), pp.758–768. Available at: http://linkinghub.elsevier.com/retrieve/pii/S1385894710008703 [Accessed July 12, 2016].

Jan, C., Asce, M. & Nguyen, Q., 2010. Discharge Coefficient for a Water Flow through a Bottom Orifice of a Conical Hopper. *Journal of Irrigation and Drainage Engineering*, 136(August), pp.567–572.

Kavanaugh, M.C. & Trussell, R.R., 1980. Design of aeration towers to strip volatile contaminants from drinking water. *Journal (American Water Works Association)*, 72(12), pp.684–692.

Lee, M., 2002. Visualization of oxygen transfer across the air–water interface using a fluorescence oxygen visualization method. *Water Research*, 36(8), pp.2140–2146. Available at: http://www.sciencedirect.com/science/article/pii/S0043135401004213 [Accessed July 1, 2016].

Lekang, O.-I., 2013. Aquaculture engineering. In *Aquaculture engineering*. Somerset, NJ, USA: Wiley-Blackwell, pp. 155–178.

Leung, S.M. et al., 2006. Air/water oxygen transfer in a biological aerated filter. *Journal of environmental engineering*, 132(2), pp.181–189. Available at: http://ascelibrary.org/doi/abs/10.1061/(ASCE)0733-9372(2006)132:2(181) [Accessed July

1, 2016].

Lewis, W.K. & Whitman, W.G., 1924. Principles of Gas Absorption. *Industrial & Engineering Chemistry*, 16(12), pp.1215–1220. Available at: http://pubs.acs.org/doi/abs/10.1021/ie50180a002 [Accessed August 20, 2016].

Lienhard, J.H., 1984. Velocity Coefficients For Free Jets From Sharp-Edged Orifices. *Journal of Fluids Engineering*, 106(1), p.13. Available at: http://fluidsengineering.asmedigitalcollection.asme.org/article.aspx?articleID=1426001 [Accessed June 2, 2016].

Liss, P.S. & Slater, P.G., 1974. Flux of Gases across the Air-Sea Interface. *Nature*, 247(5438), pp.181–184. Available at: http://www.nature.com/doifinder/10.1038/247181a0 [Accessed August 20, 2016].

Liu, M.S., Branion, R.M.R. & Duncan, D.W., 1972. Oxygen transfer to water and to sodium sulfite solutions. *Journal - Water Pollution Control Federation*, 44(1), pp.34–40. Available at: http://www.jstor.org/stable/25037274 [Accessed June 8, 2016].

Lyberatos, G. & Pullammanappallil, P.C., 2010. Anaerobic Digestion in Suspended Growth Bioreactors. In L. K. Wang, V. Ivanov, & J.-H. Tay, eds. *Environmental Biotechnology*. Totowa, NJ: Humana Press, pp. 395–438. Available at: http://link.springer.com/10.1007/978-1-60327-140-0.

Lytle, D.A. et al., 1998. Using aeration for corrosion control. *American Water Works Association*, 90(3), pp.74–88.

McGhee, T.J. & Steel, E.W. (Ernest W., 1991. *Water supply and sewerage* 6th ed., New York: McGraw-Hill.

Montgomery, D.C., 2001. *Design and analysis of experiments* 5th ed., New York: John Wiley.

La Motta, E.J., 1995. Chemical analysis of CO2 removal in tray aerators. *Journal of the American Water Resources Association*, 31(2), pp.207–216. Available at: http://doi.wiley.com/10.1111/j.1752-1688.1995.tb03374.x [Accessed August 20, 2016].

La Motta, E.J. & Chinthakuntla, S., 1996. Corrosion Control of Drinking Water Using Tray Aerators. *Journal of Environmental Engineering*, 122(7), pp.640–648. Available at: http://ascelibrary.org/doi/10.1061/%28ASCE%290733-9372%281996%29122%3A7%28640%29 [Accessed August 20, 2016].

Moulick, S. et al., 2010. Aeration characteristics of a rectangular stepped cascade system. *Water Science & Technology*, 61(2), p.415. Available at: http://wst.iwaponline.com/cgi/doi/10.2166/wst.2010.828 [Accessed July 1, 2016].

Mueller, J.A., Boyle, W.C. & Pöpel, H.J., 2002. *Aeration : principles and practice*, Boca Raton: CRC Press.

Nakasone, H., 1987. Study of Aeration at Weirs and Cascades. *Journal of Environmental Engineering*, 113(1), pp.64–81. Available at: http://ascelibrary.org/doi/10.1061/(ASCE)0733-9372(1987)113:1(64).

Odawara, R. & Loayza, N. V., 2010. *Infrastructure And Economic Growth In Egypt*, The World Bank. Available at: http://elibrary.worldbank.org/doi/book/10.1596/1813-9450-5177 [Accessed October 1, 2016].

Ohtsu, I., Yasuda, Y. & Takahashi, M., 2001. Discussion of "Onset of Skimming Flow on Stepped Spillways." *Journal of Hydraulic Engineering*, 127(6), p.522. Available at: http://link.aip.org/link/JHEND8/v127/i6/p522/s1&Agg=doi [Accessed August 20, 2016].

Özbek, B. & Gayik, S., 2001. The studies on the oxygen mass transfer coefficient in a bioreactor. *Process Biochemistry*, 36(8–9), pp.729–741.

Sabry, T.I., El-Gendy, A.S. & El-Gohary, F.A., 2011. An Integrated Anaerobic - Aerobic System for Wastewater Treatment In Rural Areas. In *An Integrated Anaerobic – Aerobic System for Wastewater Treatment In Rural Areas*. IWA Conferences.

Sabry, T.I., Hamdy, W. & AlSaleem, S.S., 2010. Application of Different Methods of Natural Aeration of Wastewater and their Influence on the Treatment Efficiency of the Biological Filtration. *Journal of American Science*, 6(12), pp.944–952. Available at: http://www.jofamericanscience.org/journals/am-sci/am0612/.

Schladow, S.G. et al., 2002. Oxygen transfer across the air-water interface by natural convection in lakes. *Limnology and Oceanography*, 47(5), pp.1394–1404. Available at: http://onlinelibrary.wiley.com/doi/10.4319/lo.2002.47.5.1394/full [Accessed July 1, 2016].

Scott, G.R. et al., 1955. Aeration of Water: Revision of "Water Quality and Treatment," Chapter 6. *Journal (American Water Works Association)*, 47(9), pp.873–885. Available at: http://www.jstor.org/stable/41254169 [Accessed June 2, 2016].

Shammas, N.K. & Wang, L.K., 2010a. Aerobic and Anaerobic Attached Growth Biotechnologies. In L. K. Wang, V. Ivanov, & J.-H. Tay, eds. *Environmental Biotechnology*. Totowa, NJ: Humana Press, pp. 671–720. Available at: http://link.springer.com/10.1007/978-1-60327-140-0.

Shammas, N.K. & Wang, L.K., 2010b. Aerobic and Anoxic Suspended-Growth Biotechnologies. In L. K. Wang, V. Ivanov, & J.-H. Tay, eds. *Environmental Biotechnology*. Totowa, NJ: Humana Press, pp. 623–670. Available at: http://link.springer.com/10.1007/978-1-60327-140-0 [Accessed June 20, 2016].

Stoica, A., Sandberg, M. & Holby, O., 2009. Energy use and recovery strategies within wastewater treatment and sludge handling at pulp and paper mills. *Bioresource Technology*, 100(14), pp.3497–3505.

Swamee, P.K. & Swamee, N., 2010. Discharge equation of a circular sharp-crested orifice. *Journal of Hydraulic Research*, 48(1), pp.106–107. Available at: http://www.scopus.com/inward/record.url?eid=2-s2.0-77957657979&partnerID=tZOtx3y1.

Tchobanoglous, G. et al., 2004. *Wastewater engineering : treatment and reuse*, McGraw-Hill.

Thacker, N.P., Katkar, S.L. & Rudra, A., 2002. Evaluation of Mass-Transfer Coefficient of Free Fall–Cascade-Aerator. *Environmental monitoring and assessment*, 74(1), pp.1–9. Available at: http://link.springer.com/article/10.1023/A:1013809819910 [Accessed June 2, 2016].

Toombes, L. & Chanson, H., 2005. Air–Water Mass Transfer on a Stepped Waterway. *Journal of Environmental Engineering*, 131(10), pp.1377–1386. Available at: http://ascelibrary.org/doi/abs/10.1061/(ASCE)0733-9372(2005)131:10(1377).

USGS, 2015. DO Tables. *DOTABLES*. Available at: http://water.usgs.gov/software/DOTABLES/ [Accessed November 17, 2015].

Whitman, B.Y.W.G., 1923. The Two-Film Theory of Gas Absorption. *Chemical and Metallurgical Engineering*, 29(4), pp.146–148.

Wójtowicz, P. & Szlachta, M., 2013. Aeration performance of hydrodynamic flow regulators. *Water Science and Technology*, 67(12), pp.2692–2698. Available at: http://wst.iwaponline.com/cgi/doi/10.2166/wst.2013.181 [Accessed July 1, 2016].

Annex I

```
function [ number,qh ] = jetting_threshold( Q,D)
%This function is used to develop jetting diameter and number of holes for
%a given flow rate
%   Q: flow rate in m3/sec
%   n: number of holes per tray
%   D: diameter of hole in mm
%% Assumptions
cd=0.6;
cv=0.99;
%%
%figure
mm=['o','d','s','*','x','v','^','>','<','+'];
for j=1:size(Q,2)
    for jj=1:size(D,2)
        n=1;
        d=D(jj)/1000; %#ok<*AGROW>
        d_h=d*sqrt(cd/cv);
        v_hole=Q(j)*4/(n*pi*((d_h)^2));
        BO=((997.2*9.81*((d)^2))/(2*0.073))^0.5; % dimensionless Bond number
        we=997.2*((v_hole)^2)*(d_h)/0.073; % dimensionless Webber number
        wec=4*((1+(0.37*(BO)^2)-((((1+(0.37*(BO)^2))^2)-1)^0.5))^2); % critical webber
number for transition from dripping to jetting
        while we>wec
            n=n+1;
            v_hole=Q(j)*4/(n*pi*((d_h)^2));
            we=997.2*((v_hole)^2)*d_h/0.073; % dimensionless Webber number
        end
        number(j,jj)=n-1;
        qh(j,jj)=Q(j)/number(j,jj)*1000000;
    end
end
figure
for j=1:size(D,2)
    Q1=Q*24*3600;
    plot(Q1,number(:,j), 'color','k','marker',mm(j))
    %x1=axes('units','normalized',);
    xlabel('Flow rate,\it (m^3/day)','FontSize',8,'FontName','TimesNewRoman')
    ylabel('Maximum number of holes for jetting','FontSize',
8,'FontName','TimesNewRoman')
    legendinfo{j}=['D=',num2str(D(j)),'mm'];
    hold on
end
xlim([0.5 5])
set(gca, 'XTickLabel',{'','1','1.5','2','2.5','3','3.5','4','4.5',''})
set(gca,'FontSize',8,'FontName','TimesNewRoman')
legend(legendinfo,'Location','NorthWest')
end
```

```
function [ DO,number, Aj,h1,SP] = Analytical_model( Q,H,D,h,N,T,A,hs,sp)
%this function optimizes the design of tray aerators
%   Input parameters are:
%   Q: flow rate, m3/sec (accepts different values)
%   H: Overall system height, m (single value)
%   D: Diameter of holes,mm (accepts different values)
%   h: Desired film height, m (accepts different values)
%   N: Number of trays to be tested (accepts different values)
%   T: Temperature, deg C. (single value)
%   A: tray area, m2 (accepts different values)
%   hs: Side height of tray, m (single value)
%   sp: spacing between trays (in case of verifying single spacing), m (single value)
%
%   NOTE: number of trays should be more than 1
%
%   NOTE 2: this function uses the subfuction for saturation DO "sat.m"
%
%
if N(1)==1
    disp('error, number of trays shall exceed one')
    return
end
cd=0.6;
cv=0.99;
KL=20/100/60/60;
c0=0;
CS=sat(T);%saturation level of oxygen;

mm=['o','d','s','*','x','v','^','>','<','+'];

for z=1:size(Q,2)
    for w=1:size(A,2)
        HLR(z,w)=Q(z)/A(w);
        for k=1:size(N,2)
            for j=1:size(h,2)
                v_hole(z)=(cv)*sqrt(h(j)*2*9.81); %#ok<*AGROW>
                for jj=1:size(D,2)
                    d11=D(jj)*sqrt(cd/cv)/1000;
                    n(jj,j,z)=round(Q(z)*4/(v_hole(z)*pi*((d11)^2)));
                    v_hole(z)=Q(z)*4/(n(jj,j,z)*pi*(d11^2));
                    h1(jj,j,z)=((v_hole(z)/cv)^2)/(2*9.81);
                    while h1(jj,j,z)>hs
                        n(jj,j,z)=n(jj,j,z)+1;
                        v_hole(z)=Q(z)*4/(n(jj,j,z)*pi*(d11^2));
                        h1(jj,j,z)=((v_hole(z)/cv)^2)/(2*9.81);
                    end
                    number(jj,j,z)=n(jj,j,z);
                    Aj(jj,j,z)=number(jj,j,z)*pi*(d11^2)/4;
                    BO=((1000*9.81*((D(jj)/1000)^2))/(2*0.073))^0.5; % dimensionless↙
Bond number
                    we(z)=1000*((v_hole(z))^2)*(d11)/0.073; % dimensionless Webber↙
number
                    wec=4*((1+(0.37*(BO)^2)-((((1+(0.37*(BO)^2))^2)-1)^0.5))^2); %↙
critical webber number for transition from dripping to jetting
                    while we(z)<wec
```

```
                        number(jj,j,z)=number(jj,j,z)-1;
                        v_hole(z)=Q(z)*4/(number(jj,j,z)*pi*(d11^2));
                        h1(jj,j,z)=((v_hole(z)/cv)^2)/(2*9.81);
                        Aj(jj,j,z)=number(jj,j,z)*pi*(d11^2)/4;
                        BO=((1000*9.81*((D(jj)/1000)^2))/(2*0.073))^0.5; %↙
dimensionless Bond number
                        we(z)=1000*((v_hole(z))^2)*(d11)/0.073; % dimensionless Webber↙
number
                        wec=4*((1+(0.37*(BO)^2)-((((1+(0.37*(BO)^2))^2)-1)^0.5))^2); %↙
critical webber number for transition from dripping to jetting
                    end
                    number(jj,j,z)=number(jj,j,z)-1;
                    v_hole(z)=Q(z)*4/(number(jj,j,z)*pi*(d11^2));
                    h1(jj,j,z)=((v_hole(z)/cv)^2)/(2*9.81);
                    Aj(jj,j,z)=number(jj,j,z)*pi*(d11^2)/4;
                    BO=((1000*9.81*((D(jj)/1000)^2))/(2*0.073))^0.5; % dimensionless↙
Bond number
                    we(z)=1000*((v_hole(z))^2)*(d11)/0.073; % dimensionless Webber↙
number
                    wec=4*((1+(0.37*(BO)^2)-((((1+(0.37*(BO)^2))^2)-1)^0.5))^2); %↙
critical webber number for transition from dripping to jetting

                    SP(k)=H/(N(k));

                    L_jet(k,z)=SP(k)-h1(jj,j,z);
                    v_jet(k,z)=sqrt(((v_hole(z))^2)+(2*9.81*(L_jet(k,z))));
                    d22(k,z)=d11*sqrt(v_jet(k,z)/v_hole(z));
                    dm(k,z)=(d11+d22(k,z))/2;
                    v_mean(k,z)=(v_jet(k,z)+v_hole(z))/2;
                    ad(k,z)=4/dm(k,z); % area to volume ratio in case of falling↙
stream, assuming diameter equal hole diameter
                    td(k,z)=(L_jet(k,z))/v_mean(k,z);
                    %abc(k,z,jj)=ad(k,z)*td(k,z);

                    L_jet2(k,z)=sp-h1(jj,j,z);
                    v_jet2(k,z)=sqrt(((v_hole(z))^2)+(2*9.81*(L_jet2(k,z))));
                    d222(k,z)=d11*sqrt(v_jet2(k,z)/v_hole(z));
                    dm2(k,z)=(d11+d222(k,z))/2;
                    v_mean2(k,z)=(v_jet2(k,z)+v_hole(z))/2;
                    ad2(k,z)=4/dm2(k); % area to volume ratio in case of falling↙
stream, assuming diameter equal hole diameter
                    td2(k,z)=(L_jet2(k,z))/v_mean2(k,z);


                    %% estimation of DO

                    DO(jj,j,k,z,w)=CS-((CS-c0)*exp(-KL*(((1)/HLR(z,w))+((1)*ad(k,z)*td↙
(k,z))));
                    DO2(jj,j,k,z,w)=CS-((CS-c0)*exp(-KL*(((N(k))/HLR(z,w))+((N(k))*ad2↙
(k,z)*td2(k,z))));
                    DOT(jj,j,k,z,w)=CS-((CS-c0)*exp(-KL*(((N(k))/HLR(z,w))+((N(k))*ad↙
(k,z)*td(k,z))));
                    %qh(jj,j,z)=Q(z)./number(jj,j,z);
                end
            end
```

```
        end
    end
end

%% Create figure for DO from one tray and number of holes with const. jet area

figure
%axes('Position',[0.0380673499267936 0.0557935784749302 0.956808199121523↙
0.908388704318937])
for i=1:size(D,2)
    plot(number(i,:,1),DO(i,:,4,1,2), 'color','k','marker',mm(i))
    legendinfo{i}=['Hole Diameter=',num2str((D(i))),'mm'];
    hold on
    xlabel('Number of holes per tray','FontSize',↙
7,'FontName','Arial','FontWeight','bold');
    ylabel('DO influent to second tray           ','FontSize',↙
7,'FontName','Arial','FontWeight','bold')
    title('Typical DO profile Vs. number of holes at different hole diameters',...
        'FontSize',7,'FontName','Arial','FontWeight','bold');
end
 ylim([1.3 1.8])

set(gca,'FontSize',8,'FontName','Arial','FontWeight','bold')
legend(legendinfo,'Location','NorthWest')

% %% Create figure for DO from one tray for flow rate per hole and diameter
%
% figure
% for i=1:size(D,2)
%     plot(qh(i,:,1)*1000000,DO(i,:,4,1,2), 'color',[rand(1),rand(1),rand(1)])
%     lgendinfo{i}=['Hole Diameter=',num2str((D(i))),'mm'];
%     hold on
%     xlabel('Flow rate per hole (x10^-^6 m^3/sec/hole)','FontSize',14);
%     ylabel('DO influent to second tray (mg/L)','FontSize',14)
%     title('Typical DO profile Vs. flow per hole for different hole diameters',...
%         'FontSize',16);
% end
% ylim([1 2])
%
% set(gca,'FontSize',14)
% legend(lgendinfo,'Location','NorthWest')

%% Create figure for DO from one tray for jet area and spacing

figure
for i=1:size(N,2)
    plot((D),DO(:,1,i,1,2), 'color','k','marker',mm(i))
    lgendinfo{i}=['Spacing between trays=',num2str(SP(i)), ' m'];
    hold on
    xlabel('Hole Diameter          ','FontSize',↙
7,'FontName','Arial','FontWeight','bold');
    ylabel('DO influent to second tray           ','FontSize',↙
7,'FontName','Arial','FontWeight','bold');
    title('Typical DO profile Vs. spacing between trays for single tray system',...
        'FontSize',7,'FontName','Arial','FontWeight','bold');
```

```
end
% xlim([2 7])
% set(gca, 'XTickLabel',{'','3','4','5','6',''})
ylim([1.3 1.8])
set(gca,'FontSize',8,'FontName','Arial','FontWeight','bold')
legend(lgendinfo,'Location','NorthWest')

%% Create figure for DO from system and number of trays at fixed spacing

% figure
% for i=1:size(D,2)
%     ee=DO2(i,1,:,1,2);
%     eee=permute(ee,[1,3,2,4,5]);
%     plot((N),eee, 'color','k','marker',mm(i))
%     lgendinfo{i}=['Hole Diameter=',num2str((D(i))),'mm'];
%     hold on
%     xlabel('Number of trays','FontSize',7,'FontName','Arial','FontWeight','bold');
%     ylabel('DO effluent from the system                    ','FontSize',
7,'FontName','Arial','FontWeight','bold');
%     title('Typical DO profile Vs. number of trays for fixed tray spacing',...
%         'FontSize',7,'FontName','Arial','FontWeight','bold');
% end
% ylim([0 CS])
% set(gca,'FontSize',8,'FontName','Arial','FontWeight','bold')
% legend(lgendinfo,'Location','NorthWest')% Create figure for number of trays

%% Create figure for system performance for a fixed height

figure
for i=1:size(D,2)
    ee=DOT(i,1,:,1,2);
    eee=permute(ee,[1,3,2,4,5]);

 plot(N,eee,'color','k','marker',mm(i))
    leegendinfo{i}=['Hole Diameter=',num2str((D(i))),'mm'];
    hold on
end
legend(leegendinfo,'Location','NorthWest')
xlabel('Number of trays','FontSize',7,'FontName','Arial','FontWeight','bold');
ylabel('DO effluent from the system          ','FontSize',
7,'FontName','Arial','FontWeight','bold');
set(gca,'XTickLabel',N)
title('Typical DO profile Vs. number of trays for a 1m height system',...
    'FontSize',7,'FontName','Arial','FontWeight','bold');
ylim([0 CS])
set(gca,'FontSize',8,'FontName','Arial','FontWeight','bold')
first_axis = gca;
sqz = 0.1; %// distance to squeeze the first plot
set(first_axis,'units','normalized', 'Position', get(first_axis, 'Position') + [0 sqz
0 -sqz ]);
ax2 = axes('Position', get(first_axis, 'Position') .* [1 1 1 0.001] - [0 sqz 0
0],'Color','none');
xlim([SP(size(SP,2)) SP(1)]);
set(get(gca, 'XLabel'),'String','Spacing between trays       ','FontSize',
7,'FontName','Arial','FontWeight','bold');
```

```
set(gca,'XTickLabel',SP)
set(ax2, 'XScale', get(first_axis, 'XScale')); %// make logarithmic if first axis is↙
too
set(gca,'FontSize',8,'FontName','Arial','FontWeight','bold')


%% Create figure for change in tray area and flow rate

figure
for w=1:size(A,2)
    aaa=DOT(1,1,k,:,:);
    aa=permute(aaa,[4,5,1,2,3]);
    plot(Q*1000*1000,aa(:,w),'color','k','marker',mm(w))
    leeegendinfo{w}=['Tray Area=',num2str((A(w))),' m'];
    hold on
    xlabel('Flow rate e6 m^3/sec'            ,'FontSize',↙
7,'FontName','Arial','FontWeight','bold');
    ylabel('DO mg/l'                         ,'FontSize',↙
7,'FontName','Arial','FontWeight','bold');
    title('Typical DO profile Vs. flow rate for a 1m height system',...
        'FontSize',7,'FontName','Arial','FontWeight','bold');
end
ylim([0 CS])
set(gca,'FontSize',8,'FontName','Arial','FontWeight','bold')
legend(leeegendinfo,'Location','SouthWest')
end
```

Annex II

Q (L/min)	d (mm)	n	SP (cm)	C0 (mg/L)	C2 (mg/L)	C4 (mg/L)	C6 (mg/L)	C8 (mg/L)
.6 L/min	6 mm	8	25 cm	0.88	3.14	4.89	6.51	7.13
1.153 L/min	6 mm	8	25 cm	0.88	2.91	4.73	6.07	6.86
1.614 L/min	6 mm	8	25 cm	0.88	2.85	4.33	5.91	6.46
.6 L/min	6 mm	8	20 cm	0.5	3	4.86	6.07	6.67
1.153 L/min	6 mm	8	20 cm	0.55	2.6	3.93	5.21	6.21
1.614 L/min	6 mm	8	20 cm	0.57	2.63	4.1	4.98	5.69
1.295 L/min	6 mm	8	30 cm	0.55	3.29	4.83	5.97	6.73
.773 L/min	6 mm	8	30 cm	0.55	3.66	5.67	6.67	7.17
1.959 L/min	6 mm	8	30 cm	0.96	3.04	5.08	5.55	6.26
.773 L/min	3 mm	8	15 cm	0.48	3.09	4.08	4.98	5.67
1.295 L/min	3 mm	8	15 cm	0.02	1.07	2.37	3.59	4.58
1.959 L/min	3 mm	8	15 cm	0.32	1.96	3.59	4.55	5.44
.773 L/min	4 mm	8	15 cm	1.17	2.58	3.88	4.8	5.61
1.295 L/min	4 mm	8	15 cm	1.56	2.69	3.91	4.72	5.56
1.959 L/min	4 mm	8	15 cm	1.17	2.63	3.87	4.78	5.25
.773 L/min	3 mm	8	20 cm	0.39	2.34	3.78	4.78	5.72
1.295 L/min	3 mm	8	20 cm	0.23	1.88	3.86	4.68	5.48
1.959 L/min	3 mm	8	20 cm	1.09	2.53	4.09	5.23	5.82
1.959 L/min	4 mm	8	20 cm	1	1.98	3.36	4.57	5.4
.773 L/min	3 mm	8	15 cm	0.3	2.5	3.31	4.55	5.5
1.295 L/min	3 mm	8	15 cm	0.01	1.23	2.46	3.75	4.63
1.959 L/min	3 mm	8	15 cm	0.34	2.01	3.78	4.84	5.83
.773 L/min	4 mm	8	15 cm	0.7	2.23	4.65	5.28	5.87
1.295 L/min	4 mm	8	15 cm	0.53	1.99	3.27	4.83	5.41
1.959 L/min	4 mm	8	15 cm	0.62	1.97	3.43	4.12	4.96
.773 L/min	3 mm	8	20 cm	0.45	2.51	3.62	4.86	5.54
1.295 L/min	3 mm	8	20 cm	0.7	2.52	3.97	4.75	5.44
.773 L/min	4 mm	8	20 cm	0.53	2.74	4.52	5.21	5.88
1.295 L/min	4 mm	8	20 cm	0.27	2.47	3.87	4.87	5.57
1.959 L/min	4 mm	8	20 cm	0.27	2.08	3.54	4.61	5.45
.773 L/min	3 mm	8	15 cm	0.21	2.25	3.68	4.46	5.24
.773 L/min	4 mm	8	15 cm	0.79	2.45	4.14	4.86	5.46
1.295 L/min	4 mm	8	15 cm	0.87	2.66	4	4.57	5.42
1.959 L/min	4 mm	8	15 cm	1.51	2.26	3.49	4.66	5.13
.773 L/min	4 mm	8	25 cm	0.66	2.65	4.74	5.63	
.773 L/min	4 mm	6	25 cm	0.58	2.9	4.49	5.45	
.773 L/min	4 mm	6	15 cm	1	2.41	4.16	4.52	
1.295 L/min	4 mm	8	25 cm	0.56	2.62	4.07	5.36	
1.295 L/min	4 mm	6	25 cm	0.4	2.53	4.25	5.15	
1.295 L/min	4 mm	6	15 cm	0.8	2.22	3.46	4.48	
1.959 L/min	4 mm	8	25 cm	0.56	2.52	3.93	5.7	
1.959 L/min	4 mm	6	25 cm	0.4	2.28	4.13	5.15	
1.959 L/min	4 mm	6	15 cm	0.9	2.2	3.5	4.26	